Physicochemical Characterisation of Disease Associated Abnormal Prion Proteins

By

Lisa Ann Stone

MRC Prion Unit

Institute of Neurology

A thesis submitted for the degree of Doctor of Philosophy to the University of London

Supervisors: Dr Jonathan D. F. Wadsworth

Professor Anthony R. Clarke

ProQuest LLC
789 East Eisenhower Parkway
P.O. Box 1346
Ann Arbor, MI 48106-1346

ACKNOWLEDGEMENTS

I would like to thank members of the MRC Prion unit, past and present for their help throughout my PhD, in both science and general tutoring. My supervisors Dr Jonathan Wadsworth and Professor Tony Clarke, who provided much encouragement along the way. Thank you to Sharon Cooper for all the hard work taking my project forward, good luck! Thank you to Ray Young for technical wizardry in the presentation of my figures. Thanks to MRC for funding, and head of the department Professor John Collinge for giving me the opportunity to study in the MRC Prion Unit. Thanks also to all the scientists involved in the work described in this thesis: Dr Sabrina Cronier, Dr Francesca Properzi, Dr Peter Klöhn, Dr Graham Jackson, Dr Howard Tattum, Dr Sebastian Brandner, Jackie Linehan, Natalie Gros and Anjna Badhan. A very big thank you to Dr Mark Kristiansen for being great company working evenings and weekends, all the pints in the union afterwards and proof reading my thesis! Thanks to Mark Batchelor who also supported me as a housemate. Thanks to other fellow members of the MRC Prion Unit giving moral support accompanied by an alcoholic beverage or two: Kevin Williams, Dr Tim Szeto, Ruth Chia, Mel White, Sam Jones and Paresh Shah.

Prion unit scientists who have moved on to pastures new: Dr Andy Hill, thanks for all the advice from the other side of the globe (who could forget the world record for western blotting and your great musical taste). Dr Patrick Lewis, thanks for all the career advice. Thanks to Dr Gaia Skibinski for positive thesis thinking. Jenny Buckell, Dr Sukhi Mahal and their spirit of adventure, thanks for being there.

A big thank you to all my wonderful family for support throughout my PhD, my mum, Veronica Stone and the Byrne's clan, my dad, Mike Stone, and Kevin Howgate. My friends who have lived my journey: Sam Spence, Elly Cid and Faye Burton, thanks for being my spiritual rocks. The queen of the thesis, Dr Fred Herrmann, thanks for making me see the advantage of a scientific PhD over humanities! Thanks to Christel "Taylor" Makaloy for all the baselines. Thanks to the plastic scousers, Ali McConnell, Jenny Stroud and Liz Phelan, for being a great support back home. Thanks to my old friends from Manchester University, Dr Lynn Clark, Jess Wardlaw, Kelly Dickens and Simon Wilkins, for getting me through my first degree. Thanks to other fab friends who also organised my social activities whilst I was studying including Marianne Sundholm, Debbie O'Doherty, Nicki Wanford, Elle MacKay, Rosie Fannon, Jayne Arnold, Ali Rothwell and not forgetting Lynn Hodges, may she rest in peace. Thanks to the many artists for the uplifting soundtrack to keep me going including Peter Cox, Richard Drummie, Nick Rhodes, and Simon LeBon, amongst others.

The work in this thesis is dedicated to all my family and friends who have supported me in my scientific vocation over the years, and those who have inspired me in many different ways

"I thank you for bringing me here, for showing me home, for singing these tears, finally I've found that I belong here" Martin L. Gore ©1997

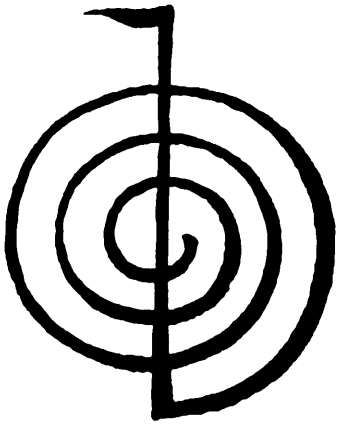

Five spiritual principles as a guide to living:

1. Just for today I will give thanks for my many blessings
2. Just for today I will not worry
3. Just for today I will not be angry
4. Just for today I will do my work honestly
5. Just for today I will be kind to my neighbour and every living thing

Dr Mikao Usui

August 15, 1865 - March 9, 1926

ABSTRACT

The central feature of prion disease is the conversion of normal host-encoded cellular prion protein, PrP^{C}, to an abnormal isoform, PrP^{Sc}. PrP^{Sc} appears to be the principal, if not the sole, component of infectious prions. Prion strain diversity seems to be encoded within PrP itself through a combination of PrP^{Sc} conformation, glycosylation and possibly other, as yet, unidentified post-translational modifications. Efficient purification of PrP^{Sc} will facilitate detailed chemical characterisation and investigation of conformations or assembly states required for prion infectivity. Purification of denatured PrP^{Sc} has been achieved through enrichment from brain homogenate using selective precipitation followed by chemical and thermal denaturation and isolation by immunoaffinity chromatography. These methods have isolated PrP^{Sc} from rodent prion strains with a yield of ~ 50 % and purity of > 90 % of total protein and for the first time permit isolation of full length denatured PrP^{Sc} facilitating comprehensive structural analysis. Purified denatured PrP is expected to have all the covalent post-translational modifications that may be required for prion infectivity. In attempts to reconstitute prion infectivity, denatured PrP was refolded under different solvent conditions and assessed for changes in solubility, resistance to proteolytic digestion and infectivity in bioassay. Although distinct changes in the physicochemical properties of PrP were observed, to-date no evidence for reconstitution of prion infectivity has been found. In the course of these studies, it was discovered that Cu^{2+} ions inhibit proteinase K activity and a detailed kinetic description of this inhibition was obtained. The lack of prion infectivity seen in refolded preparations of denatured PrP^{Sc} suggests a requirement for other as yet unidentified co-factors. The identity of PrP^{Sc} interacting proteins was investigated during the purification of PrP^{Sc} under differential extraction conditions in which prion infectivity was observed using an *in vitro* assay. Proteinase K digestion gave a change in prion infectivity implying that a correlation with the removal of a protease sensitive component occurred. Continuation of these studies may facilitate the identification of co-factors required for specific prion infectivity.

Abbreviations

All amino acid abbreviations as standard

α-PrP	PrP in a predominantly α-helical conformation
AEBSF	4-(2-aminoethyl)-benzenesulphonyl fluoride
βME	β-mercaptoethanol
β-PrP	PrP in a predominantly β-sheet conformation
BSE	bovine spongiform encephalopathy
BSA	bovine serum albumin
CD	circular dichroism
CJD	Creutzfeldt-Jakob disease
CSF	cerebral spinal fluid
CWD	chronic wasting disease
$CuSO_4$	copper sulphate
DMP	dimethyl pimelimidate
DMSO	dimethyl sulphoxide
D-PBS	Dulbecco's phosphate buffered saline lacking Ca^{2+} and Mg^{2+} ions
DTT	dithiothreitol
DY	drowsy prion strain
ECL	enhanced chemiluminescence
EDTA	ethylenediaminetetraacetic acid
EEG	electroencephalogram
EM	electron microscopy
EtOH	ethanol
fCJD	familial Creutzfeldt-Jakob disease
FCS	foetal calf serum
FDC	follicular dentritic cell
FFI	fatal familial insomnia
fM	femtomolar
g	gravitational force
GFAP	glial fibrillary acidic protein
GPI	glycosyl phosphatidyl inositol
GSS	Gerstmann-Sträussler-Scheinker disease
Ha	hamster
H&E	haematoxylin and eosin
HPLC	high pressure liquid chromatography
HY	hyper prion strain
i.c.	intracerebrally
ID	infectious doses
ID_{50}	infectious dose with 50 % attack rate
Ig	immunoglobulin
IU	infectious units
kDa	kilo Daltons
KI	potassium iodide
LD_{50}	lethal dose with 50 % attack rate
M	molar

MeOH	methanol
MEM	minimal essential medium
Mo	mouse
MRI	magnetic resonance imaging
mRNA	messenger ribonucleic acid
NaAc	sodium acetate
NaH_2PO	sodium phosphate
NaPTA	Sodium phosphatungstic acid
NEM	N-ethyl morpholine
NMR	nuclear magnetic resonance
NP40	nonidet P40
OFCS	Opti-MEM-10 % v/v FCS fetal calf serum
OPRI	Octapeptide repeat insertion
ORF	open reading frame
PAGE	polyacrylamide gel electrophoresis
PBS	phosphate buffered saline
PBST	PBS containing Tween 20
PEG	polyethylene glycol
pI	isoelectric point
PIPLC	phosphatidylinositol-specific phospholipase C
PK	proteinase K
PMCA	protein misfolding cyclic amplification
PMSF	phenylmethylsulphonyl fluoride
p-NA	para-nitrophenyl acetate
PNGase F	N glycosidase F
Prnp	mouse PrP genetic transcript
PRNP	human PrP genetic transcript
$Prnp^{0/0}$	transgenic mouse lacking PrP genetic transcript
PrP	prion protein
$PrP^{27\text{-}30}$	protease resistant core of PrP^{Sc}
PrP^{C}	cellular prion protein
PrP^{RES}	PrP that is partially protease resistant and may or may not be infectious
PrP^{Sc}	disease associated prion protein
PTFE	polytetrafluoroethylene
PVC	polyvinyl chloride
PVDF	polyvinylidene fluoride transfer membrane
RML	Rocky Mountain Laboratory (mouse adapted scrapie)
rpm	rotations per minute
rPrP	recombinant PrP
sarkosyl	lauroyl sarcosine, sodium salt
Sc237	hamster adapted scrapie
SCA	scrapie cell assay
SCEPA	scrapie cell endpoint assay
sCJD	sporadic Creutzfeldt-Jakob disease
SDS	sodium dodecyl sulphate
sFI	sporadic fatal insomnia
SN	supernatant
TAB	tropix assay buffer

TBST	tris buffered saline containing tween 20
Tg	transgenic
Tris	2,3-dibromopropyl phosphate
TME	transmissible mink encephalopathy
TSE	transmissible spongiform encephalopathy
Tween 20	polyoxyethylene (20) sorbitan monolaurate
U	units
vCJD	variant Creutzfeldt-Jakob disease
v/v	volume to volume ratio
w/v	weight to volume ratio

Table of Contents

Index of Figures and Tables

1 General introduction

Prion diseases are rare and fatal neurodegenerative diseases of humans and animals. This group of diseases were originally called transmissible spongiform encephalopathies (TSE's) prior to the discovery of the major component of the infectious agent and this name is still used today. Due to the infectious nature of the disease causing agent it was originally thought that it was a "slow-virus", but now a wealth of evidence shows that the causative agent is primarily composed of a disease associated isoform of the prion protein, PrP, designated PrP^{Sc}, which is resistant to methods used to inactivate nucleic acids. There is a host cellular form of PrP, PrP^{C}, of unknown function, and is converted to the disease associated isoform (PrP^{Sc}) by an unknown mechanism. The fact that these diseases occur as inherited and sporadic disorders, as well as transmissible infections, make prion diseases biologically unique. Despite a wealth of research into prion disease it is still unknown what the role of PrP^{Sc} is in disease progression or indeed, if it is the sole component of the infectious agent.

1.1 The discovery of the prion protein

TSE's were first seen as a transmissible disease in sheep and goats over 250 years ago with the unusual feature of a prolonged incubation period. In 1954, the term "slow virus" was coined to describe the transmissibility of the infectious agent and the slow progression of disease (1). However, after studies using procedures that modify or hydrolyze nucleic acids failed to inactive the scrapie agent (2-5) theories started to turn towards proteins being the causative agent (3;6-8). In fact as early as 1967, a protein hypothesis of transmission was proposed by Griffith (9), which was dismissed at the time. Although the exact components of prions are still unknown, it is now widely believed that the infectious agent is primarily proteinaceous (10).

1.1.1 Biochemical properties of the infectious agent

Isolation of the infectious agent responsible for TSE was a formidable task. Without a marker for the infectious agent, and simple infectivity assays, work had to be done using animals with prolonged incubation periods to end point before assessment of results. Prior to the development of the mouse bioassay using Chandler mice in 1961 (11) work had to be done using sheep and goats which was costly and time consuming.

Purification studies provided a variety of information on the physicochemical properties of the infectious agent including; association with cellular membranes (12-16), co-purification with microsomes (17), detachment from membranes with ultracentrifugation (18), heterogeneity of density in sucrose, NaCl, metrizamide and CsCl gradients (19;20) and properties of aggregation and hydrophobicity were shown using differential centrifugation (21;22).

More importantly, the properties of the infectious agent showed that it was primarily proteinaceous. It was found to be stable in detergent conditions that wouldn't denature proteins but unstable in detergent conditions that were denaturing. Non-denaturing detergent conditions could separate the infectious agent from other cellular components if followed by differential centrifugation or precipitation (23;24). The infectious agent was also resistant to both nuclease digestion and some forms of protease treatment (25). These studies provided the basis for further purification methods that were greatly facilitated by the development of a short incubation time in bioassay in Syrian hamsters using a hamster adapted scrapie prion strain (24).

1.1.2 Purification of the prion protein

A partial purification method that gave convincing data for the infectious agent being a protein was developed by Prusiner et al in 1981 (26). Methods included ultracentrifugation

with 0.5 % w/v sodium deoxycholate to solubilise membranes and digestion with micrococcal nuclease and proteinase K. Proteinase K (PK) treatment under certain conditions was found to significantly reduce the infectivity, suggesting that the infectious agent was proteinaceous. The agarose electrophoresed material was treated to produce chemical modification of amino acid residues by diethylpyrocarbonate which carbethoxylates proteins and was shown to reduce infectivity (26).

The culmination of all these studies led Prusiner to define the infectious agent of scrapie as "small proteinaceous infectious particles which are resistant to inactivation by most procedures that modify nucleic acids", with the *pro*teinaceous *in*fectious term taken to conjure the word "prion" (5).

Purification to isolate the prion protein was finally achieved in 1982 by Prusiner et al who adapted their earlier methods (27). The main modification to the earlier protocols was centrifugation over a sucrose gradient. The infectious agent was found in 2 main peaks, but was seen all over the sucrose gradient. The peak near the top of the gradient also contained other contaminating proteins but the main peak near the bottom at the interface between 25-60 % sucrose contained predominantly one protein thought to associate as aggregates with other hydrophobic molecules. This peak was seen over several preparations and on average had a 1-10 % yield, and 410 fold purification with 1.4×10^{10} ID_{50} U/mg of protein. To further analyse the infectious agent, purified samples were radio-iodinated and analysed by SDS-PAGE. Using this method no nucleic acids were seen but protein bands were visualised between 27 and 30 kDa (27). A protein of similar molecular weight was found in uninfected tissue but was digested with PK, whereas the disease associated protein remained stable (28). However, under denaturing conditions the disease associated protein was also digested. At this point it was unknown if the protein was a product of disease or a component of the infectious agent but since then many studies have shown that infectivity is correlated with concentration of the protease resistant core of PrP^{Sc}, PrP^{27-30} (27-32) (reviewed in (33)).

The amino acid sequence of this protein was obtained in 1984 (34) which enabled further analysis, and the production of anti-PrP antibodies (35). These antibodies were seen to label proteins from both normal and disease associated material.

1.1.3 Location of the PrP gene

After the N-terminal amino acid sequence had been obtained from the purified disease associated prion protein, oligonucleotides could be synthesised to identify the PrP gene. Surprisingly, the gene was found in both normal and disease associated tissues (34;36;37). No evidence has been shown to suggest that the PrP gene undergoes rearrangement during disease and there was no evidence or genetic basis for any alternative splicing (38). The mRNA of PrP doesn't increase in concentration throughout the disease (37) and normal and infected animals have the same open reading frame (ORF) sequences to the genome (39). Amino acid sequencing of the N-terminus of purified PrP^{C} and PrP^{Sc} showed extreme similarity and the difference in these proteins is likely to be due to a post-translational event (31).

The ORF of many PrP genes from different species have now been sequenced showing that they encode a protein of about 250 amino acids which is highly conserved amongst mammals, and is present in many other vertebrates including marsupials, birds and fish, suggesting an important role in evolution (40;41). The amino acid sequence of PrP from 11 mammalian species is shown in **Figure 1.1**.

Figure 1.1: Amino acid sequences of PrP from 11 species

Amino acid sequence of PrP from eleven mammalian species, adapted from Collinge et al 1997 (42). Numbering of amino acids is based on the human sequence in the first row. All sequences are taken from data submitted to the EMBL database (http://ca.expasy.org/sprot/). The mouse sequence corresponds to that of the NZW short incubation time allele and differs from the long incubation allele at positions indicated here as 109 (Leu/Phe) and 190 (Thr/Val). Because of the absence of glycine at position 55 in the mice these residues are 108 and 189 in the mouse sequence. The cow allele is shown as having six octapeptide repeats between residues 51 and 92, but bovine PrP contains either five or six repeats. The final repeat of mink, sheep and goat contain nine amino acids rather than usual eight and are shown displaced from the final octapeptide of the human sequence (between 91-92) aligned with the sixth repeat of cow which also contains nine amino acids. Amino acids which are identical in all species shown are outlined.

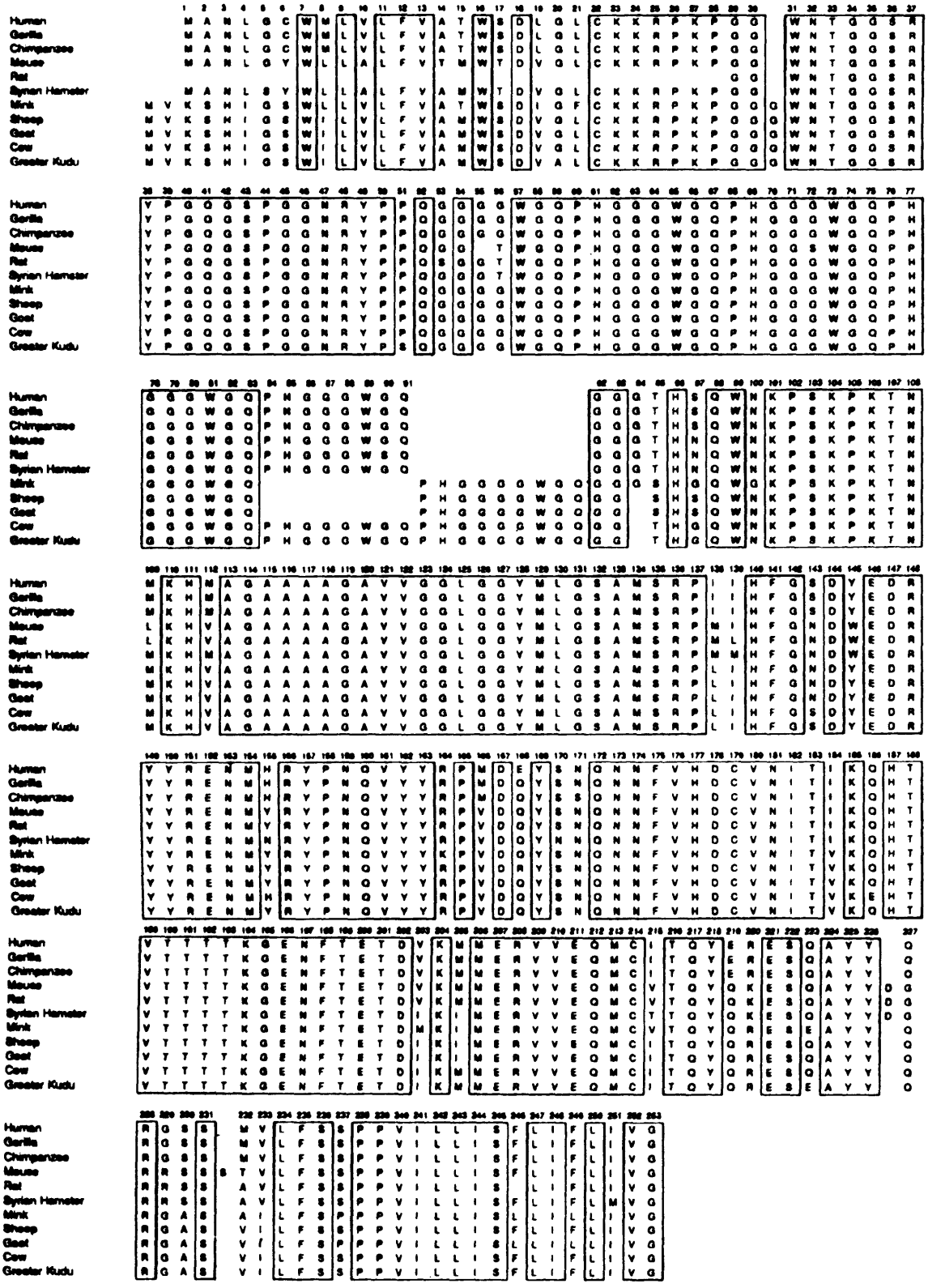
Human
Gorilla
Chimpanzee
Mouse
Rat
Syrian Hamster
Mink
Sheep
Goat
Cow
Greater Kudu

1.2 PrP conformation and disease propagation

After the isolation of PrP showing that it is host encoded, research has focussed on characterising the properties of PrP and what the differences are between the cellular form, PrP^{C}, and the disease associated form, PrP^{Sc}. PrP^{Sc} differs from PrP^{C} by being partially protease resistant and prone to aggregation, making conformational and structural studies difficult. As both forms of the protein have the same primary sequence, differences between PrP^{C} and PrP^{Sc} could be due to covalent post-translational modifications or simply conformational change. How these different properties occur from the same primary sequence and how they might be implicated in disease has been an area of intense research. Although some progress has been made on investigating the conformation of native PrP^{Sc} most research has been focused on the refolding of recombinant PrP (rPrP) to conformations that adopts either PrP^{C} or PrP^{Sc} properties.

1.2.1 Structure of PrP

After translation PrP is processed through the endoplasmic reticulum (ER) where the N-terminal and C-terminal regions of the protein are cleaved. The N-terminal signal peptide is removed at lysine residue 22 and C-terminal truncation occurs between 2 serine residues at positions 230/231 in order to attach a phosphatidylinositol glycolipid (GPI) anchor (see **Figure 1.2A**) (43;44).

GPI anchors consist of a phospholipid chain that spans a cellular membrane and a head group comprising of a phosphodiester-linked inositol at the top of the phospholipid chain. The inositol is linked to a chain of glucosamine, 3 mannose sugars and a phosphoethanolamine which links the sugars to the protein. The tetra-saccharide backbone can have numerously diverse side chains and the phospholipids can have many compositional differences giving rise to multiple GPI moieties (45). Studies into possible

differences between PrP^C and PrP^{Sc} have shown that the GPI anchor of both contain sialic acid (46;47). PrP^C can be cleaved from membranes at the GPI moiety using phosphatidylinositol-specific phospholipase C (PIPLC) (48) but PrP^{Sc} is resistant to such cleavage (49;50) indicating that a conformational change prevents accessibility of PIPLC. Other studies have shown that another enzyme, cathepsin D, can cleave PrP^{Sc} in the C-terminus liberating the GPI anchor with retention of prion infectivity (51) and transgenic mice expressing PrP lacking a GPI anchor can still propagate prions (52) suggesting that the GPI anchor is not a prerequisite component of the infectious prion (53).

PrP^C contains two N-linked glycosylation sites (Asn181IleThr and Asn197PheThr of human PrP; asparagine residues 180 and 196 of mouse PrP) (see **Figure 1.2A**). Glycosylation occurs as PrP is processed in the golgi, where neither, either or both sites can be modified with carbohydrate. Studies on purified hamster PrP^C and PrP^{Sc} show that there are at least 50 different sugar chains that can be attached to the glycosylation sites, with an increase of bi- tri- and tetra-antennary complex sugar chains in PrP^{Sc} (54-57). Finally a disulphide bond is formed between two cysteine residues (178 and 213 in mouse PrP) near the C-terminus, situated either side of the glycosylation sites (see **Figure 1.2A**).

Analysis of secondary and tertiary structures of PrP by nuclear magnetic resonance (NMR) using rPrP (58-65) and purified bovine PrP^C (66) have shown that PrP^C structure is highly conserved amongst mammalian and other species. The C-terminal portion of the protein is structured and shown to have 3 α-helices and a short anti parallel β-sheet. Crystal structure analysis confirmed these PrP folds using ovine PrP (67;68) and a human PrP dimer (69). The structural features of mouse PrP, representative of all mammalian PrP's, is shown in **Figure 1.2A** and a 3D structural model based on work using mouse rPrP (58) showing all the post-translational modifications is shown in **Figure 1.2B** (61).

Figure 1.2: Cellular processing of mouse PrP and 3D structural model

(**A**) Representative diagram showing the processing of PrP from its genetic transcript to the primary protein sequence. Known post translational modifications including N-terminal cleavage of a signal peptide, C-terminal attachment of a GPI anchor, formation of a disulphide bond and N-linked glycosylation are shown together with regions of known secondary structure. (**B**) 3D structure derived from data determined by NMR of recombinant mouse PrP^{21-231} (61) shows the positions of the post translational modifications and α-helix and β-sheet secondary structure. Globular structure of the protein shown in red with the 3 α-helices, glycosylations at 180 and 196 shown in blue, disulphide bond shown in yellow and GPI anchor in gold.

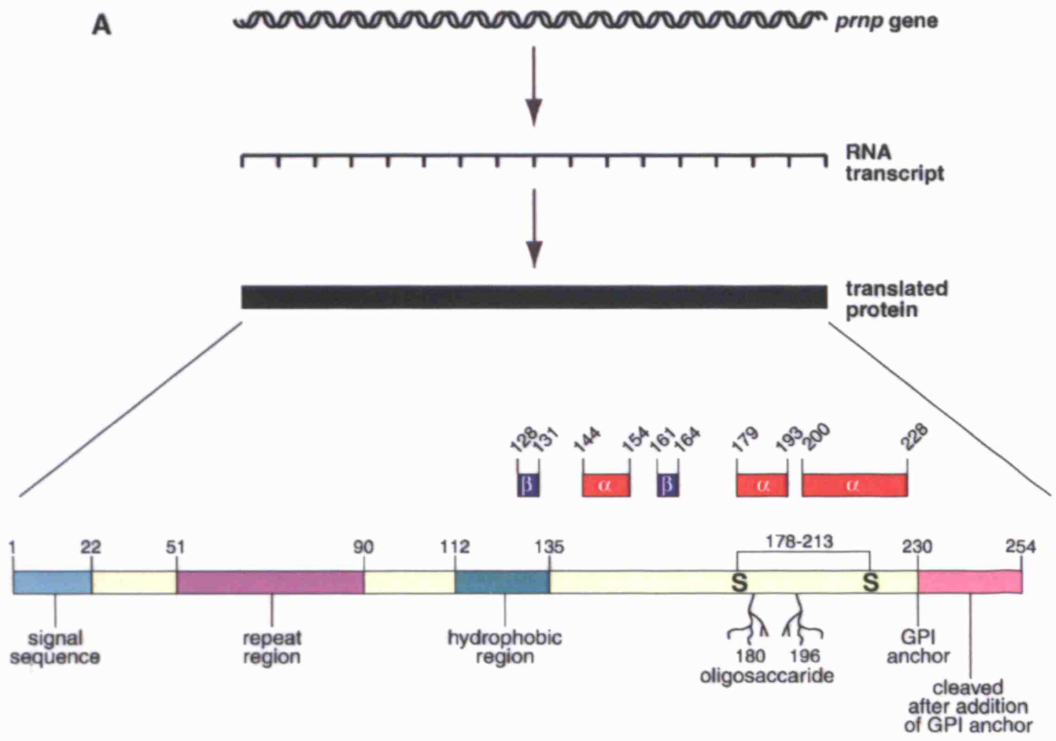
A
prnp gene
RNA transcript
translated protein
128 131 144 154 161 164 179 193 200 228
β α β α α
1 22 51 90 112 135 178-213 230 254
S S
signal sequence
repeat region
hydrophobic region
180 196 oligosaccaride
GPI anchor
cleaved after addition of GPI anchor

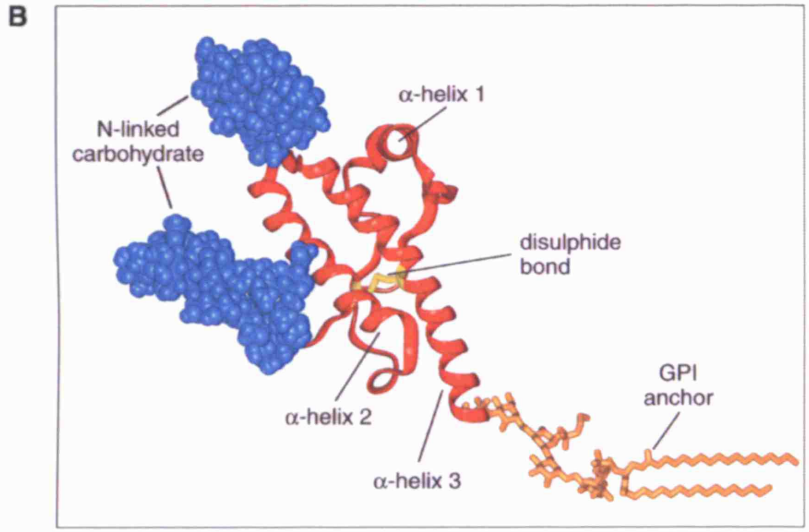
B
α-helix 1
N-linked carbohydrate
disulphide bond
GPI anchor
α-helix 2
α-helix 3

1.2.2 Properties of PrP

N-terminus

Although the structure of the C-terminal globular domain has been characterised for PrP^C, studies have failed to determine a structure for the N-terminal third of the protein. However, the N-terminus is the most highly conserved region of the prion protein and contains a unique sequence motif comprising octapeptide repeats suggesting that it might be involved in the cellular function of PrP^C. The repeat contains amino acids PHGGGWGQ which is preceded by 2 copies of a 6 amino acid sequence GG(S/N)RYP. The copy numbers vary slightly in different species (see **Figure 1.1**), for example mouse PrP has 5 repeats, while human PrP has a nonapeptide followed by 4 octapeptide repeats. This region is flexible and preceded by a region of basic amino acids suggesting a region of concentrated positive charge. The octapeptide repeats are known to bind Cu^{2+} and Zn^{2+} ions with high affinity and could be structured upon binding such transition metals, suggesting a possible role in regulation or signalling of the ions (61;70-73). A role for Cu^{2+} ions has been implicated in PrP^C function involving movement out of lipid rafts (74;75). Mutations of the N-terminus of PrP are known to cause inherited prion disease suggesting that it is important in some conformations of PrP^{Sc} and/or disease manifestation (76-80).

Hydrophobic domain

A 24 amino acid region between 112 and 135 is hydrophobic (see **Figures 1.1** and **1.2A**) and also highly conserved in mammalian PrP. Research showing that PrP^C can be released from cell membranes by PIPLC indicates that this region does not serve as a transmembrane domain at the cell surface (48). However, in synthetic systems it has been shown that peptides from this region can span membranes and this could occur as part of PrP^C function during cellular trafficking (81;82). Small PrP peptides that cover the

hydrophobic region have been refolded under differing conditions to generate conformations that can induce apoptosis and to form amyloid fibrils suggesting it could also be an important part of an infectious prion (83-86).

Codon 129 polymorphism

A variety of mutations have been found in the human PrP gene that cause inherited prion disease (discussed in **Section 1.3.2**) and such mutations and non-pathogenic polymorphisms are of structural interest in their role in determining PrP^{Sc} conformation. A polymorphism of the prion protein at codon 129, coding for either a methionine (M) or a valine (V), which was originally mistaken for a pathogenic mutation was found not to be linked to disease (87) but still has a great impact on human prion disease. 51 % of the Caucasian population are MV heterozygotes, 37 % MM homozygotes and 12 % are VV homozygotes (88;89). Homozygosity gives a predisposition to some forms of human prion disease, iatrogenic and sporadic CJD patients and those who have developed kuru predominantly have either MM or VV alleles, rarely MV (88;90-92) and in the case of variant CJD, so far, only MM alleles (77). Studies have shown that there is little difference between the folding and stability of each polymorph in the PrP^{C} fold but rPrP with methionine at codon 129 has a greater propensity to aggregate and form fibrils (65;93-95).

Conformational differences of PrP^{C} and PrP^{Sc}

Native conformational studies have been hindered by the insolubility of PrP^{Sc} and the low quantities of PrP^{C} available. Work investigating PrP from different species and prion strains using Fourier transform infrared spectroscopy and circular dichroism (CD) have shown that in contrast to PrP^{C} with a predominantly α-helical structure, PrP^{Sc} had a higher amount of β-sheet (96;97) that can differ in PrP associated with different prion strains (98-101).

PrP^{Sc} deposits in brain tissues have been observed to have varying size and morphology including amyloid plaques. Although no evidence has shown fibrils in human prion disease (102), structured fibrils have been synthesised using recombinant PrP material (93;103) giving an insight to prion conformations.

With the exception of Cu^{2+} ion binding (74;75), studies investigating PrP^{C} interacting molecules have yet to identify any candidate with unequivocal *in vivo* relevance (reviewed in (104)). There has also been no reported evidence for any PrP^{Sc} co-factors directly influencing prion infectivity.

1.2.3 PrP folding and infectious conformations

Studies have looked at PrP conformation and the change in structure from a native fold to one resembling that of PrP^{Sc}. Recombinant PrP expressed in *Escherischia coli* has provided PrP for most of the structural studies and attempts to fold rPrP into conformations resembling either PrP^{C} or PrP^{Sc} has been achieved by several methods in different groups (93;94;105-107). Jackson et al showed that rPrP can adopt the predominantly α-helical conformation with an intact disulphide bond resembling a PrP^{C}-like structure by refolding at neutral pH without reducing conditions (94). Conditions for refolding PrP into a β-sheet conformation involved low pH and reducing agents. These studies have produced informative data on PrP (94;106;108) including increased PrP resistance to PK digestion (109). Studies by Jackson et al have shown that inoculation of α-helical refolded rPrP into $Prnp^{0/0}$ mice generated antibodies with specific affinity towards PrP^{C} whereas inoculation with β-sheet refolded rPrP generated antibodies with affinity for PrP^{Sc} (110) thus confirming highly distinct conformations of PrP generated under the different refolding conditions. Oxidising conditions leading to the formation of a β-sheet conformation of PrP with an intact disulphide bond has also been reported (93;111).

Studying PrP pathways of folding and equilibrium states can give important information as to the possible mechanisms by which PrP^{C} can be converted into PrP^{Sc}. By titrating in a denaturant, unfolding of PrP can be observed to see if there are any intermediate equilibrium states. Several studies have shown that PrP in an α-helical form needs to unfold before refolding to a β-sheet form, by using denaturants such as GuHCl (94) or urea (108;112). The structured C-terminal domain of PrP folds and unfolds reversibly in response to chaotropic denaturants and it appears that there are no equilibrium intermediates (61;113) or kinetic intermediates (114) in the folding reaction and that PrP displays unusually rapid rates of folding and unfolding. These data suggest that PrP^{Sc} is unlikely to be formed from a kinetic folding intermediate, as has been hypothesised in the case of amyloid formation in other systems, and is more likely to be formed from the unfolded state of PrP (reviewed in (115;116)). These studies have given further insight to the conversion of PrP^{C} into PrP^{Sc} whereby native PrP^{C} must adopt an unfolded state before conversion. How this conformational change occurs and if any other molecules are needed for the conversion is still unknown.

As well as conformational studies, attempts have been made to reconstitute infectivity, or at least gain PrP^{Sc}-like properties, from previously uninfectious PrP, either rPrP, PrP^{C} or denatured PrP^{Sc}. Dilution from denaturants such as urea, GuHCl and SDS failed to reconstitute infectivity of isolated denatured PrP in buffer lacking or containing phospholipids (117). Other researchers have shown that Cu^{2+} ions convert PrP to a PrP^{Sc} like structure with marginal PK resistance (118-122). Other studies with Zn^{2+} ions have shown effects on increased PrP aggregation, trafficking and protease resistance (72;73). Other transition metals such as Mn^{2+} has been shown to induce aggregation (123) and Co^{2+} and Ni^{2+} ions are shown to increase protease resistance (72).

Recently, a β-sheet conformation of PrP with intact disulphide bond has been shown to generate PrP fibrils and these preparations cause disease in PrP overexpressing mice (124;125). This is a tremendous breakthrough in the prion field supporting the protein only

hypothesis. However, affected animals had a prolonged incubation period near their lifespan indicating an extremely low infectious prion titre. Thus the nature of the infectious PrP isoform remains unknown (126). Whether another factor is required for prion disease is still unknown, and such studies are complicated by the possibility that such factors may be acquired *in vivo* post-inoculation.

1.2.4 Models of PrP^{Sc} replication

Conformational studies on PrP have sought to establish disease associated structural properties and in particular how the conformation of PrP^{Sc} arises and what structural properties of PrP^{Sc} confer prion infectivity. To examine PrP replication based on methods of increased protease resistant PrP (PrP^{RES}) and to see if a cellular processing system is required, differing models have been used. An *in vitro* amplification model was first shown in 1994, by radiolabelling PrP^{C} to prove *de novo* production of PrP^{Sc} using a PrP^{Sc} seed (127). This method was used to look at transmision barriers in replacement to bioassay (128-130) and could also be used to screen for therapeutics (131-133). However, these methods for conversion were extremely inefficient and such a large proportion of PrP^{Sc} seed was required that correlation of increases in specific infectious titre due to *de-novo* generated material was impossible (134).

Further attempts at *in vitro* amplification systems, now termed protein misfolding cyclic amplification (PMCA), have improved on amplification (135;136) and more recently infectivity (137). Steps include dissociation of aggregates by sonication to produce aggregate seeds for amplification (138;139). Such studies show that the generation of infectious material can occur without a cellular processing system.

Cell lines have also been developed to look at propagation of PrP^{Sc} or protease resistant PrP, including rat PC12 cells (140), murine N2a cells (141) and human GT1 cells (142).

Thought to be more representative of an *in vivo* situation compared to a PMCA system and could be used for analysing disease propagation and therapeutic targets. Cell based models are now as sensitive as bioassay and can replace bioassays in some cases, with the caveat of only replicating certain strains (143;144).

1.2.5 Disease propagation and neurotoxicity

Studies have also investigated how neurotoxicity is caused and to look at preventing disease with potential therapeutic compounds. It is still unknown how PrP^{Sc} replicates in cells, and furthermore how this replication procedure causes neurotoxicity and disease. As stated above, several studies have shown that for PrP to convert from an α-helical form to a β-sheet form, the structure needs to unfold. The rapid rate of refolding suggests that PrP fluctuates between a dominant native state, PrP^{C}, and a series of minor conformations (113). A proportion of these minor conformations are thought to self-associate in an ordered manner to produce an infectious PrP^{Sc} seed, composed of misfolded PrP monomers. Evidence so far supports this as studies have shown that the number of PrP^{Sc} molecules needed per infectious unit is between 1000 and 4000 molecules (145;146) and that oligomers comprising of 14-28 units of PrP^{Sc} are thought to be the most infectious (147). These PrP^{Sc} oligomers are thought to increase during disease and seed other PrP aggregation processes by recruiting other misfolded PrP monomers (see **Figure 1.3**). This mechanism could underlie prion propagation and would account for the transmitted, sporadic and inherited aetiologies of prion disease.

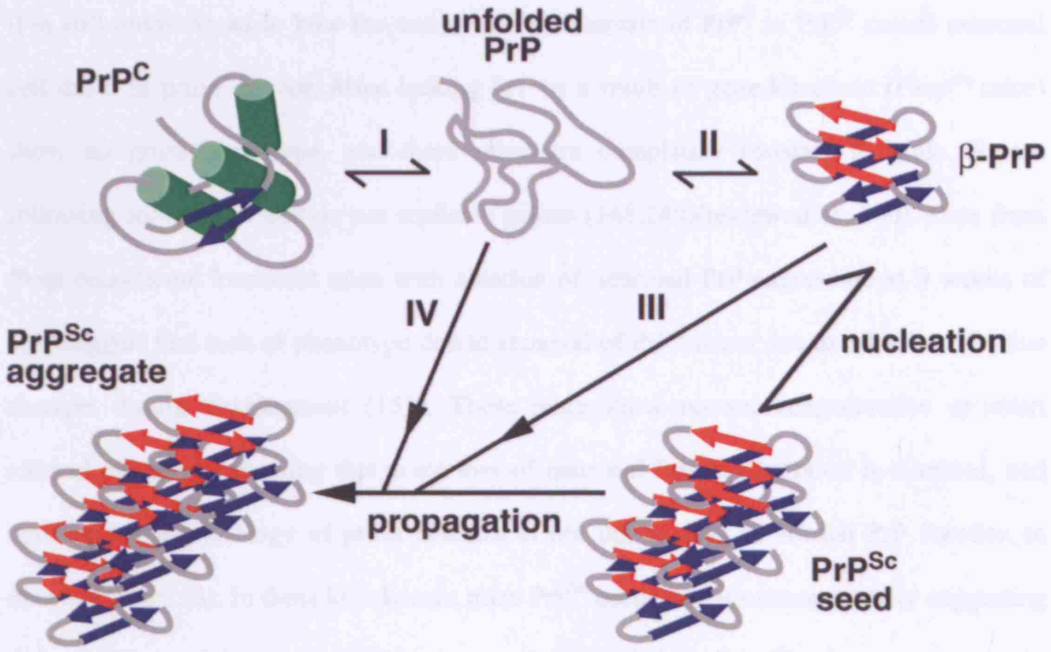

Figure 1.3: Theoretical model of prion disease propagation

Adapted from Collinge (115). The normal cellular isoform of prion protein, PrP^{C}, is rich in α-helix (green cylinders) and can be reversibly interconverted **(I,II)** to a β-sheet-rich (arrows) conformation, β-PrP. β-PrP has an increased propensity to aggregate, and the formation of a crucial seed size leads to essentially irreversible propagation of the disease-related isoform of the prion protein, PrP^{Sc}, through the recruitment of further β-PrP monomers **(III)** or unfolded PrP **(IV)**. Subsequent mechanical breakage or cleavage of elongating fibrils would lead to an exponential rise in prion titre. Such a model can accommodate the different aetiologies of human prion diseases; prion propagation might be initiated by the introduction of a seed (acquired prion disease); by spontaneous seed production as a rare stochastically mediated event that involves wild-type PrP (sporadic prion disease); or as an essentially inevitable event with PrP that contains a pathogenic mutation (inherited prion disease). Following such initiating events, the process of propagation is driven thermodynamically by intermolecular association.

It is still unknown as to how the conversion mechanism of PrP^{C} to PrP^{Sc} causes neuronal cell death in prion disease. Mice lacking PrP as a result of gene knockout (*Prnp*$^{o/o}$ mice) show no gross phenotype, and these mice are completely resistant to prion disease following inoculation and do not replicate prions (148;149)(reviewed in (150). Data from *Prnp* conditional knockout mice with ablation of neuronal PrP expression at 9 weeks of age, suggest that lack of phenotype due to removal of PrP^{C} is not due to effective adaptive changes during development (151). These mice show no neurodegeneration or overt clinical phenotype showing that acute loss of neuronal PrP in adulthood is tolerated, and that the pathophysiology of prion diseases is not due to loss of normal PrP function in neurons (152;153). In these knockdown mice PrP^{Sc} accumulates extraneuronally suggesting that specific toxicity occurs within neurones (152). While *Prnp*$^{o/o}$ mice are completely resistant to prion infection, reconstitution of such mice with PrP transgenes restores susceptibility to prion infection in a species-specific manner and allows a reverse genetics approach to study structure-function relationships in PrP, (for review see (150;154)). The importance of the location of PrP^{C} in prion disease is also shown with transgenic mice lacking the GPI anchor (52). These mice accumulated abnormal PrP deposits after inoculation with prions but did not succumb to prion disease. The cummulation of these data indicate that PrP^{Sc} or an intermediate species has a toxic gain of function which is also mediated by the location of the toxic species causing cell death.

Cell death is thought to occur via an apoptotic mechanism (155-157) and a variety of studies have investigated how apoptosis occurs in prion disease. PrP^{Sc} (158) or shorter PrP peptide fragments (83) have shown toxicity *in vitro*, suggesting a toxic gain of function of PrP^{Sc}. Other studies have suggested that a toxic gain of function is due to altered trafficking of PrP^{C} (159;160). Studies analysing the basis of neuronal toxicity have shown proteasome impairment with either PrP^{C} (159;160) or PrP^{Sc} (157). The latter study gave convincing evidence for the role of compartmentalised cytosolic PrP^{Sc} aggregesomes causing apoptosis via a caspase-dependent mechanism (157). A role of the ubiquitin-proteasome system has

also been implicated in other neurodegenerative diseases such as Huntington's disease, Parkinson's disease and Alzheimer's disease (161). Aggregated proteins are inefficiently degraded via the proteosome (162) and in some cases actually impair proteasome function in cell models (163). Aggregated proteins impairing proteasome function to cause cell death via apoptosis has not been unequivocally proven in any given neurodegenerative disease, but studies lean towards this as a possible mechanism in prion disease. Further studies may show exactly how PrP^{Sc} aggresomes cause apoptosis via the ubiquitin-proteasome system and enable identification of the toxic PrP species in prion disease.

1.3 Clinical characterisation of prion diseases

Prion diseases of humans and animals present with a wide variety of clinical symptoms. Clinical pathology includes spongiosis, astrocytosis and amyloid deposition. Amyloid deposits can be labelled with antibodies that recognise the prion protein. How the highly conserved prion protein fits in to disease propagation to present such diverse clinical symptoms remains unknown. But the clinical characterisation has given insight to prion strain differences and disease aetiology.

1.3.1 Animal prion diseases

An animal TSE was first seen in Europe in the 18th century with what was described as "scrapie" in sheep. Despite not being shown to be transmissible until the 20th century it was widely believed that flocks could be infected and the matter was of such economic importance that it was brought to the House of Commons (164). Since then, prion disease has been seen in a variety of other animals.

Scrapie

This disease of sheep was called "scrapie", due to the predominant symptom of sheep scraping themselves against field posts, and is still one of the names for prion disease today (165). This disease was investigated by veterinarians subsequently in the 19th century who showed that neuronal vacuolation was a characteristic feature (166). The transmissibility of scrapie infection was also attempted in the 19th century, with no success. However, initial negative results were likely due to the failure to recognise a long incubation period. The first transmission experiment was in 1936 showing a long incubation period of 14-22 months to clinical symptoms dependent on route of transmission (167). The transmissibility

of the agent was further confirmed after an outbreak that was connected to a vaccine prepared with sheep brain, spinal cord and spleen (168). It was subsequently shown that this transmissibility could cross the species barrier to laboratory mice (11) but has never been shown to pose a risk to human health (169) (reviewed in (165)).

Chronic Wasting Disease

Chronic wasting disease (CWD) is a TSE that affects elk and deer in the US and Canada. Originally seen in captive animals in the 1960's, is now found in wild populations of deer in certain areas of Wyoming and Colorado. Wild elk are also seen to be affected but not as common (170-173). It is still unknown as to the origin of this disease or the transmission as prions have not been found in the environment from either faeces or vegetation surrounding infected carcasses (174). It is likely that environmental prions are the infectious source but at levels below detection, as studies have shown that although deer forage near infected carcasses, they did not consume infected tissues (174).

Transmissible Mink Encephalopathy

Transmissible mink encephalopathy (TME) is believed to be an acquired disease. It is thought to originate from scrapie infected sheep or TSE infected cattle in feeds (175). Although after experimental evidence showing transmission to hamsters,TME is thought not to be related to BSE in cattle (176) aside from one farming source (177).

Bovine Spongiform Encephalopathy

Bovine spongiform encephalopathy (BSE) is probably the most widely known of the animal TSE's occurring as an epidemic in the UK in the early 1990's. BSE is an acquired disease spread by infected tissues from BSE positive cattle. It is however, unknown as to whether the origin was via feeds containing sheep scrapie or an unrecognised bovine TSE (178). It is estimated that over a million cows were affected with BSE although only 170,000 were seen to develop clinical disease (179;180). Epidemic proportions were reached by the reprocessing of bovine carcasses into cattle feed, instead of discarding infected cattle material. Despite the knowledge of the transmissibility of the agent, it was 1989 before a change in handling of bovine offals and prevention of processing into various food chains was proposed (181). Due to a species barrier effect (182) it was thought that BSE wouldn't be a risk to human health. However a new prion disease of humans "variant CJD" (vCJD) was seen in the 1990's which was found to be causally linked to the BSE epidemic (183-187).

BSE has since been seen in other European countries, the United States, Canada and Japan (188-192). Other animals have been shown to develop TSE from contaminated feeds including, other bovines, nyala, greater kudu, cheetahs, oryx, puma and domestic cats (193-195) showing the prevelance of this prion strain.

1.3.2 Human prion diseases

Human prion diseases can be sporadic, inherited or acquired and have many different clinical and pathological features. Unlike animals, where prion disease isn't known to be inherited, human inherited forms provide strong evidence for the protein only hypothesis and the role of PrP^C in disease.

Sporadic/classical CJD

The human prion disease, Creutzfeldt-Jakob disease (CJD) was first documented in the 1920's (196-198). Today classical or sporadic CJD (sCJD) clinically affects 1 in 1,000,000 worldwide (199) with a mean age of onset between 55-60 years. It is recognised by rapid neurological degeneration after onset and a clinical duration much shorter than other neurodegenerative diseases. Most patients die within 12 months (200), but 10 % of cases have a longer duration of 2 years (201).

Clinical symptoms begin with dementia, followed by movement disorders, and death is usually by systemic infection (202). Most cases have the predominant symptom of cognitive impairment, but about 10 % present with cerebellar ataxia (202;203). Other subsets include patients with Heidenhain's CJD whom develop cortical blindness (204) and a panencephalopathic variant seen in Japan that also shows degeneration of cerebral white matter as well as spongiosis of grey matter (202;203). For 70 % of cases, electroencephalogram (EEG) readings show a periodic synchronous discharge in a disease specific pattern of periodic triphasic waves at 1-2 cycles, a symptom not seen in other forms of CJD. Magnetic resonance imaging (MRI) also shows signal changes in basal ganglia, although may not be seen in all cases (205).

Definitive diagnosis of sporadic CJD, however, is by post mortem or brain biopsy for neuropathalogical confirmation of abnormal PrP deposition and spongiform encephalopathy. Pathological findings also show astrocytosis and loss of neurones. Recent diagnostic tests include elevated levels of protein 14-3-3 in the cerebral spinal fluid (CSF) (206;207).

Inherited prion disease

Familial forms of TSE are caused by autosomal dominant mutations of the *PRNP* gene located on chromosome 20 (208;209) and substantiate the protein only hypothesis of prion propagation. Syndromes classified prior to the discovery of PrP and the *PRNP* gene include Gerstmann-Sträussler-Scheinker syndrome (GSS), fatal familial insomnia (FFI) and familial CJD (fCJD) (reviewed in (77;210)). Clinical symptoms and pathology differ depending on the type of mutation involved. Variation in clinical symptoms also occurs even within the same mutation of PrP (80;211-213). Inherited prion disease comprises 10-15 % of CJD cases and pathogenic mutations include point mutations which can result in an amino acid change or stop codon, and octapeptide repeat insertions (OPRI) (77;80;214) or a 2 repeat deletion (215). Over 30 mutations are known to cause inherited prion disease (see **Figure 1.4**). Some are associated with one particular clinical classification and others with a varying spectrum showing that although amino acid sequence has great importance on pathogenic PrP^{Sc} conformations, other factors may be involved in determining phenotype. Although the classification of the different syndromes are still used, since the discovery of prion disease genetics the lines between them are no longer well defined (77).

The most common familial CJD, fCJD, mutation is E200K but others include; OPRI, D178N, E196K, and T183A. Even though there are variations between the familial cases, on average there is an earlier onset and longer disease duration than with sporadic CJD (216-220). Symptoms are generally the same as sporadic CJD but some cases have atypical phenotypes (221-224). PrP staining of the brain can be varied with differing mutations including number of OPRI repeats and also with the same mutation and differences in codon 129 polymorphism (225-227). Spongiform encephalopathy may also be absent (224;228).

GSS is different from fCJD by predominance of chronic cerebellar ataxia, a longer clinical duration and the presence of large amyloid plaques (42). The most common mutation in

GSS is P102L (208;213;229). Other mutations include P105L (230), A117V (231), F198S (232), A117V, Y145X, H187R, G131V and D178N. There is varying phenotype, disease onset and duration dependent on mutation.

FFI can be sporadic (called sporadic fatal insomnia - sFI) but is mainly found as an inherited autosomal dominant disorder (233;234). The most common mutation is D178N (235-237) but E200K has also been found (238;239). Methionine homozygosity at codon 129 has shown to have an association with an FFI phenotype with D178N mutation whereas valine homozygosity at codon 129 is more likely to have a fCJD phenotype (240). Symptoms are very different to other forms of CJD, insomnia as the name suggests, being the main clinical feature. Pathology is also different, spongiosis and PrP deposition is limited, and neuronal loss is located in the thalamus. It is classified as a TSE due to its transmissibility (241) and mutation of the *PRNP* gene.

The varying phenotypes of inherited prion disease show that small changes in specific amino acids can have different disease causing effects. The knowledge of differing phenotypes within cases of the same mutation complicates this matter further and a detailed understanding of the physicochemical characteristics of PrP^{Sc} is needed to explain disease associated conformational changes with differing mutations (76;202;213).

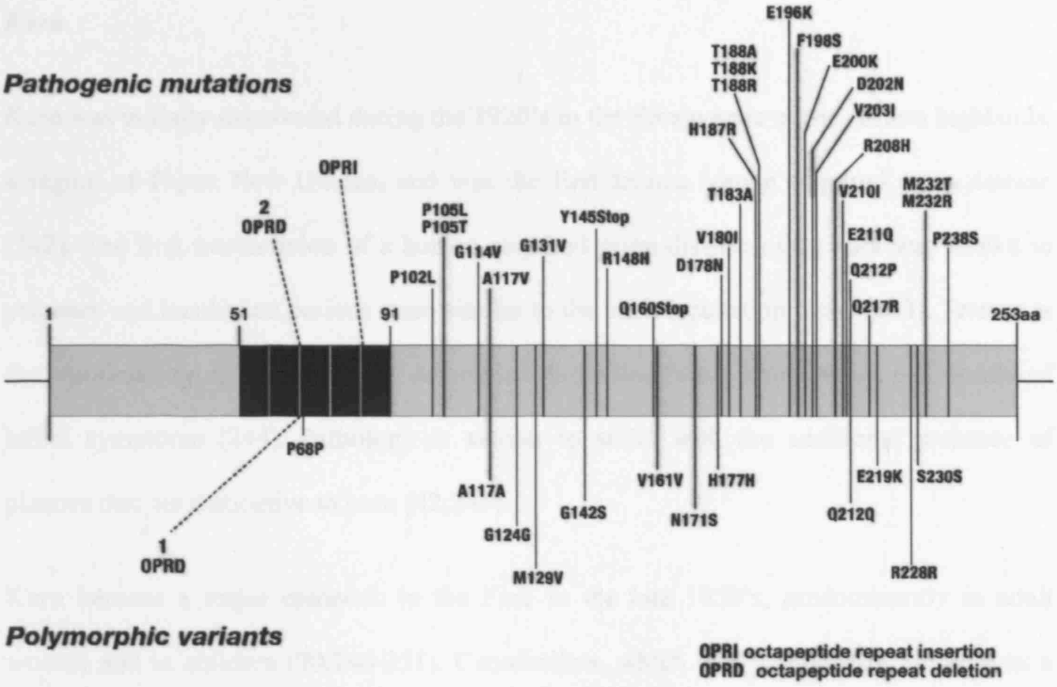

Figure 1.4: Pathogenic mutations and polymorphic variants of human PrP

Adapted from (77). Definite or suspected pathogenic mutations are shown above the representation of the prion protein. Neutral or prion disease susceptibility/modifying polymorphisms are shown below.

Kuru

Kuru was initially discovered during the 1920's in the Fore people of the eastern highlands, a region of Papua New Guinea, and was the first known human acquired prion disease (242). The first transmission of a human acquired prion disease using kuru was shown in primates and incubation periods were similar to the kuru incubation times (243). Tremor is the prominent symptom of disease, dementia follows and death occurs within 6-9 months of initial symptoms (244). Pathology is similar to sCJD with the additional presence of plaques that are distinctive to kuru (42;245).

Kuru became a major epidemic in the Fore in the late 1950's, predominantly in adult women and in children (90;246-251). Cannibalism, which was practiced in the Fore as a ritual for the deceased, is the cause of kuru (90). Cannibalism was banned by the Australian government in the late 1950's and since then there has been no cases of kuru in individuals born after the ban and the number of cases have now declined to almost zero (90). Kuru has a mean incubation of around 12 years providing interesting data on an acquired human prion disease epidemic (181). Susceptibility has been shown with the codon 129 polymorphism. The MM genotype has been shown to have the shortest incubation period (252), with the youngest reported case of 4-5 years (90). VV genotypes have longer incubation times, and MV heterozygotes reported to have incubation times in excess of 50 years (88;90). Kuru imposed a strong balancing selection on the Fore population essentially eliminating *PRNP* 129 homozygotes. Elderly survivors of the kuru epidemic, who had multiple exposures at mortuary feasts are, in marked contrast to younger unexposed Fore, predominantly *PRNP* 129 heterozygotes. Worldwide *PRNP* haplotype diversity and coding allele frequencies suggest that kuru-like epidemics imposed a strong balancing selection at this locus during the evolution of modern humans (88;90).

Variant CJD

Variant CJD, causally linked to the BSE strain of prion disease, has different clinical symptoms to classical CJD including earler age of onset and a prolonged clinical duration of up to 2 years (183;253). Clinical features include behavioural and psychiatric disturbances, early features being dysphoria, withdrawal, anxiety, insomnia, and apathy. Neurological features develop 4 months into the disease and include loss of memory, pain, unsteady gait, and even later in disease, more common features seen are the cerebellar signs such as myoclonus, chorea, dystonia, some upper motor neurone signs and visual impairment (254). Elevation of protein 14-3-3 in CSF, seen in sCJD, is not often seen in vCJD and cannot be used as a marker for disease (255). Also the EEG differences seen in sCJD are not seen in vCJD. However, MRI is helpful, showing a high signal in the posterior thalamus (256). Pathological differences include the presence of amyloid plaques that are surrounded by vacuoles giving a "florid" appearance, similar to what is seen in kuru.

The difference to classical CJD gave it the term "variant" and studies subsequently showed the strong association between the new variant of CJD and the BSE strain (184-186;257). Based on these data it is now thought that exposure of BSE infected bovine products to humans caused this new strain. The genetic phenotype of those who have developed clinical disease with new variant CJD have been homozygous M/M at codon 129 of the *PRNP* gene (258). Iatrogenic transmission to a codon 129 heterozygote occurred after a blood transfusion from an asymptomatic variant CJD carrier, however this person did not develop clinical disease and subclinical PrP^{Sc} was only discovered after the person died of other causes (259). Overall, susceptibility to disease with a homozygous phenotype is clear, having been shown in other forms of CJD, such as kuru (77;252). To date there are 159 cases of vCJD mainly in the UK and it is currently impossible to predict the amount of future cases. The peak exposure to humans of BSE was in 1992-1993 and suggests that the

proportion of the population exposed is far greater than those who have developed clinical disease so far (www.cjd.ed.ac.uk) (90;115).

1.4 Prion strains and transmission barriers

With the knowledge that there are multiple disease aetiologies, the role of PrP^{Sc} in disease seems complex if it is the sole infectious agent. In the non-experimental TSE's, there are multiple non-prion related genetic and environmental factors that may contribute to disease aetiology. However, prion strains are defined as distinct PrP^{Sc} isolates that can be serially passaged in genetically identical inbred mice, producing distinct incubation times, and neuropathology. These findings show that even with no other genetic or environmental factors multiple prion disease phenotypes exist (260). Prion strains have been difficult to accommodate within the protein only model of prion propagation and the protein-only hypothesis has to postulate multiple stable PrP^{Sc} conformations, assembly states, or other post-translational modifications which can be "transmitted" to PrP in host species. There is considerable evidence ruling out the involvement of a nucleic acid (145;261-263), although in 1991 Charles Weissmann posed the "unified theory" that it may be possible that small nucleic acids are associated with the infectious agent to encode strains (264). However, to date, no evidence exists for co-factors associated with PrP^{Sc} encoding strain specific properties and therefore it is likely that the structural properties of PrP^{Sc} alone encode strains (5).

Evidence for distinct PrP^{Sc} conformations encoding prion strain properties was first seen after passage of mink TME into hamsters (101;265;266). In these transmissions two distinct pathological phenotypes were observed termed hyper (HY) and drowsy (DY). The DY phenotype retained its ability to cause disease in mink whereas the HY phenotype lost pathogenicity in mink. The HY phenotype was similar to the Sc237 hamster prion strain with a similar short incubation time whereas the DY phenotype has distinct neuropathology and longer incubation time (266). It was concluded that the DY isoform was the predominant mink TME isoform which could be passaged in hamsters with distinct transmission barrier, whereas the HY isoform was a minor component of TME not observed in mink but had a greater pathogenicity in hamsters (265). Although the DY

isoform is not stable on serial passage in hamsters (267), analysis of PrP^{Sc} in these transmissions showed distinct physicochemical properties. Following limited proteolysis, PrP^{Sc} associated with the HY and DY phenotype showed distinct migration patterns of PrP^{Sc} by immunoblotting that relate to different N-terminal ends of HY and DY PrP^{Sc} following protease treatment implying differing conformations of HY and DY PrP^{Sc} (101;266). These findings established PrP^{Sc} conformation as a basis of prion strain diversity.

Other PrP^{Sc} structural properties that may determine prion strain characteristics include the differences in GPI anchor, glycosylation or other as yet undetected post-translational modifications. Post-translational modifications could determine PrP conformations that encode strains or have strain specific effects directly, by influencing cellular targetting or prevention of PrP clearance from particular cells. As multiple PrP conformations are possible from one amino acid sequence (113), a further understanding of how one conformation is preferentially stabilised over another is needed. Knowledge of PrP^{Sc} structural properties will enable a detailed understanding of potential strain specific changes in PrP that may encode distinct disease phenotypes.

The role of the GPI anchor has been shown to be important in disease as transgenic mice lacking the GPI anchor are resistant to clinical prion disease yet accumulate abnormal PrP in amyloid plaques (52). It is known that the GPI anchor is readily cleaved by PIPLC in PrP^{C} but not in PrP^{Sc} (48-50) but little is known of the involvement of the GPI anchor in disease propagation and prion strains. There could be important differences in the GPI anchor of different prion strains involved in membrane localisation and therefore disease aetiologies.

The role of glycosylation in the formation of prion strains and disease propagation is still mostly unknown, and studies are contradictory (reviewed in (268)). *In vitro* experiments have shown that unglycosylated PrP is preferentially converted into protease resistant PrP

(269). However glycosylated PrP^{Sc} has shown to have stronger efficiency in crossing transmission barriers (270). Glycan effects could be due to shielding the protein from enzymatic cleavage or targeting of PrP^{Sc} in cells (56;271). In general most strains show similarity in their glycosylation pattern after crossing a species barrier. The BSE strain maintains is strain characteristics of PrP^{Sc} after transmission to humans and vCJD, shows a different glycosylation pattern to other human CJD types (76;272). PrP^{Sc} glycoforms associated with sporadic and iatroigenic CJD are predominantly monoglycosylated, whereas PrP^{Sc} in vCJD is predominantly diglycosylated, and this is one of the characteristics that showed that vCJD was caused by BSE transmission (184).

Prion strain dependence on PrP conformation has been substantiated by a study using an immunoaffinity assay (273). The assay looked at the affinity of different strains, passaged in Syrian hamsters, to bind to the same anti-PrP antibody, 3F4 (274). 3F4 is an IgG_{2a} and binds to hamster, human and feline primary sequences reacting with epitope 104-113 which is unstructured in PrP^{C}. As N-terminal epitopes are known to not be recognised after conversion into PrP^{Sc} (275) the structure specific recognition could be exploited to analyse conformation between the strains. Each strain showed a unique binding pattern to the antibody under different conditions that would change conformation.

1.4.1 Human PrP^{Sc} types

As the prion diseases of humans are seen on differing genetic and environmental backgrounds, their classification is segregated into types rather than defined as strains as in genetically identical mice. However, the principle of differing PrP^{Sc} isoforms is the same. PrP^{Sc} types, encompassing sporadic, inherited and acquired forms of human prion disease, are classified by their disease aetiologies and fragment sizes of PrP^{Sc} on SDS-PAGE after digestion samples using PK. These different types are known to roughly correlate with disease aetiology (type 4 associated with vCJD only) and amino acid sequence as evidence

by mutations in inherited prion disease and segregation of PrP^{Sc} types with codon 129 polymorphism. However, further knowledge of properties associated with human PrP^{Sc} types is needed to fully correlate these with disease aetiology. Also, knowledge of other genetic and environmental factors that could be related to disease aetiology may provide further information on specific prion infectivity and susceptibility to disease (276;277).

The N-terminus of the prion protein is unstructured in PrP^{C} and the conformational differences in the N-terminal cleavage sites of the human PrP^{Sc} types a matter of interest as the amino acid sequence of all is identical, with the exception of some of the mutants in inherited prion diseases. As to what causes the conformational rearrangement of the protease resitant core of the human PrP^{Sc} types is unknown. Four major human PrP^{Sc} types are associated with sporadic and acquired human prion diseases, these isofoms are differentiated on immunoblots after limited proteinase K digestion of brain homogenates (272;278;279). PrP^{Sc} types 1-3 are seen in classical (sporadic or iatrogenic) CJD brain, while type 4 PrP^{Sc} is uniquely seen in vCJD brain (272;278;279). However, this knowledge of PrP^{Sc} isoforms is further complicated by different classifications of the human PrP^{Sc} types in different laboratories. An earlier classification of PrP^{Sc} types seen in classical CJD described only two banding patterns (280) with PrP^{Sc} types 1 and 2 that is described by Hill et al corresponding with the type 1 pattern of Gambetti et al, and the type 3 fragment size described by Hill et al corresponding to the type 2 pattern of Gambetti et al (279;281;282). While type 4 PrP^{Sc} is readily distinguished from the PrP^{Sc} types seen in classical CJD by a predominance of the di-glycosylated PrP glycoform, type 4 PrP^{Sc} also has a distinct proteolytic fragment size (272) although this is not recognized by the alternative classification which designates type 4 PrP^{Sc} as type 2b (281). Hill et al also reported that a single case of sporadic CJD is associated with type 6 PrP^{Sc} (type 5, observed only in experimental transmissions, see **Section 1.4.2** and **Figures 1.6** and **1.7**) indicating that further heterogeneity is possible (272). Codon 129 polymorphism constrains the propagation of distinct PrP^{Sc} conformers and glycoforms in sporadic and acquired CJD (see

Figure 1.5A). Further diversity in PrP^{Sc} is observed in inherited prion disease (76;213). Cases of inherited prion disease caused by point mutations in the *PRNP* gene show glycoform ratios distinct from those observed in sporadic CJD and vCJD, and individuals with the same *PRNP* mutation can propagate PrP^{Sc} with distinct fragment sizes (76). These observations provide an insight into how diverse clinical phenotypes may arise in patients with the same *PRNP* mutation.

Efforts to produce an unified international classification and nomenclature of human PrP^{Sc} types has been complicated by the fact that the N-terminal conformation of some PrP^{Sc} subtypes seen in sporadic CJD can be altered *in vitro* via changes in metal-ion occupancy (272;279) (see **Figure 1.5B**) or solvent pH (283;284). While it has recently been proposed that pH alone determines PrP^{Sc} N-terminal structure (284), this interpretation has not been supported by other studies (285;286), and strain-specific PrP^{Sc} conformations show critical dependence upon the presence of copper or zinc ions under conditions where pH 7.4 is strictly controlled (279). Further complexity is evident from studies showing that multiple PrP^{Sc} conformations and glycoform ratios may exist in the same patient (213;287;288). Although agreement has yet to be reached on methodological differences, nomenclature and the biological importance of relatively subtle biochemical differences in PrP^{Sc}, there is strong agreement between laboratories that phenotypic diversity in human prion disease relates to the propagation of disease-related PrP isoforms with distinct physicochemical properties (202;272;278-280;282;289;290). Further investigation into what PrP^{Sc} structural components encode different prion strain types is needed to further the knowledge of what constitutes an infectious prion and provide an understanding of prion disease aetiology.

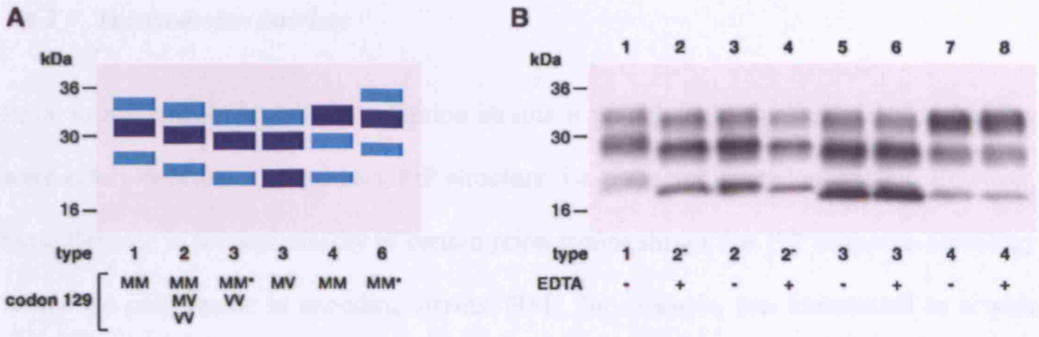

Figure 1.5: Molecular strain types of human prion disease

(**A**) Adapted from Hill et al (272), representative cartoon of human strain types observed on SDS-PAGE after proteolytic digestion, dominant glycoform shown in dark, different glycoform ratios can be associated with codon 129 polymorphism, (*) single cases only. (**B**) Adapted from Wadsworth et al (279), difference in human strain types under conditions of metal ion chelation. PrP^{Sc} types 1 and 2 show a difference in fragment size after proteolytic digestion in the presence of 20 mM EDTA, the smaller fragment size termed 2-, PrP^{Sc} types 3 and 4 are unaffected by metal ion chelation.

1.4.2 Transmission barriers

Prior to the current knowledge of prion strains it was thought that transmission barriers were solely dependent on primary PrP structure, i.e. a species dependent barrier. However, the difference in transmissibility of certain prion strains shows that PrP sequence homology is not the only factor in encoding strains. BSE, for example, has transmitted to a wide variety of hosts maintaining BSE prion strain characteristics, even on subsequent passage to laboratory mice (291). Other strains have shown to have difficulty in transmitting to differing species even with similar sequence homology having low attack rates, a change in strain type or subclinical prion disease (292-296). These data show that although sequence homology is important in the transmissibility of prions, strain type is also highly important (115;297).

Human molecular strain types can be propagated in transgenic mice expressing human PrP showing strain associated characteristics (184;278;295;298). As discussed above there is phenotypic diversity in human prion disease and polymorphism at codon 129 of the human *PRNP*, significantly affects susceptibility to human prion diseases and disease aetiology. This has also been seen in the transgenic human *PRNP* mouse models after inoculation with either BSE or vCJD prions (184;278;295;298;299) (see **Figures 1.6** and **1.7**). The PrP^{Sc} conformations from each polymorphic variant are completely distinct after inoculation with either BSE or vCJD prions (295). Depending on the origin of the inoculum (cattle BSE prions or vCJD (human-passaged BSE) prions) and the PrP codon 129 genotype of the host, transmission can result in four distinct prion disease phenotypes (184;295;299). Human PrP MM homozygous transgenic mice propagate either type 2 or 4 PrP^{Sc} with respective neuropathologies consistent with human sporadic CJD or vCJD (295;298), whereas human PrP VV homozygous transgenic mice either propagate a novel type 5 PrP^{Sc} and have a distinct pattern of neuropathology, or develop clinical prion disease in the absence of detectable PrP^{Sc} (184;295) (see **Figures 1.6** and **1.7**). A similar phenomenon has been observed with primary transmission of BSE to SJL inbred mice (298;300)(see **Figure 1.8**).

These findings indicate that BSE derived prion infection and secondary infection by iatrogenic routes in humans, may not be restricted to a single disease phenotype. The differing PrP^{Sc} isoforms and disease aetiologies observed in transgenic mice with the polymorphic variants of human *PRNP* codon after inoculation with BSE or vCJD prions emphasise the importance of understanding PrP^{Sc} structural properties that encode different prion strains for correct evaluation of the aetiology underlying acquired forms of prion disease.

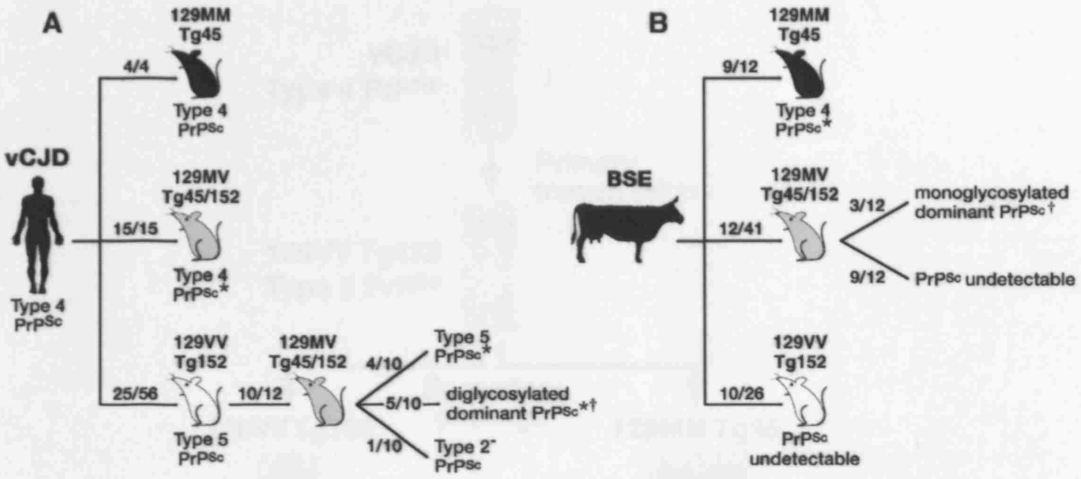

Figure 1.6: Transmission of vCJD and BSE into human transgenic mice

Adapted from Wadsworth et al (295). Schematic summary of transmissions of vCJD and BSE prions to transgenic mice expressing human PrP. Transgenic mice background as reported by Asante et al (301).

The total number of prion affected mice (both clinical and subclinical) is reported for each inoculated group: 129MM Tg45 mice (black), 129MM Tg35 mice (gray), 129VV Tg152 mice (white). Animals were scored by clinical signs, immunoblotting, and/or immunohistochemistry. In transmissions that result in bifurcation of propagated PrP^{Sc} type, the number of samples positive for type 2 or type 4 PrP^{Sc} is reported as a proportion of the total number of samples examined by immunoblotting.

(*) The occurrence of subclinical prion infection only.

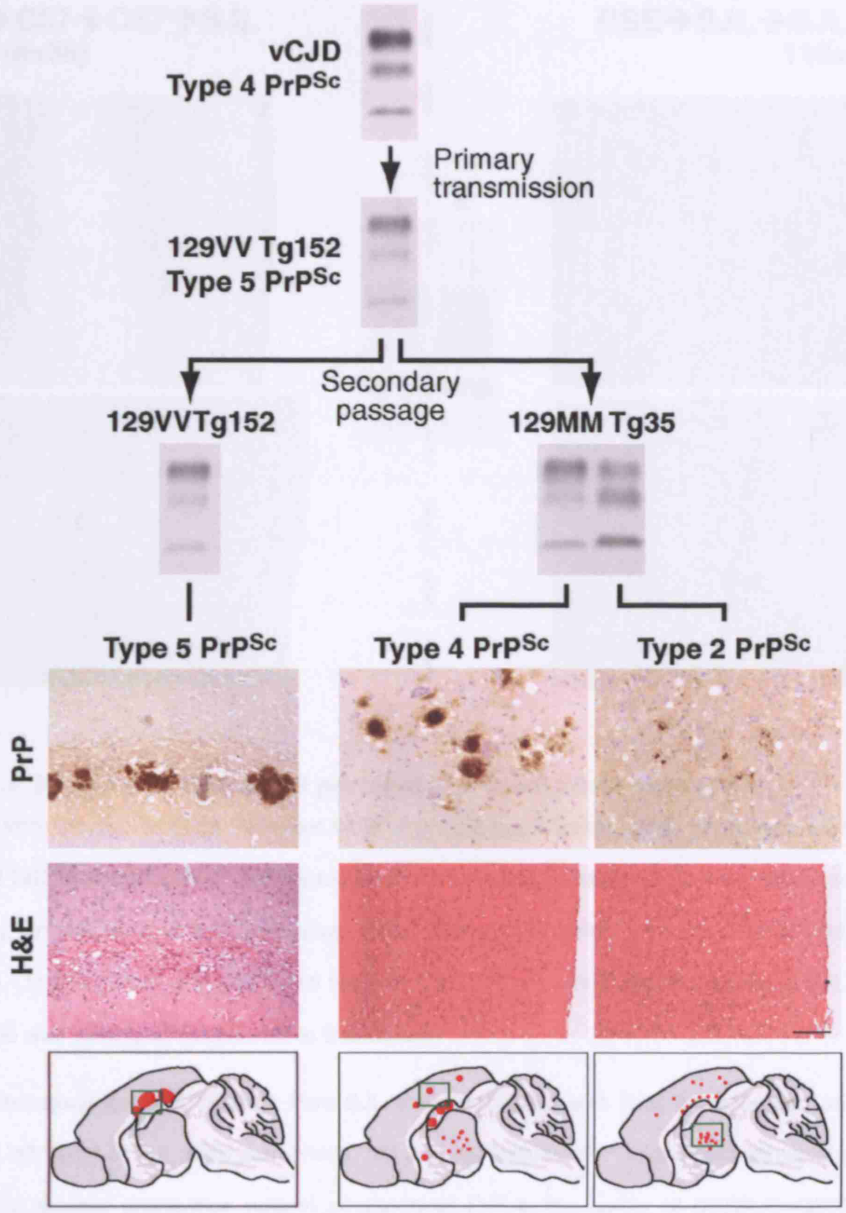

Figure 1.7: Neuropathological analysis of strain types in vCJD transmission in transgenic mice

Adapted from Wadsworth et al (295). Primary transmission of vCJD prions in 129VV Tg152 mice produces type 5 PrP^{Sc} that is maintained after secondary passage in 129VV Tg152 mice but induces propagation of either type 2 or type 4 PrP^{Sc} after passage in 129MM Tg35 mice. Immunohistochemistry (PrP) shows abnormal PrP immuno-reactivity, including PrP-positive plaques, stained with monoclonal antibody 3F4 against PrP. Sections stained with hematoxylin and eosin (H&E) show spongiform neurodegeneration (left, corpus callosum; middle and right, parietal cortex). Scale bar, 100 μm. Lower panels show the regional distribution of abnormal PrP deposition. Green boxes in the sketches denote the area from which PrP-stained sections are derived.

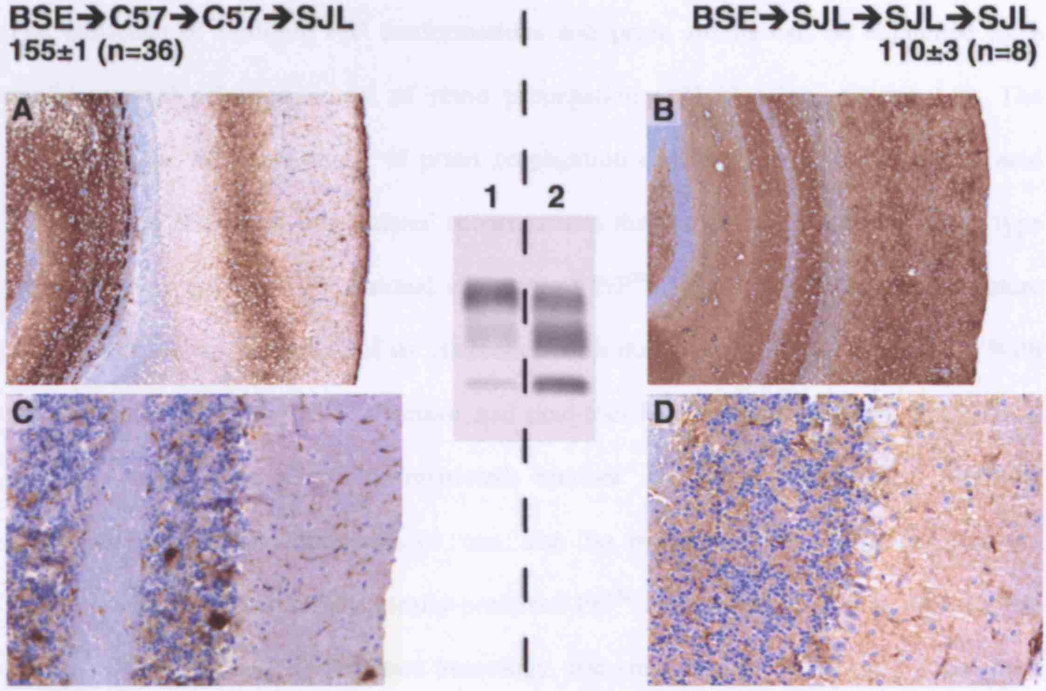

Figure 1.8: Strain differences of BSE passaged in different inbred mouse lines

Adapted from Lloyd et al (300). Western blots of proteinase K-treated brain homogenates from cattle BSE and BSE transmission and subpassage in inbred mice. Western blots were analysed by high-sensitivity enhanced chemiluminescence (ECL) using biotinylated anti-PrP monoclonal antibody ICSM-35. (**1**) BSE strain was passaged twice in C57BL/6 mice and then passaged in SJL mice; (**2**) BSE strain was passaged three times in SJL mice.

Neuropathological analysis of brain from SJL mice inoculated with BSE following two passages in C57BL/6 left panel or SJL right panel mice. (**A**) and (**B**) indicate PrP immunohistochemistry showing the distinct laminar distribution pattern of abnormal PrP in the cortex of C57BL/6>C57BL/6>SJL-passaged BSE (**A**), while the PrP immunoreactivity in SJL>SJL>SJL-passaged BSE is uniformly distributed (**B**). The cerebellum of the former group (**C**) mainly shows plaques and very little diffuse staining, while the latter group (**D**) predominantly shows diffuse staining and no plaques.

The existence of multiple PrP conformations and prion strains can be explained by a conformational selection model of prion propagation (181;302) (see **Figure 1.9**). The conformational selection model of prion propagation explains that both PrP amino acid sequence and other post-translational modifications that make up a particular strain type will determine the three dimensional structure of PrP^{Sc}. This three dimensional structure will then affect the efficiency of its interaction with host PrP for prion propagation. With the influence of primary PrP structure and post-translational modifications, PrP from a certain species can adopt a restricted number of thermodynamically preferred conformations. These conformations can also be propagated in a different species dependent on their thermodynamically preferred PrP^{Sc} conformations. These isoforms are not just dependent on PrP sequence homology, but are crucially influenced by the prion strain, some of which may be thermodynamically preferred in several species, for example BSE. Glycosylation could be important for stabilising these particular conformers, as well as other as yet unknown post-translational modifications.

Figure 1.9: Conformational selection model of prion propagation

Adapted from Hill & Collinge (302) Prion propagation involves conversion of host-encoded PrP^{C} into PrP^{Sc}. Distinct strains of prions are associated with distinct PrP^{Sc}-types that can be differentiated by different patterns of proteolytic cleavage (thought to represent distinct PrP^{Sc} conformers) and glycosylation. Inoculated prions preferentially convert PrP^{C} into one of these preferred conformers, leading to prion propagation and disease. PrP glycosylation might be important in stabilizing particular PrP^{Sc} conformations. Mammalian PrP genes are highly conserved and it is hypothesised that only a restricted number of different PrP^{Sc} conformations (that are highly stable and can therefore be serially propagated) will be permissible thermodynamically. These will constitute the range of prion strains seen. Although a significant number of different PrP^{Sc} conformations might be possible among the range of mammalian PrP proteins, only a subset of these would be allowable for a given single mammalian PrP. Substantial overlap between the favoured conformations for PrP^{Sc} derived from species **A** and species **B** might therefore result in relatively easy transmission of prion diseases between these two species, whereas two species with no preferred PrP^{Sc} conformations in common would have a large barrier to transmission (and indeed transmission would necessitate a change of strain-type). There is overlap between the allowable PrP^{Sc} conformers between species **A** and species **B**. This overlap facilitates transmission between these species involving the 'green' and 'red' strains. However, inoculation with the 'blue' or 'yellow' strains would only result in propagation if a strain switch to red or green occurred. There is no overlap or allowed conformers between species **A** or **B** with species **C** resulting in a substantial transmission barrier between species **C** and **A**, or **C** and **B**. Passage of strains through an intermediate host might allow the adaptation of a particular strain to a new host.

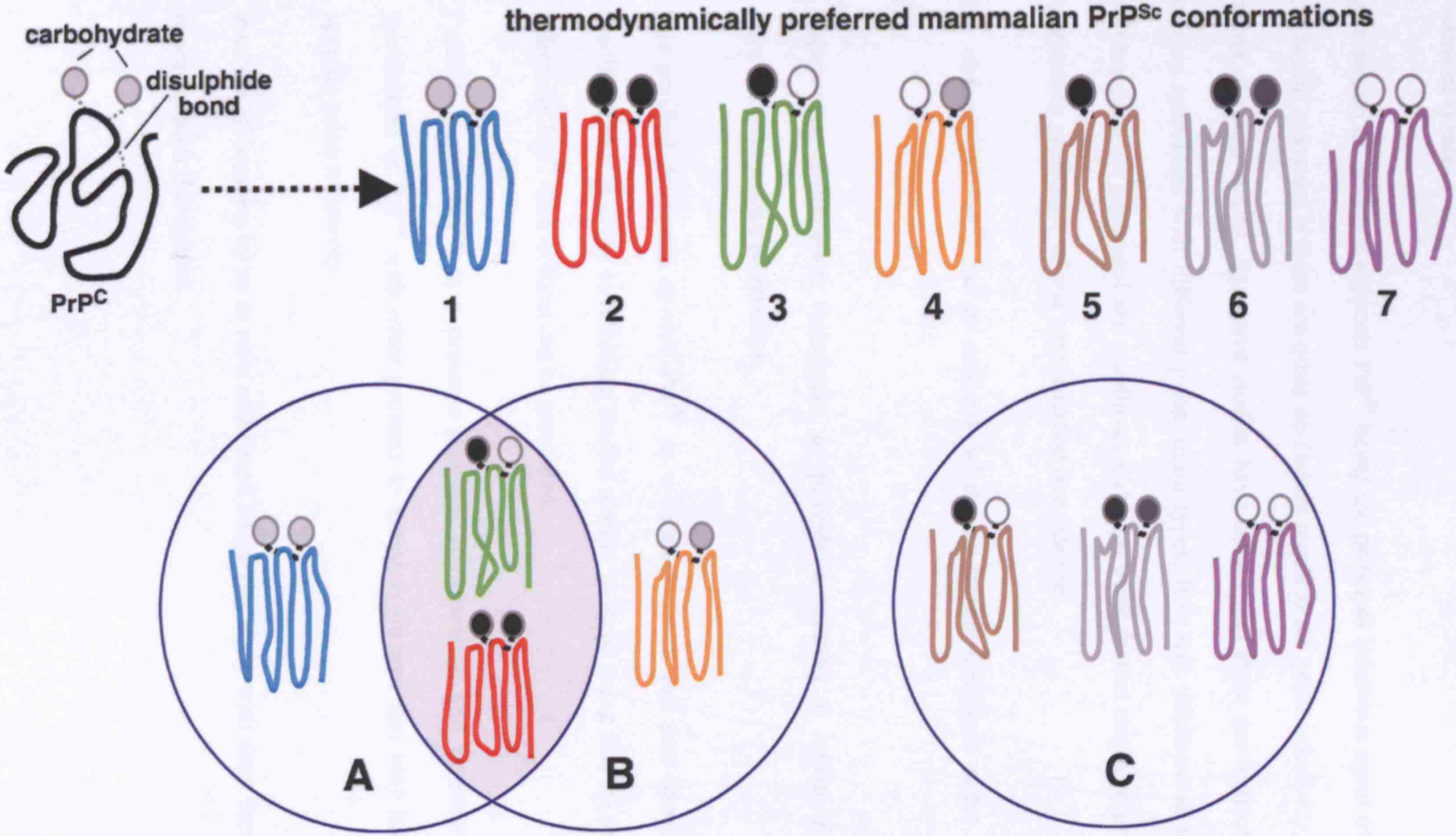
carbohydrate
disulphide bond
PrP^C
thermodynamically preferred mammalian PrP^Sc conformations
1
2
3
4
5
6
7
A
B
C

1.5 Aims of thesis

Although a wealth of evidence supports PrP^{Sc} being the principal infectious agent of prion disease, it is still unknown if there are other co-factors required for prion infectivity or the determinants of prion strains. Extensive studies have shown that there are distinct PrP^{Sc} conformations associated with different prion strain types. It is still unknown as to how these conformations are generated and stabilised, and what other factors might be involved in the determining preference of one conformation over another.

To further characterise PrP^{Sc} and to establish what may be the infectious agent it was sought to:

- Improve on purification techniques to provide a method to isolate PrP for physicochemical characterisation.
- Use purified denatured *ex-vivo* PrP^{Sc} as a substrate (with full post-translational modifications) in apply to refolding studies similar to those using rPrP to see if an infectious PrP^{Sc}-like isoform can be generated.
- Partially purify PrP^{Sc} in a protease resistant conformation and investigate co-purification of PrP^{Sc} with other proteins to assess co-factors that may influence specific prion infectivity.
- Analyse all samples by an *in vitro* cell-based infectivity assay with short incubation times for high throughput.

2 Purification of PrP^{Sc} in a denatured state by immunoaffinity chromatography

2.1 Introduction

Studies on the infectious agent have shown that it is hydrophobic and prone to aggregation and these properties have been exploited for its purification. Purification to isolate the prion protein, found to be a major component of the infectious agent, was achieved in 1982 by Prusiner et al (27). Initial methods included ultracentrifugation with 0.5 % w/v sodium deoxycholate to solubilise membranes and digestion with micrococcal nuclease and proteinase K (PK). Gross debris was removed from homogenates by a brief centrifugation and supernatants were adjusted with EDTA and dithriothreitol (DTT). Subsequent methods avoid prolonged ultracentrifugation with sodium deoxycholate, which was time consuming, and were replaced with sedimentation using polyethylene glycol (PEG 8000). Samples were then digested sequentially with micrococcal nuclease and PK before addition of 2 % w/v sodium cholate and further precipitation with 30 % w/v ammonium sulphate. Final pellets were resuspended in 2 % v/v Triton X-100 and 0.8 % w/v SDS before centrifugation over a sucrose gradient. Infectivity was distributed over the entire gradient but was consistently found to associate with one predominant protein peak. The infectivity isolated had on average a 1 % to 10 % yield, and 410 fold purification with 1.4×10^{10} ID_{50} U/mg of protein. The protein was seen to migrate between 27 and 30 kDa on SDS PAGE, and was shown to be disease associated by its absence from normal hamster brain (28). Purification methods were subsequently further improved to increase yield and fold purification. This was achieved by employing continuous flow zonal rotor centrifugation for the sucrose density separation (303). The purification of PrP was between 3000 and 10000 fold and the introduction of the continuous flow procedure enabled 95 % of the prion infectivity loaded on the sucrose gradient to be isolated in a single protein peak. The final purification protocol is summarised in **Figure 2.1**.

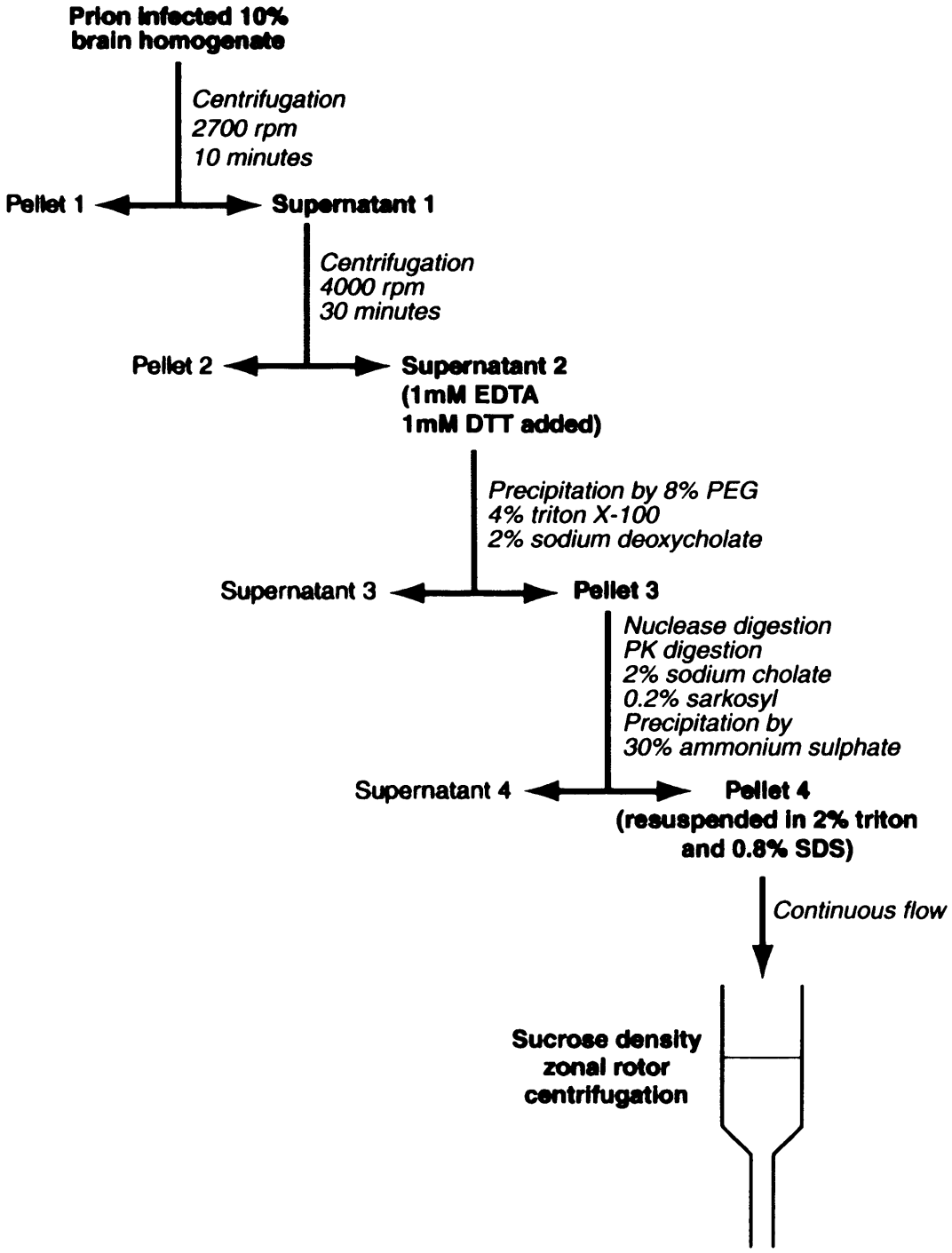

Figure 2.1: Sequence of steps that first isolated disease associated PrP

Adapted from methods described elsewhere (27;303). Methods of Prusiner et al for the purification of infectious prions, exploiting the PrP^{Sc} characteristics of hydrophobicity, detergent insolubility and partial resistance to digestion with endonuclease and protease. These methods led to isolation of the prion protein and were pioneering in the field.

Although the methods described by Prusiner et al were a huge breakthrough in the prion field and the main aim of the purification to discover a disease associated protein was achieved, development of other purification methods is still required. The original methods were laborious and complex and were marred by low yield which necessitated an input of 10 l of 10 % w/v starting homogenate (303). Furthermore these methods have been difficult to apply to human brain due to lower concentrations of PrP^{Sc} and difficulties with protein contaminants not encountered with hamster brain. Development of new purification methods for PrP^{Sc} to improve on yield and to permit analyses of other prion strains is required. The concentration of both PrP^{C} and PrP^{Sc} in terminal hamster brain is about 7 μg/g wet weight brain (304) and as ~10% w/w of the wet weight of brain is protein, a ~14000 fold purification is required to isolate pure PrP^{Sc}.

Other researchers have attempted to develop novel methods for purification of PrP^{Sc} (reviewed in (305)), however, most of these protocols are based on Prusiner's methods and again exploit the PrP^{Sc} properties of insolubility and protease resistance. Hilmert & Diringer adapted Prusiner's methods on a smaller scale involving solubilisation with the detergent sarkosyl, precipitation with NaCl, sonication at various stages and PK digestion as a final step, giving a 20 % yield of PrP^{Sc} (306;307). Marsh et al adapted Hilmert & Diringer's methods slightly and also confirmed a similar yield of PrP^{Sc} (308). Bolton et al further adapted Prusiner's methods and used solubilisation in sarkosyl and NaCl precipitation before centrifugation over a sucrose cushion (309;310). Methods were also adapted by Riesner et al to investigate prion infectivity in relation to nucleic acid components (261;262). To date only a few groups have adapted some of these methods to purify other prion strains including a mouse adapted Obihiro prion strain (311) and mouse ME7 prion strain (312).

Immunoaffinity purification of PrP^{Sc} was reported by Gabizon in 1988 (313;314) giving a 4000 fold purification and 4 % yield. Several further attempts have been made at immunoaffinity purification of PrP^{Sc} but these were marred by low yield and contamination

by immunoglobulins from the affinity matrices (31;315). All of these attempts at immunoaffinity purification of PrP^{Sc} sought to keep the protein in a conformation that retained prion infectivity. However for the analysis of possible post-translational modifications that may distinguish PrP^{Sc} isoforms associated with distinct prion strains, retention of PrP^{Sc} conformation is not required.

2.1.1 Aims

The aim of the research described in this chapter was to develop a robust method for isolation of denatured PrP^{Sc} from the brain of terminally infected animals at a sufficiently high yield that permits structural analysis of post-translational modifications to amino acids and facilitates investigation of the structure of N-linked carbohydrate. These novel methods would also provide a substrate for refolding studies to investigate conditions where denatured PrP^{Sc} could be refolded to an infectious isoform.

2.2 General Materials and Methods

All reagents were of highest analytical grade from Sigma unless otherwise stated.

2.2.1 Origin of tissue samples, ethical approval and research governance

Tissues were collected at autopsy with consent of relatives from patients with CJD or control patients without neurological disease. Research using human tissue was performed under approval from the Institute of Neurology/National Hospital for Neurology and Neurosurgery Local Research Ethics Committee. Transmission studies in rodents were performed under authority granted by the UK Home Office and care of animals was according to institution guidelines.

2.2.2 Safety procedures

All procedures involving infectious prions were performed within designated class 1 microbiological safety cabinets situated within an ACDP level III containment laboratory. No unsealed biological material (tissue or derivative homogenate or samples thereof) was manipulated outside of the class 1 microbiological safety cabinet. Disposable gloves, safety gown and safety glasses were worn at all times. Microfuges were situated on the open bench next to class 1 cabinets and prion infected material was microfuged at 16,100 x g within 1.5 ml screw-top microfuge tubes containing a rubber O-ring.

2.2.3 Decontamination procedures

All disposable plastic-ware (tubes, tips etc) and solutions containing biological material were discarded into a pot of 50 % (v/v) sodium hypochlorite (chloros) (Solmedic) (>20,000

ppm available chlorine) prepared in water and situated within the microbiological safety cabinet. Materials were decontaminated by exposure to chloros solution for at least 1 h prior to disposal of the liquid phase down designated laboratory sinks within the containment laboratory. Decontaminated plastic-ware was transferred to a sharps bin. Sharps used within designated class 1 microbiological safety cabinets were disposed of immediately after use into a sharps bin situated within the class 1 cabinet. Sealed sharps bins were transferred to autoclave bags and autoclaved out of the laboratory according to the general code of practice of the ACDP level III containment laboratory before incineration.

2.2.4 Preparation of homogenates

Prion infected tissue specimens, stored in sealed pots within the designated freezers of the ACDP level III containment laboratory, were transferred to a class 1 microbiological safety cabinet designated suitable for the preparation of either human or animal tissue homogenates. Specimens were partially thawed from -80 °C and transferred to a petri dish. A suitable quantity of tissue was excised using a scalpel and sealed in a disposable plastic pot and weighed. Brain and other tissue samples were prepared as a 10 % w/v brain homogenate using glass-glass tissue homogenisers in sterile Dulbecco's phosphate buffered saline lacking Ca^{2+} and Mg^{2+} ions (D-PBS) (Gibco Cat. N°. 14190-185). Homogenates were aliquotted and either stored at –80 °C or used immediately.

2.2.5 Sodium phosphatungstic acid (NaPTA) precipitation

Selective precipitation by sodium phosphatungstic acid (NaPTA), originally developed for a conformational dependent immunoassay (CDI) (273), was performed as described previously (316) with a reduction of incubation time and the added step of digestion with

benzonase for improved viscosity of the samples during centrifugation. Aliquots of tissue homogenate, either freshly prepared or thawed if frozen, were diluted with an equal volume of 4 % w/v lauroylsarcosine, sodium salt (sarkosyl) (Calbiochem Cat. N°. 428010) in PBS and incubated at 37 °C for 10 min. Benzonase, purity grade 1 (Merck Cat N°. 395064H) was added from original stock of 25000 U/ml to a final concentration of 50 U/ml and incubated at 37 °C for 30 min. Stock NaPTA solution was prepared at a concentration of 4 % w/v with 170 mM $MgCl_2$ at pH 7.4 and pre-warmed to 37 °C prior to addition to samples to avoid the formation of insoluble magnesium salts. NaPTA was added at a final concentration of 0.3 % in the sample and incubated at 37 °C for 30 min. Samples were centrifuged at 16,100 x g for 30 min. Supernatants were discarded and the pellets thoroughly resuspended in 0.1 % w/v sarkosyl in PBS to volumes typically between 10 µl and 500 µl. Pellets were often pooled before proteinase K digestion.

2.2.6 Proteinase K digestion

Samples were digested with proteinase K (PK) (EC 3.4.21.14) derived from the fungus *Tritirachium album* (VWR Cat N°. 124568). This enzyme has a minimum activity of 30 mAnson U/mg and was used at a final concentration of 50 µg/ml (unless otherwise stated) by addition from a stock concentration of 1 mg/ml PK in H_2O, and incubated at 37 °C for 1 h. Samples for sodium dodecyl sulphate polyacrylamide gel electrophoresis (SDS-PAGE) were processed as described below (see **Section 2.2.8**). For other samples, inhibition of PK activity was achieved by the addition of phenylmethylsulphonyl fluoride (PMSF) (from a stock concentration of 200 mM in dimethylsulphoxide (DMSO) or methanol (MeOH)) to 10 mM final concentration in the sample. Samples were centrifuged at 16,100 x g for 15 min, the supernatants discarded and the pellets resuspended in 0.1 % w/v sarkosyl in PBS containing 10 mM PMSF. The process of centrifugation and resuspension was repeated

twice and final pellets resuspended in 0.1 % sarkosyl in PBS containing 10 mM PMSF to approximately $1/10^{th}$ of the original starting volume.

2.2.7 Deglycosylation

A stock solution of 5 % w/v SDS and 10 % v/v β-mercaptoethanol (βME) in H_2O was added to PrP samples to give a final concentration of 0.5 % SDS and 1 % β-mercaptoethanol (βME). If samples already contained SDS, the stock solution was adjusted accordingly. The reducing agent, βME, was omitted in some cases. Protein was solubilised by boiling at 100°C for 10 min, equilibrated to room temperature then centrifuged at 16,100 x g for 1 minute. The supernatants were transferred to a new centrifuge tube and the pellet discarded. The supernatant was diluted 5 fold by the addition of 4 volumes of 50 mM sodium phosphate (NaH_2PO), containing 1 mM ethylenediaminetetraacetic acid (EDTA), 4 mM 4-(2-aminoethyl)-benzenesulphonyl fluoride (AEBSF) (Melford Laboratories Cat N°. MB2003), and 1.25 % v/v nonidet P40 (NP40), pH 7.0, to give final concentrations of 0.1 % SDS and 1 % NP40. Deglycosylating enzyme, N glycosidase F (PNGase F) (Roche Cat N°. 1365193), stored at 250 U/ml in 50 % glycerol at -20 °C, was added to a final concentration of 30 U/ml. Enzymatic digestion was typically accomplished by incubation for 4 h at 37 °C with constant agitation. Samples were stored at -80 °C if not used immediately. Protein was recovered by ice-cold MeOH precipitation by addition of 4 volume equivalents of MeOH (pre-cooled at -20 °C) to the sample and immediate centrifugation at 16,100 x g for 30 min. The supernatant was carefully removed and discarded and the pellets air-dried.

2.2.8 SDS Polyacrylamide Gel Electrophoresis (SDS-PAGE)

For discontinuous SDS-PAGE samples were mixed with 2 x stock of SDS-PAGE sample buffer (125 mM Tris-HCl, 20 % v/v glycerol, 4 % w/v SDS, 0.05 % w/v bromophenol blue, pH 6.8). 2 x sample buffer also contained 8 mM AEBSF if PK was present in the sample and 4 % v/v βME for reducing conditions. Samples were boiled for 10 min at 100 °C and loaded into a well on a pre-cast 16 % Tris glycine 1.5 mm or 1.0 mm gel (Invitrogen Cat N°. EC64985). See-blue prestained molecular weight markers (Invitrogen Cat N°. LC5625) were loaded typically at 10 µl, and at least one well loaded per gel. Running buffer was diluted from a 10 x stock (National Diagnostics Cat N°. EC-870) to give a final concentration of 25 mM Tris-HCl, 192 mM glycine, 0.1 % w/v SDS at pH 8.0 in H_2O. Gels were run at 200 V for 80 min.

SDS-PAGE gels can produce reactive species that will N-terminally block proteins preventing amino acid sequencing. It is generally unknown what the reactive species are or how the N-terminal blockage occurs, but there are many steps known to reduce the generation of reactive species, one of which is the use of reducing agents (317). Accordingly for SDS-PAGE, for the purposes of amino acid sequencing, running buffer was diluted from a 10 x stock as above and glutathione (100 mM stock in distilled deionised water) added to the cathode reservoir to a final concentration of 50 µM. One well was loaded with 10 µl of sample buffer, and the gel was electrophoresed at 50 V for 30 min until the band of bromophenol blue was seen to be about halfway down the gel. The buffer was then discarded. Samples were mixed with SDS-PAGE sample buffer as above, boiled for 10 min at 100 °C and loaded into a well on the pre-electrophoresed gel. Running buffer was composed from a 10 x stock (National Diagnostics Cat N°. EC-870) and 100 µM sodium thioglycolate from a 100 mM w/v stock in H_2O added to the cathode reservoir. Gels were run at 200 V for at least 80 min, until the band of bromophenol blue had reached the end of the gel.

2.2.9 Electroblotting

After SDS-PAGE, electroblotting was performed by transfer onto Immobilon polyvinylidene fluoride (PVDF) membrane. Immobilon-P (0.45 μm pore size, 131 μg/cm^2 binding capacity of BSA, Millipore Cat No. IPVH 000 10) was used for immunoblotting and Immobilon-P^{SQ} membrane (0.2 μm pore size 340 μg/cm^2 binding capacity of bovine serum albumin (BSA), Millipore Cat N°. ISEQ 000 10) was used for coomassie staining and amino acid sequencing. Membrane sections, cut to the same size as the gel, were pre-soaked in 100 % MeOH (as they are not easily hydrated) before transfer into blotting buffer. Blotting buffer was diluted from a 10 x stock (National Diagnostics Cat N°. EC-880) to final concentrations of 25 mM Tris-HCl, 192 mM glycine, and 20 % v/v MeOH, pH 8.0 for immunoblotting and 50 mM boric acid, 50 mM Tris and 20 % MeOH, pH 8.5 for coomassie staining and sequencing. Proteins were transferred from the gel to the membrane at either 35 V for 90 min or 15 V overnight.

2.2.10 Immunoblotting

After electroblotting, membranes were transferred to square tissue culture dishes and washed in phosphate buffered saline, containing 0.05 % v/v tween 20, (PBST). PBS was diluted from a 10 x low phosphate stock containing 4.4 g/l of sodium dihydrogen orthophosphate and 12.8 g/l di-sodium hydrogen orthophosphate, pH 7.4 (BDH Cat. N°. 437117K). Incubation with blocking solution, 5 % w/v non fat milk powder (Marvel), made up in PBST, was for 1 h with gentle agitation.

Anti-PrP monoclonal antibodies were used at a final concentration of 0.2 μg/ml in PBST. Biotinylated anti-PrP monoclonal antibodies were used at a final concentration of 0.5 μg/ml in PBST unless otherwise stated. Incubation of primary antibody was between 60 and 90 min or overnight with the buffer containing 0.1 % w/v sodium azide. Washing after primary

antibody incubation was for 1 h with 4 changes of PBST. Primary antibodies used were mouse monoclonal anti-PrP antibody 3F4 (IgG2a) (Signet Labs Cat. N°. 9620-10) (274); and mouse monoclonal anti-PrP antibody ICSM 18 (IgG1κ) (DGen Ltd, London Cat. N°. 0130-01810) (110;318).

Secondary antibodies were diluted 1/10,000 in PBST and Dako avidin/biotin alkaline phosphatase kit made up as per manufacturers instructions (see below). Incubations were between 45 min and 1 h and washing after secondary antibody was between 30 and 45 min with 4 changes of PBST. Secondary antibodies used were goat anti-mouse Fab specific human Ig absorbed IgG alkaline phosphatase conjugate (Sigma Cat. N°. A-2179), and goat anti-mouse IgG and IgM whole molecule, human Ig absorbed IgG alkaline phosphatase conjugate (Biosource Cat. N°. AMI3705) Dako alkaline phosphatase biotinylated secondary kit (Dako Cat. N°. K0376) with solution A, containing 1 ml of avidin from chicken's egg and solution B, containing 1 ml biotinylated alkaline phosphatase from calf intestinal mucosa was used to probe biotinylated antibodies. Aliquots of 6 µl of each reagent were mixed in 20 ml of PBST 30 min prior to application.

For high sensitivity enhanced chemiluminescence (ECL) methods were as described previously (316). After incubation in alkaline phosphatase conjugated secondary antibodies, membranes were washed in 20 mM Tris-base, 1 mM $MgCl_2$, at pH 9.8 (tropix assay buffer – TAB) for 2 x 5 min. and developed using chemiluminescent substrate, CDP Star (Tropix Inc. Cat. N°. MS250R). Membranes were then placed between acetate sheets and transferred to a photographic cassette. Biomax MR films (Kodak, Anachem Cat. N°. 8941114) were developed using Kodak developer and fixative by hand or by using an Xograph imaging machine (Xograph Imaging Systems, Tetbury, UK). Developed films were scanned using an Epson scanner for electronic format and densitometry of digital images was performed using a Kodak Image Station 440 CF (Kodak).

2.2.11 Silver Staining of SDS-PAGE gels

Silver staining was performed using the Plus One silver stain kit (Amersham Cat. No. 17-1150-01) which detects proteins at 0.2-0.6 ng protein per band and is based on the methodology of Heukeshoven and Dernick (319). This method uses thiosulfate to increase the reducing potential of the proteins to enhance the signal and the reduction of silver nitrate to metallic silver with the use of formaldehyde.

Gels were placed in clean dishes and fixed in 40 % v/v ethanol (EtOH) and 10 % v/v glacial acetic acid in H_2O for 30 min with gentle agitation. The gel was then incubated with sodium thiosulfate sensitising solution for 30 min followed by 3 x 5 minute washes with H_2O. Silver reaction was then incubated for 20 min followed by 2 x 1 minute washes with H_2O and developed for approximately 5 min until protein bands were visible. Once the protein bands were visible the reaction was stopped using EDTA stopping solution. If the gels were to be kept long term they were washed after stopping solution with H_2O for 3 x 5 min and kept in preserving solution.

Gels were photographed on a light box using a Polaroid gel camera and black and white film at optimum exposure times. Developed polaroids were scanned using an Epson scanner.

2.2.12 Coomassie staining of Immobilon-P^{SQ} membrane

After electroblotting, membranes were transferred to clean square tissue culture dishes and fixed in 30 % v/v MeOH for 15 min. Membranes were then stained with 0.1 % w/v Coomassie blue R_{250} in 30 % MeOH until membranes turned blue (typically for 5-15 min). Membranes were then destained in 30 % MeOH until the protein bands were visible. Specific bands were excised using a scalpel and forceps and transferred to a microfuge tube and sealed.

2.2.13 Amino acid sequencing

Protein bands for sequencing were cut from Coomassie stained membranes using a clean disposable scalpel and transferred into a clean centrifuge tube. The samples were sent to the University of Bristol, where amino acid sequencing was performed by Dr Will Mawby using a Procise 492cLC protein sequencer (Applied Biosystems) on standard cycles.

2.3 Methods developed for purification of PrP^{Sc} in a denatured state by immunoaffinity chromatography

2.3.1 Coupling of antibodies to protein A sepharose beads

As the affinity of mouse IgG1 is low for protein A, it was necessary to couple in high salt conditions (320). A PD10 column (Pharmacia Biotech Cat. N°. 17-0851-01) was equilibrated with a high salt coupling buffer, 50 mM sodium borate, 3 M NaCl, pH 9.0, and mouse anti-PrP monoclonal antibody ICSM18, typically 3 mg/ml, filtered through the column to transfer into the buffer. ICSM18 was eluted with high salt buffer and allowed to filter through via gravity. 10 x 1 ml fractions were collected and protein concentration quantified by transfer of fractions into a quartz cuvette and determination of absorbance at A280 nm using a spectrophotometer. ICSM 18 is an IgG1 molecule and 1.35 absorbance units are equal to a 1 mg/ml concentration (321). Concentration of IgG1 (mg/ml) can be calculated using absorbance at 280 nm divided by 1.35 to give the concentration. Peak fractions were pooled and diluted with buffer to give a final concentration of 1mg/ml in a volume that was usually 10 ml.

Protein A sepharose fast flow beads (Amersham Cat. N°. 17-1279-01), have a particle size 60-165 μm and a binding capacity for IgG of 50 mg/ml of beads. Beads were washed in high salt buffer batch wise with a bed volume of 5 ml of beads and 45 ml buffer. The beads were gently agitated and allowed to settle at room temperature. The supernatant was carefully removed using a pipette followed by resuspension of beads in 45 ml buffer. This was repeated 3 times so the beads were devoid of original storage buffer.

ICSM18 was added to high-salt equilibrated beads at a ratio of 1 mg antibody per 300 μl of beads and incubated overnight at room temperature with constant agitation. Beads were subsequently washed twice batch wise in 10 volumes of the high salt buffer over a period of typically 30 min by letting the beads settle in the tube and removal of the supernatant using a pipette. Beads were then resuspended in 10 volumes of high salt buffer and dimethyl

pimelimidate (DMP) (Pierce Cat. N°. 21666) added from solid to give a final concentration of 20 mM followed by incubation for 30 min with agitation (DMP is a homobifunctional imido ester susceptible to nucleophilic attack by free amino groups under certain conditions, to form an amidine, (see **Figure 2.2**.). Beads were washed once in 10 volumes of 200 mM ethanolamine, pH 8.0, once by letting the beads settle in the tube and removing the supernatant using a pipette, after which a further 10 volumes of ethanolamine buffer was added and the beads incubated for 2 h at room temperature with constant agitation. Beads were then washed in D-PBS containing 0.01 % w/v thimerosal 4 times batch wise to remove ethanolamine buffer as described above. Beads were then made up to the full volume of the tube with D-PBS containing 0.01 % thimerosal for storage at 4 °C. To check coupling efficiency, washed beads with bound ICSM18 prior to addition of DMP and the final DMP-coupled ICSM18-protein A beads were analysed by reducing and non-reducing SDS-PAGE and immunoblotting with alkaline phosphatase conjugated goat anti-mouse IgG antibody (Biosource).

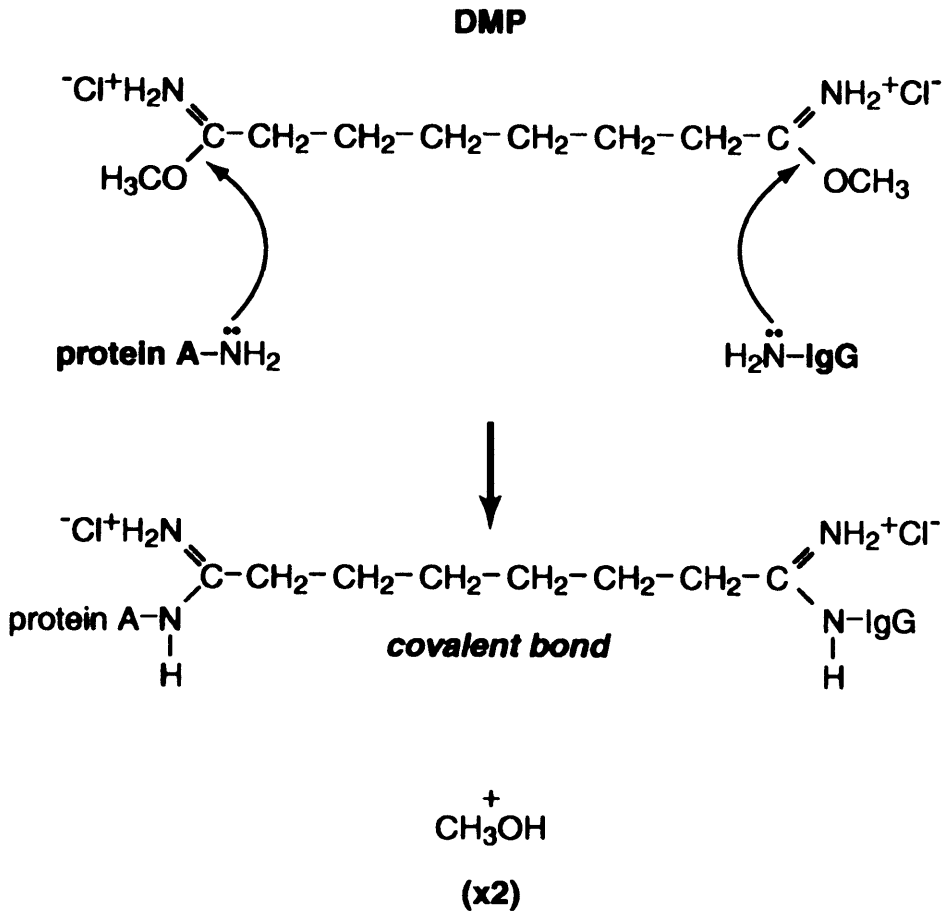

Figure 2.2: Coupling reaction of DMP

Dimethyl pimelimidate (DMP) is a homobifunctional imido ester that covalently couples Protein A to IgG via a nucleophilic reaction involving free amino groups (predominantly lysine residues) of protein A and IgG.

2.3.2 Preparation of Immunoaffinity columns

A chromatography column, non-jacketed, 1.7 x 10 cm (Sigma Cat. N°. C3669), was extensively washed with D-PBS and connected with polyvinyl chloride (PVC) collared tubing (1.42 mm, 1.65 mm, 3.16 mm; Anachem Cat. N°. s 116-0532-200, 116-0549-130, 116-0549-120), and poly(tetrafluoroethylene) (PTFE) capillary tubing (Anachem Cat. N°. 19-0041-01) to a Gilson mini pulse pump model MP2 (Anachem Cat N°. E5501) and fraction collector model 2110 (Biorad Cat. N°. 731-8120). Protein A sepharose beads covalently coupled to ICSM18 were loaded onto the column to give a bed volume of 1 ml and the column was washed again with PBST.

2.3.3 Immunoaffinity purification of PrP

Solubilisation and equilibration of PrP

PrP^{Sc} enriched material, 200 µl in volume, derived from 12 ml starting 10 % w/v homogenate, that had been NaPTA precipitated and PK digested, had SDS added to a final concentration of 0.5 %, from a 10 % w/v stock in H_2O, and boiled for 10 min. Following this procedure PrP in the sample is now denatured and should now be referred to simply as PrP rather than PrP^{Sc}. The sample was centrifuged for 1 minute at 16,100 x g and pellet discarded (or retained for further analysis where appropriate). The supernatant was diluted 50 fold, to a final volume of 10 ml, with D-PBS containing 0.1 % v/v Tween 20, and 5 x incomplete protease inhibitor cocktail (lacking EDTA), and equilibrated for 60 min at room temperature.

Removal of endogenous immunoglobulins

To remove any possible contaminating immunoglobulins from the denatured PrP sample, native protein A and protein G sepharose beads (Protein G sepharose beads, Amersham Cat N°. 17-0618-01) were used at a ratio of 20 µl of combined bed volume of beads to 1 ml sample. Protein A and G beads at a 1:1 ratio were washed thoroughly in D-PBS to remove storage buffer and made into a 50 % slurry in D-PBS before addition to the PrP samples. Samples were agitated gently for 30 min by rotation. After rotation, samples were centrifuged for 1 minute at 100 x g to pellet the beads. Supernatants were pooled into a 50 ml tube and a sample of the beads taken for analysis by SDS-PAGE to monitor removal of immunoglobulins.

Immunoaffinity chromatography

The PrP sample was circulated three times on the affinity column at a flow rate of 0.5 ml/min using a Gilson mini pulse pump. The column was then washed with 10 ml of D-PBS containing 0.1% v/v Tween 20 (PBST) and the eluate collected into a 50 ml tube.

The column was attached to a fraction collector (set to collect 2 minute fractions) and washed with 4 ml of 20 mM Tris-base, 1 mM $MgCl_2$, at pH 9.8 (tropix assay buffer – TAB)(316). This was expected to remove loosely bound contaminating proteins that interact non-specifically with ICSM18, protein A or the bead matrix. Bound protein was subsequently eluted with 10 ml of 1 % w/v SDS in H_2O, collected in 1 min fractions. Aliquots from all steps in the chromatography were analysed by SDS-PAGE and immunoblotting using mouse monoclonal anti-PrP antibody ICSM18. During this analysis, chromatography fractions were stored at -80 °C.

2.3.4 Detection and concentration of peak fractions of purified PrP

Peak SDS eluate fractions of PrP that had been identified by SDS-PAGE were thawed from -80 °C storage and warmed to 37 °C in a thermomixer to ensure solubilisation of SDS that might otherwise interfere with sample concentration. Peak fractions were concentrated through a Microcon centrifugal filter (Millipore Cat. N°. 42421) with a membrane size that will retain proteins greater than 10 kDa. Fractions were sequentially loaded onto the filter and centrifuged at 16,100 x g for 30 min until an appropriate volume was acquired (usually 5 µl for each equivalent of 1 ml starting homogenate). The filter used was then inverted into new microfuge tube and centrifuged at 100 x g for 3 min to collect purified concentrated PrP. Purified PrP samples were stored at -80 °C if not used immediately. Purity and yield of each purified sample was analysed by SDS-PAGE followed by either silver staining or immunoblotting using anti-PrP monoclonal antibodies (3F4 for hamster Sc237 derived material and ICSM18 for mouse RML derived material). For amino acid sequencing SDS-PAGE gels were electroblotted onto immobilon-P^{SQ} sequencing membrane and coomassie stained prior to excision of PrP bands for analysis.

2.4 Results

In this study methods were sought to efficiently isolate disease associated prion protein with high yield and purity. The first step was to enrich PrP^{Sc} from homogenate by means of precipitation. This allows concentration of PrP^{Sc} in a small volume, thereby providing the opportunity to work with large amounts of starting homogenate in each preparation. To isolate PrP with high purity, immunoaffinity purification using an anti-PrP antibody with high affinity for multiple PrP primary sequences was considered to be the method of choice. For immunoaffinity purification PrP needs to be soluble for efficient chromatography and this has to be achieved by methods that will not compromise the antibody-antigen interaction. Conditions for elution should ensure that PrP will be removed efficiently in a solvent suitable to maintain the solubility of small quantities of isolated protein.

2.4.1 Efficient enrichment of PrP^{Sc} from hamster Sc237 and mouse RML brain by NaPTA precipitation

To achieve enrichment of PrP^{Sc} from brain homogenate sodium phosphotungstic acid (NaPTA) (273) precipitation was considered to be the method of choice. Methods were performed as described previously (316) (see **Section 2.2.5**).

10 % homogenates in PBS prepared from the brain of Syrian hamsters terminally infected with Sc237 prions or CD-1 mice terminally infected with RML prions were NaPTA precipitated and pellets and supernatants were analysed by SDS-PAGE and immunoblotting.

Figure 2.3 shows the recoveries of PrP^{Sc} from hamster Sc237 and mouse RML strains by NaPTA precipitation (representative of over 15 preparations). Due to the degradation of PrP^{C} by endogenous proteases over the 1 h incubation at 37 °C the quantification of PrP^{C} in

the supernatant is hard to determine, but by the proportions of PrP^{Sc} and total PrP recovery in the pellet it is likely that two thirds of the total PrP recovered is PrP^{Sc} and >90 % of PrP^{Sc} is recovered in the pellet.

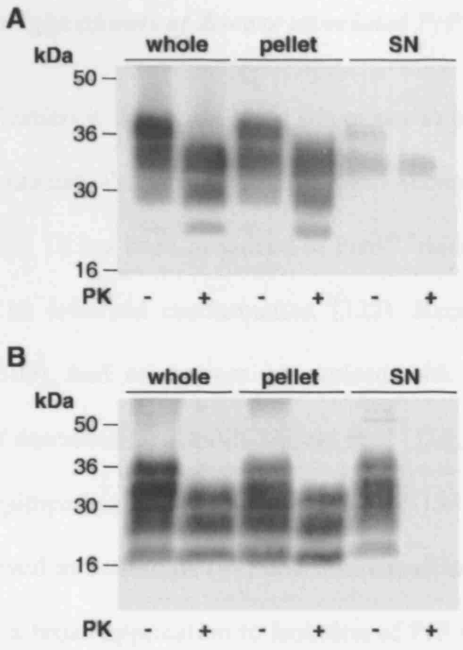

Figure 2.3: PrP^{Sc} enrichment by NaPTA precipitation of Sc237 infected hamster brain homogenate

NaPTA selectively precipitates PrP^{Sc} from 10 % hamster Sc237 brain homogenate (**A**) and 10 % mouse RML brain homogenate (**B**). The equivalent of 5 µl starting homogenate is in each lane. PrP^{Sc} fragments are shown after digestion with 100 µg/ml (**A**) or 50 µg/ml (**B**) PK, 1 h, 37 °C. Immunoblots were labelled with mouse anti-PrP monoclonal antibody 3F4 (**A**), mouse anti-PrP monoclonal antibody ICSM18 (**B**) and developed using high sensitivity ECL.

2.4.2 ICSM18 detects all glycoforms of disease associated PrP from multiple species

For immunoaffinity purification it was considered important to use an antibody with high affinity for multiple mammalian PrP primary sequences. Accordingly, anti-PrP antibody ICSM18 was chosen. ICSM 18 has been produced in $PrnP^{0/0}$ mice immunised with human recombinant PrP^{91-231} in its α-helical conformation (322). Recombinant α-PrP^{91-231} was produced as described (109), and mice were immunised with this material to produce monoclonal antibodies, as described by Khalili-Shirazi et al (110;318). ICSM18 is an IgG1 immunoglobulin and its epitope lies within the sequence 142-153 of human PrP(318). This sequence is highly conserved in mammals (41) and immunoaffinity purification using this antibody is likely to have a broad application to isolation of PrP associated with numerous prion strains.

To show ICSM18 recognition of denatured PrP, 10 % brain homogenates from 5 prion strains propagated in different species were processed for SDS-PAGE and immunoblotting with and without PK digestion. Selected prion strains were mouse RML, hamster Sc237, human vCJD, cattle BSE and sheep scrapie. As shown in **Figure 2.4**, ICSM18 detects disease associated PrP fragments from all these prion strains/species conformations.

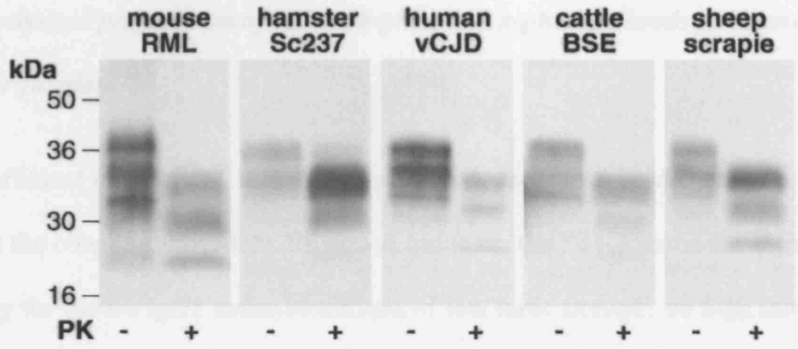

Figure 2.4: ICSM18 detects PrP from 5 different species

Five prion strains, mouse RML, hamster Sc237, human vCJD, cattle BSE and sheep scrapie were processed with and without PK digestion at 50 µg/ml for 1 h at 37 °C (100 µg/ml PK for hamster). The volume of 10 % brain homogenate analysed in each case was 5 µl for mouse RML, 2 µl for hamster Sc237, and 10 µl for human vCJD, cattle BSE and sheep scrapie. Immunoblots were labelled with anti-PrP monoclonal antibody ICSM18 and developed using high sensitivity ECL.

2.4.3 Optimised preparation of ICSM18-protein A sepharose beads for immunoaffinity purification

To show efficient coupling of ICSM18 to protein A sepharose beads, samples were taken throughout the coupling procedure. Protein A binds via the Fc region of the antibody with a low affinity for mouse IgG1 under conditions of low ionic strength, so high salt conditions were required for efficient binding (323). IgG immunoglobulins have an approximate molecular weight of 150 kDa comprising two heavy chains of 2 x 50 kDa and 2 light chains of 2 x 25 kDa linked together via disulfide bonds. Before coupling with DMP the constitutent chains can be seen via SDS-PAGE after solubilisation under reducing conditions. After covalent coupling, only the light chain should be liberated from the ICSM18-protein A sepharose complex under reducing conditions.

Figure 2.5 shows analysis of the antibody throughout the coupling procedure to protein A sepharose beads (representative of many preparations). ICSM18 IgG1 migrates as intact antibody at 150 kDa without reducing agent whereas with reducing agent both the heavy and light chains are visible. This is also shown after overnight incubation with protein A sepharose beads and washing, showing that the antibody has bound efficiently. After the covalent crosslinking with DMP there is a very marked reduction in overall ICSM18 signal strength indicating that DMP has worked efficiently. In the presence of reducing agent IgG light chain is liberated, however the low signal strength and shift in molecular mass to ~34 kDa indicates extensive covalent modification of IgG light chain with DMP.

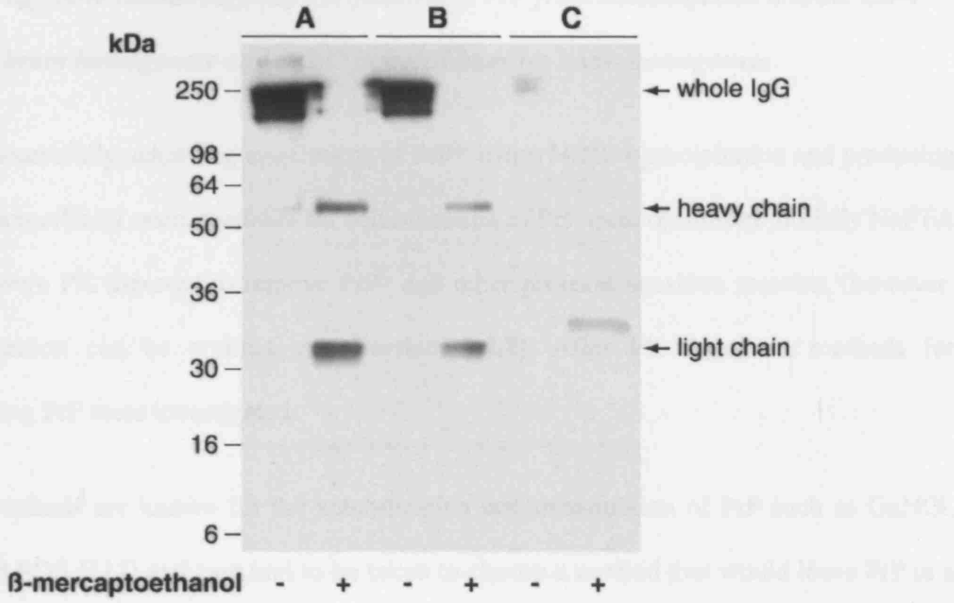

Figure 2.5: Efficient covalent coupling of ICSM18 to protein A sepharose beads

After equilibration of ICSM18 overnight with protein A sepharose beads and after covalent coupling with DMP, samples were taken and ICSM18 analysed by immunoblotting with antimouse IgG secondary antibody. The paired samples were boiled with SDS-PAGE sample buffer with and without reducing agent βME. Paired lanes (**A**) shows anti-PrP antibody ICSM18 prior to coupling. Without reducing agent, the whole antibody migrates with high molecular mass whereas the presence of reducing agent IgG heavy and light chains are liberated. Paired lanes (**B**) shows ICSM18 bound to protein A sepharose beads after overnight coupling but before treatment with DMP. A similar signal to paired lanes (**A**) shows the antibody has efficiently bound to the beads and is retained after washing. Paired lanes (**C**) shows ICSM18, detected on beads after covalently coupling with DMP. The lack of signal in the non-reduced sample shows that the whole IgG molecule has been successfully covalently crosslinked to protein A. In the presence of βME, light chain is liberated and migrates with slightly higher molecular mass indicating that DMP has been covalently incorporated. Immunoblots were labelled with alkaline phosphatase conjugated goat anti-mouse polyclonal secondary and developed with high sensitivity ECL.

2.4.4 Effective immunoaffinity purification of PrP from RML infected murine CD-1 brain homogenate and Sc237 infected hamster brain homogenate

After successfully achieving enrichment of PrP^{Sc} using NaPTA precipitation and producing an immunoaffinity resin, methods for solubilisation of PrP were optimised. Initially NaPTA pellets were PK digested to remove PrP^{C} and other protease sensitive proteins, (however, PK digestion can be omitted, see **Section 2.4.7**). After PK digestion, methods for solublising PrP were investigated.

Many methods are known for the solubilisation and denaturation of PrP such as GuHCl, urea and SDS (117) and care had to be taken to choose a method that would leave PrP in a solution compatible with immunoaffinity chromatography. As exchange of buffers by dialysis or other methods could result in a loss of PrP, it was elected not to choose high concentrations of chaotrope. Instead, SDS and heat was chosen as only a low concentration of SDS would be needed to solubilise PrP, and heat would also destroy protease activity. Subsequently the denaturing effects of SDS can be countered by the addition of a non-ionic detergent to the sample to enable immunoglobulin binding (213;320). It was found that as little as 0.5 % w/v SDS and boiling at 100 °C for 10 min was sufficient to solubilise all PrP. This material was then diluted 50 fold into D-PBS containing 0.1 % v/v Tween 20, and 5 x complete protease inhibitor.

With PrP solublised and in a solution suitable for immunoglobulin capture, methods needed to be optimised for efficient binding of PrP to the resin and minimal contamination of the PrP eluate. One obvious interaction that is likely to take place is the binding of endogenous immunoglobulins in the PrP sample with any free protein A binding sites. To prevent this, a pre-adsorption step was introduced in which PrP samples were incubated with protein A and protein G sepharose beads for 30 min to remove endogenous immunoglobulins. Following this pre-adsorption step the PrP sample was directly circulated on the immunoaffinity column. Subsequently the column was washed sequentially with

equilibration buffer followed by a high pH buffer that is utilised to reduce non- specific background signal of immunoblots (316).

With PrP efficiently bound to the immunoaffinity resin and efforts made to remove any possible contaminants, PrP then had to be eluted efficiently, under conditions that removed all PrP but minimised elution of ICSM18 or protein A from the resin. Applying the knowledge that sufficient concentrations of anionic detergents disrupts protein-antibody interactions (320) and that SDS would be a suitable solution for subsequent analysis by SDS-PAGE, 10 ml of 1 % w/v SDS was used to elute PrP.

Analysis of samples taken at all stages of immunoaffinity purification show the efficiency of the methods (see **Figures 2.6** and **2.7**). Panels **A** from both figures show SDS elution fractions of PrP. Panels **B** show purified material after concentration and analysis on silver stain to show total protein. The expected PrP glycoform ratio is apparent by both methods of analysis showing that the conditions for immunoaffinity purification gives quantitative recovery of di, mono and non-glycosylated PrP.

Although stringent steps were taken to avoid contamination due to endogenous antibody binding to protein A or ICSM18 eluting off the column, some variable contamination with IgG was seen in some preparations. This is more likely to be endogenous immunoglobulins as ICSM18-protein A sepharose beads have been shown to be stable under conditions of boiling SDS (see **Figure 2.5**). To eliminate possible contamination of samples, for amino acid sequencing gels were electrophoresed under non-reducing conditions to prevent co-migration of PrP and immunoglobulin light chain.

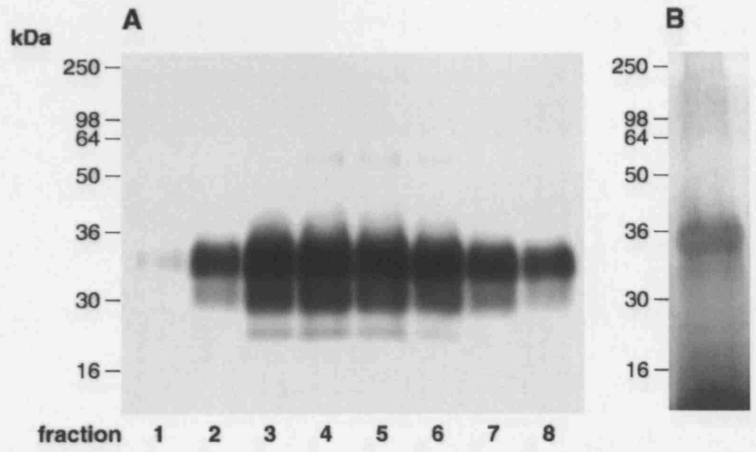

Figure 2.6: Elution profile of hamster Sc237 derived PrP from immunoaffinity purification and silver stain of concentrated material

(A) Immunoblot of peak fractions eluted with SDS from the immunoaffinity column (fractions 1-8 collected at 1 min intervals). The blot was labelled with mouse anti-PrP monoclonal antibody ICSM18 and developed with high sensitivity ECL. **(B)** Silver stain of immunoaffinity purified PrP concentrated peak fractions equivalent to 3 ml starting 10 % hamster Sc237 brain homogenate, developed using Amersham plus one kit.

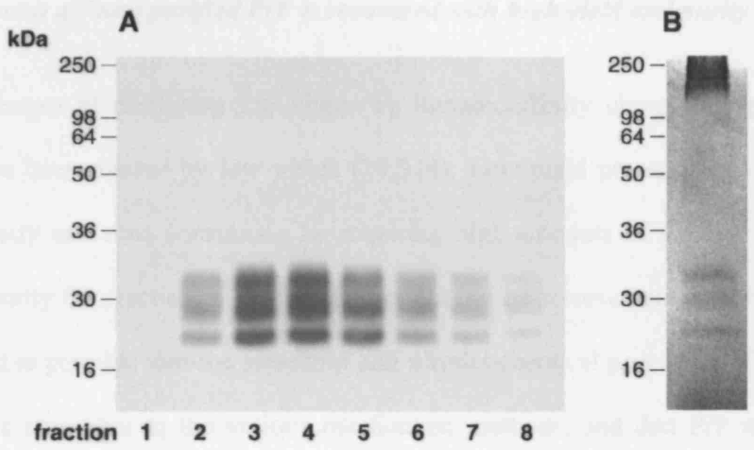

Figure 2.7: Elution profile of mouse RML derived PrP from immunoaffinity purification and silver stain of concentrated material

(A) Immunoblot of peak fractions eluted with SDS from the immunoaffinity column (fractions 1-8 collected at 1 min intervals). The blot was labelled with mouse anti-PrP monoclonal antibody ICSM18 and developed with high sensitivity ECL. **(B)** Silver stain of immunoaffinity purified PrP concentrated peak fractions equivalent to 2 ml starting 10 % mouse RML brain homogenate, developed using Amersham plus one kit.

2.4.5 Immuno affinity purified PrP is recovered with high yield and purity

Previous attempts at purifiying PrP either by immunoaffinity chromatography or other methods have been marred by low yields (27;314). Low yield presents a problem as not only is it costly and time consuming by requiring high amounts of starting material, but more importantly the fraction of PrP isolated might not be representative of the whole PrP population. It is possible that the structural and physicochemical properties of isolated PrP make it more amenable to the various purification methods, and that PrP with alternate properties are excluded.

Concentrated purified PrP was diluted and compared by volume with the starting homogenate. Example yields from purified mouse RML and hamster Sc237 PrP are shown in **Figure 2.8**. Yield of PrP from both hamster Sc237 and mouse RML were typically ~ 50 % (n=15) as determined by densitometry of developed films scanned using an Epson scanner for electronic format and densitometry on digital images performed using a Kodak Image Station 440 CF (Kodak).

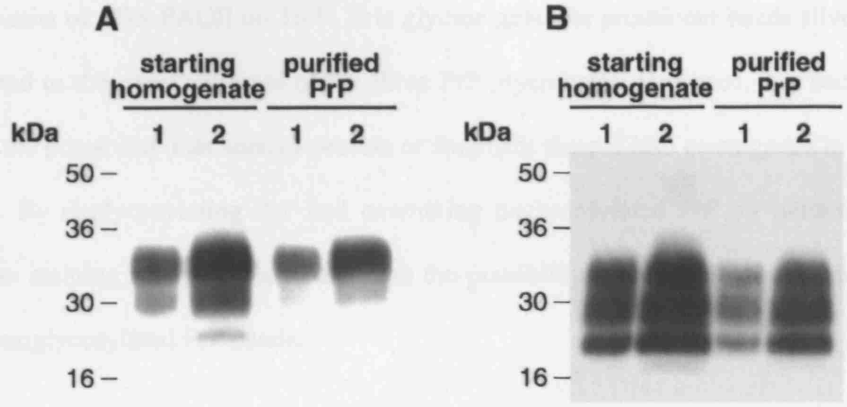

Figure 2.8: High yields of immunoaffinity purified PrP from mouse RML and hamster Sc237 infected brain homogenate

Comparison of PrP levels before and after immunoaffinity purification show that an approximate yield of about 50 % is achieved. (**A**) hamster Sc237 derived PrP, volume equivalents of starting homogenate in lane 1, 5 µl, and lane 2, 40 µl. Immunoblotted with mouse anti-PrP monoclonal antibody 3F4. (**B**) mouse RML derived PrP, volume equivalents of starting homogenate in lane 1, 5 µl, and lane 2, 20 µl. Immunoblotted with mouse anti-PrP monoclonal antibody, ICSM18. Both developed using ECL. Yield in both cases is ~ 55 % as determined by densitometry of developed films scanned using an Epson scanner for electronic format and densitometry on digital images performed using a Kodak Image Station 440 CF (Kodak).

By the limits of SDS-PAGE on 16 % Tris glycine gels, the prominent bands silver stained correspond to the expected mass of the three PrP glycoforms. However, it is necessary to exclude the possibility that another protein or fragment thereof also co-migrates in the same position. By deglycosylating PrP and examining unglycosylated PrP by immunoblotting and silver staining it is possible to examine the possibility of contaminants underlying the di or monoglycosylated PrP bands.

Figure 2.9 shows deglycosylation of purified material from mouse RML and hamster Sc237 preparations. Immunoblotting shows efficient deglycosylation of PrP and silver staining shows an equivalent band shift revealing no other detectable proteins. These data indicate that other proteins do not co-migrate with glycosylated PrP.

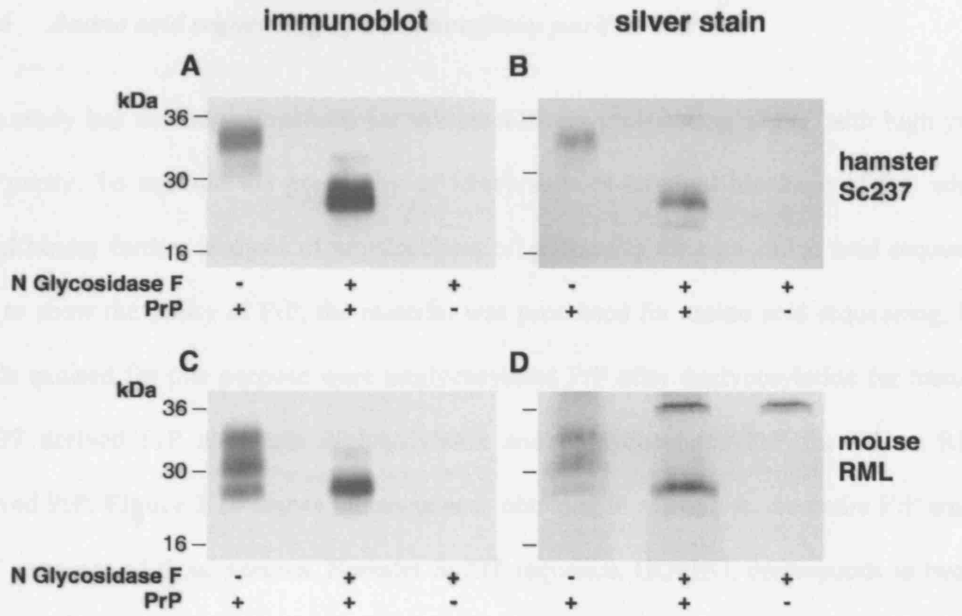

Figure 2.9: Deglycosylation of immunoaffinity purified PrP from mouse RML and hamster Sc237 infected brain homogenate

Immunoaffinity purified mouse RML and hamster Sc237 PrP before and after digestion with N Glycosidase F and processed via SDS-PAGE. (**A**) and (**B**) hamster Sc237 PrP, (**C**) and (**D**) mouse RML PrP. (**A**) and (**C**) immunoblots (developed using high sensitivity ECL) loaded with the equivalent of 10 µl starting 10 % brain homogenate. (**A**) mouse anti-PrP monoclonal antibody, 3F4. (**C**) mouse anti-PrP monoclonal antibody, ICSM18. (**B**) and (**D**) silver stained SDS-PAGE gels (developed using Amersham plus one kit) showing the equivalent of 3 ml (**B**) and 2 ml (**D**) starting 10 % brain homogenate.

2.4.6 Amino acid sequencing of immunoaffinity purified PrP

This study has developed methods for immunoaffinity purification of PrP with high yield and purity. To exclude the possibility of irreversible N-terminal blockage of PrP which could hinder further analysis of physicochemical properties through amino acid sequence, and to show the purity of PrP, the material was processed for amino acid sequencing. PrP bands excised for this purpose were unglycosylated PrP after deglycosylation for hamster Sc237 derived PrP and both diglycosylated and unglycosylated PrP for mouse RML derived PrP. **Figure 2.10** shows the sequences obtained in relation to the entire PrP amino acid sequence of those species. Hamster Sc237 sequence, GQPHG, corresponds to two of the start sites Prusiner et al have characterised at positions G74, G78, G82, G86, and G90 (34). The sequence obtained from immunoaffinity purified hamster PrP isolated here corresponds to the sites of either G74 or G82. Immunoaffinity RML PrP gave a sequence of GQPHGG that would correspond to a start site of G73 or G81 in the octapeptide repeat region that corresponds well with the molecular mass of PK digested RML PrP^{Sc} fragments.

```
            10          20          30          40          50          60
Ha MANLSYWLLA LFVAMWTDVG LCKKRPKPGG WNTGGSRYPG QGSPGGNRYP PQGGGTWGQP
Mo MANLGYWLLA LFVTMWTDVG LCKKRPKPGG WNTGGSRYPG QGSPGGNRYP PQGGTWGQPH
            70          80          90         100         110         120
Ha HGGGWGQPHG GGWGQPHGGG WGQPHGGGWG QGGGTHNQWN KPSKPKTNMK HMAGAAAAGA
Mo GGGWGQPHGG SWGQPHGGSW GQPHGGGWGQ GGGTHNQWNK PSKPKTNLKH VAGAAAAGAV
           130         140         150         160         170         180
Ha VVGGLGGYML GSAMSRPMMH FGNDWEDRYY RENMNRYPNQ VYYRPVDQYN NQNNFVHDCV
Mo VGGLGGYMLG SAMSRPMIHF GNDWEDRYYR ENMYRYPNQV YYRPVDQYSN QNNFVHDCVN
           190         200         210         220         230         240
Ha NITIKQHTVT TTTKGENFTE TDIKIMERVV EQMCTTQYQK ESQAYYDGRR SSAVLFSSPP
Mo ITIKQHTVTT TTKGENFTET DVKMMERVVE QMCVTQYQKE SQAYYDGRRS SSTVLFSSPP
           250  254
Ha VILLISFLIF LMVG
Mo VILLISFLIF LIVG
```

Figure 2.10: PrP sequences of hamster or mouse PrP with N-terminal amino acid start sites of purified PrP

Full length sequences of hamster (**Ha**) and mouse (**Mo**) PrP, highlighted in red is the sequence obtained from immunoaffinity purified PrP, numbers in bold show the amino acid position.

2.4.7 Immunoaffinity purification methods can be applied to full length PrP

Although the N-terminus of PrP^{Sc} is PK sensitive and PK digested PrP^{Sc} retains infectivity (29), it cannot be excluded that the N-terminus could be important for both prion propagation or in specifying strain specific PrP^{Sc} properties. Thus, as purified full length PrP would be of great value to analyse, accordingly it was sought to change the methods to omit proteinase K digestion. Surprisingly, identical processing of RML brain homogenate by NaPTA precipitation, solubilisation and immunoaffinity chromatography produced full PrP of comparable purity to that of truncated PrP isolated after inclusion of PK digestion. The yield of full length PrP was about 50 % of starting material. As only NaPTA precipitation has been used to isolate PrP^{Sc} from PrP^{C}, approximately two thirds of purified full length PrP would be expected to be derived from PrP^{Sc}. Full length purified PrP from mouse RML shows a small amount of background staining compared with truncated PrP, but the area around the PrP glycoforms shows no other contaminating proteins (**Figure 2.11**).

Figure 2.12 summarises the steps taken in developing the immunoaffinity purification methods.

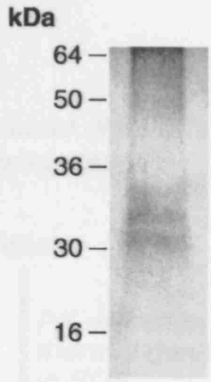

Figure 2.11: Immunoaffinity purified full length mouse RML derived PrP

SDS-PAGE silver stain showing concentrated peak fractions of immuno-affinity purified full length mouse RML PrP equivalent to 2 ml starting 10 % brain homogenate.

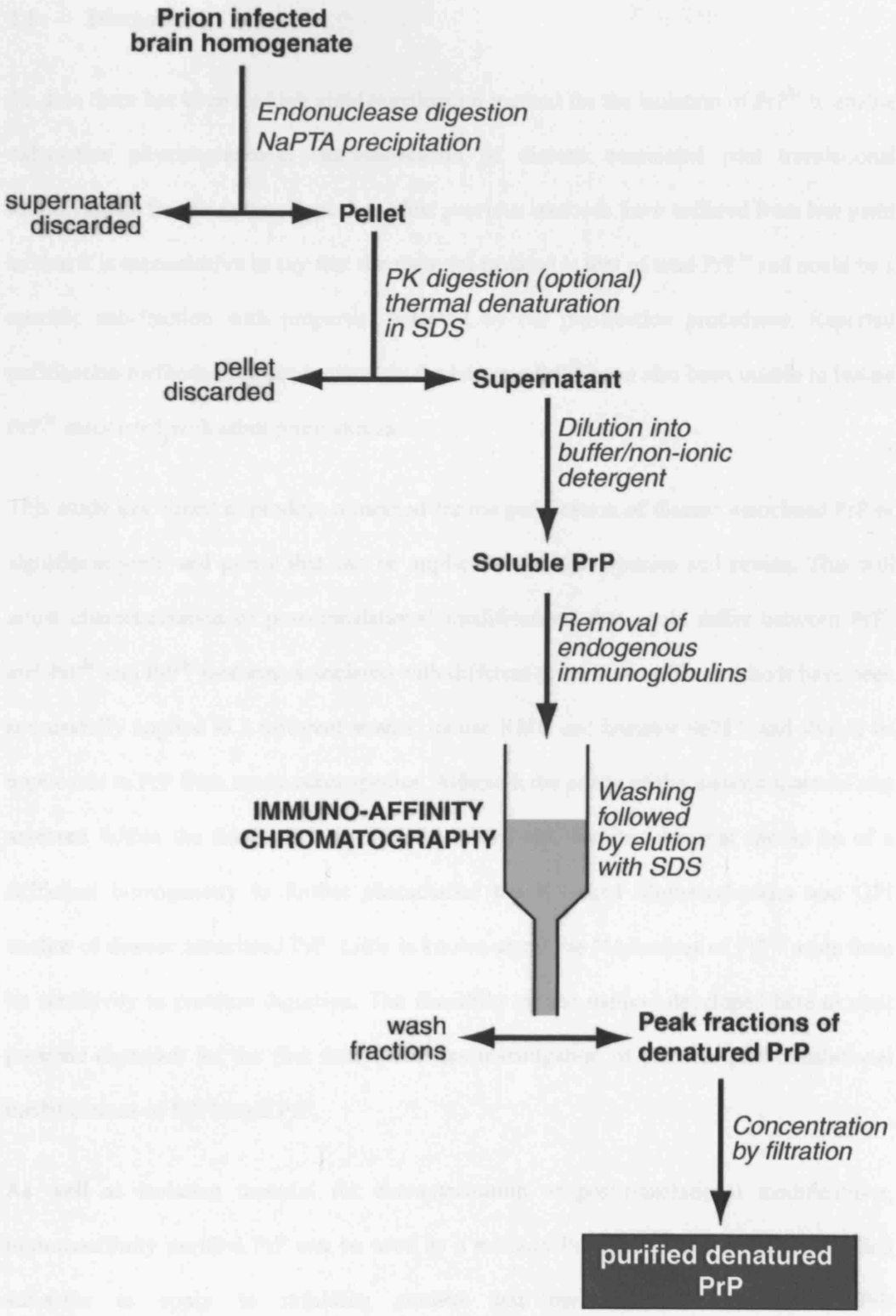

Figure 2.12: Schematic representation of purification of PrP by immunoaffinity chromatography

2.5 Discussion

To date there has been no high yield purification method for the isolation of PrP^{Sc} to enable exhaustive physicochemical characterisation of disease associated post translational modifications from a range of species. Most previous methods have suffered from low yield so that it is inconclusive to say that the material isolated is that of total PrP^{Sc} and could be a specific sub-fraction with properties selected by the purification procedures. Reported purification methods used predominantly for hamster PrP^{Sc} have also been unable to isolate PrP^{Sc} associated with other prion strains.

This study has aimed to produce a method for the purification of disease associated PrP of significant yield and purity that can be applied to multiple species and strains. This will allow characterisation of post-translational modifications that could differ between PrP^{C} and PrP^{Sc} and PrP^{Sc} isoforms associated with different prion strains. The methods have been successfully applied to 2 different strains, mouse RML and hamster Sc237, and should be applicable to PrP from many other species. Although the purity of the isolated material was assessed within the limits of a 16 % SDS-PAGE gel, isolated material should be of a sufficient homogeneity to further characterise the N-linked oligosaccharides and GPI anchor of disease associated PrP. Little is known about the N-terminus of PrP^{Sc} aside from its sensitivity to protease digestion. The flexibility of the method developed here to omit protease digestion for the first time facilitates investigation of possible post-translational modifications of full length PrP.

As well as isolating material for characterisation of post-translational modifications, immunoaffinity purified PrP can be used as a suitable fully post translationally modified substrate to apply to refolding studies that currently use recombinant PrP (94;106;108;111;324). Although it is known that PrP^{Sc} has the same amino acid sequence as PrP^{C} yet differs in conformation, the exact disease associated properties are unknown. Recombinant PrP maybe unsuitable for methods to generate infectious structures as it lacks

post translational modifications that could be required for infectivity. It has not been shown until recently that recombinant material can be refolded into a structure, which upon inoculation causes disease in transgenic mice (125). The low titres of infectivity compared to the high quantity of PrP inoculated in this study could indicate that a small proportion of PrP molecules have been modified chemically either during the refolding process or after inoculation (126). Further investigations using fully post-translationally modified PrP provides a better substrate for the refolding studies.

Although the methods described in this chapter have not shown that the purified material is completely homogeneous, there are no consistent contaminants seen by SDS-PAGE. Possible contamination by endogenous immunoglobulins binding to protein A was only seen irregularly, and such contaminants from other preparations could be easily removed using native protein A and protein G sepharose beads by pre-adsorbtion prior to immunoaffinity purification. The material produced is of a sufficiently high yield to be used in studies to investigate methods to refold PrP into a PrP^{Sc}-like structure to examine reconstitution of prion infectivity, see **Chapter 3**.

2.5.1 Conclusions and future work

Significant improvement of purification procedures to look at post translational modifications has been achieved. Further work ongoing in the MRC Prion Unit includes; the isolation of PrP from multiple species and strains and chemical analysis of carbohydrate structures and amino acids. Also the glycan sequences of each PrP species is being investigated by differential recognition by different plant and animal lectins and the use of carbohydrate specific antibodies. The determination of the N-terminal sequences of human PrP^{Sc} types 1-4 in order to accurately define strain-specific proteinase K cleavage sites will provide important information on PK resistant conformations. Investigations on the structure, and possible strain-specific differences of GPI anchors is also being undertaken.

Investigations towards the reconstitution of an infectious structure using immunoaffinity purified PrP is described in **Chapter 3**.

3 Reconstitution of PrP^{Sc} structural properties from denatured purified PrP and analysis of what is an infectious prion

3.1 Introduction

The nature of prion diseases and the protein only hypothesis, suggesting that PrP^{Sc} conformation alone encodes infectivity, challenges scientific dogma. To date a wealth of scientific evidence supports the protein only hypothesis, without involvement of a nucleic acid component of the infectious prion (145). However, it is still unknown if other cellular or proteinaceous factors are involved in the structure of the infectious prion and PrP^{Sc} replication. Due to the hydrophobic and aggregation properties of PrP^{Sc}, work towards isolation of PrP^{Sc} in its native state to prove or disprove the protein only hypothesis has been difficult. Therefore most studies have focused on isolating PrP from a previously uninfectious source, such as PrP^{C}, rPrP or denatured PrP^{Sc}, and examining conditions in which substrate PrP may gain the properties of PrP^{Sc} including prion infectivity, either alone or in combination with a particular co-factor.

Conditions giving a change in conformation of rPrP to a PrP^{Sc}-like isoform include low pH, with or without reducing conditions (93;94;103;106;108;109;111;124) and the addition of transition metals (72;73;118-122) (see **Section 1.2.3**). Such conditions have variably shown an acquisition of β sheet structure in PrP, insolubility, the generation of PrP fibrils, acquisition of PK resistance, and importantly, more recently, prion infectivity (125).

Attempts at regaining infectivity from partially purified denatured PrP^{Sc} has been previously studied (117). Partially purified material would retain potential disease associated covalent translational modifications that rPrP lacks, although being only partially purified, work with this material would not rule out the involvement of other co-factors. Notably, however, these studies did not manage to regain infectivity from

denatured PrP through dilution into buffered saline, or through dilution and the addition of phospholipids (117).

3.1.1 Aims

For the first time a purification method has been produced to give high quantities of denatured *ex-vivo* PrP^{Sc} (see **Chapter 2**). As potential unknown post translational modifications may confer prion infectivity to PrP, this substrate provides an extremely interesting starting material for experiments investigating conditions for reconstitution of prion infectivity. Accordingly, initial experiments have been performed under conditions that have been shown to generate PrP^{Sc}-like species from rPrP.

Changes in denatured *ex-vivo* PrP^{Sc} conformation and aggretation state were monitored by measuring insolubility, fibril formation, PK resistance and infectivity. If the protein only hypothesis is correct, under appropriate conditions it should be possible to change PrP to a PrP^{Sc}-like conformation and generate prion infectivity. If infectivity is not produced this may not, however, necessarily imply that PrP^{Sc} is not the sole infectious agent. In this circumstance these data could be interpreted that either the conformation may not be exactly PrP^{Sc}-like, or that additional factors are required for prion infectivity, either as an integral structural component or to act as vehicles for targeted delivery to cells. Thus if an infectious conformation is not achieved, it will be necessary to take further steps to investigate possible co-factors by means of native PrP^{Sc} purification. Accordingly, part of the work was directed toward establishing a strategy by which this may be achieved.

3.2 Methods

3.2.1 Exchange of purified concentrated PrP into appropriate denaturant

Purified denatured mouse RML or hamster Sc237 derived PrP, processed via methods in **Chapter 2**, and stored at -80 °C were retrieved from storage and thawed before exchange into appropriate denaturant (see below). To fully solubilise SDS in the samples, isolates were initially incubated at 37 °C. The PrP samples contained ~1 % w/v SDS from the immunoaffinity chromatography column elution buffer and due to the precipitation of SDS by GuHCl the SDS had to be removed by exchange into H_2O using a 10 kDa microcon centrifugal filter prior to exchange into a GuHCl buffer. Aliquots from purified material, at sufficient PrP concentration for renaturation, were pipetted on the membrane of a Microcon centrifugal filter (Millipore Cat. N°. 42421) (retains proteins greater than 10 kDa). Four wash steps with 500 µl aliquots of H_2O were required to remove SDS. This was achieved by repetitive addition of H_2O onto the filter and centrifugation at 16,100 x g for 30 min. The sample was then diluted into the denaturation buffer (6 M GuHCl, 10 mM Na acetate, 10 mM Tris-HCl, 100 mM DTT, pH 4) usually at the equivalent concentration of 5 µl per 1 ml starting 10 % homogenate and incubated for 10 min at room temperature. The filter used was then inverted into new microfuge tube and centrifuged at 100 x g for 3 min to collect purified concentrated PrP in appropriate denaturant. The sample was then boiled at 100 °C for 10 min to ensure complete denaturation. The denatured PrP was then available for refolding or was frozen at -80 °C. In the latter case samples were reboiled as above prior to use.

3.2.2 Transfer into renaturation buffers

Denatured PrP processed as above, in denaturation buffer (6 M GuHCl, 10 mM NaAc, 10 mM Tris-HCl, 100 mM DTT, pH 4) was diluted into a series of renaturation buffers. The

dilution made was 60 fold so that the final concentration of GuHCl was 100 mM, a concentration that permits refolding of PrP (94).

Many groups have reported changes in the structural properties of PrP under different conditions. In this series of experiments, published experimental methods were chosen that may produce acquisition of PrP^{Sc}-like properties from purified PrP. Jackson et al (94) reported a conformational change in recombinant PrP to give a structure with predominant β-sheet using a pH 4 buffer under reducing conditions. McKenzie et al (122) reported that PrP denatured in GuHCl, can refold to a proteinase K resistant conformation using a buffer containing Cu^{2+} ions.

Accordingly, buffers used were a reduced pH 4 buffer (10 mM Tris HCl, 10 mM NaAc, 1 M NaCl, 100 mM DTT pH 4), a buffer containing Cu^{2+} ions (10 mM Tris HCl, 130 mM NaCl, 10 mM $CuSO_4$ pH 7), and D-PBS as a control. All buffers contained 0.1 % w/v azide as a bacteriocide for prolonged incubation at 4 °C. PrP was rapidly diluted into each buffer and incubated at 4 °C for all solvent conditions over several days to weeks and aliquots at various time points sampled to monitor a change in the physicochemical properties of PrP.

3.2.3 Analysis of solubility of renatured PrP

Samples, usually 10 µl, from refolded PrP preparations were taken at different time points and centrifuged at 16,100 x g for 30 min to generate insoluble pellet and soluble supernatant fractions. Samples were analysed by SDS-PAGE and immunoblotted for detection of PrP with appropriate anti-PrP antibodies (3F4 for hamster Sc237 derived material or ICSM18 for mouse RML derived material). If PrP in D-PBS controls was found to be insoluble, further differentiation between the samples was examined by incubation with 1 % w/v SDS for 30 min at room temperature prior to centrifugation.

3.2.4 Electron microscopy of insoluble PrP preparations

Insoluble PrP fractions and denatured controls in GuHCl were analysed via electron microscopy (EM) by Dr Howard Tattum, within the MRC Prion Unit, in order to examine the aggregated structure of reconstituted PrP material. 10 µl of each reconstituted sample was used neat or diluted 5 fold in D-PBS before application on to carbon coated, glow-discharged, 300-mesh copper grids and processed as described elsewhere (103). Images were recorded at a magnification of 27,000 x in a Tecnai T10 microscope (FEI, Eindhoven, NL).

3.2.5 Analysis of proteinase K resistance of renatured PrP

To examine proteinase K (PK) resistant structures, samples of refolded PrP preparations were PK digested over a time course with varying concentrations of PK. In some cases samples were mixed with FVB PrP null (FVB $Prnp^{0/0}$ mice (325)) 10 % w/v brain homogenate to control for total protein levels. Samples without proteinase K were submitted to the same time course in the presence of PrP null 10 % brain homogenate in order to control for enzymatic degradation of PrP due to endogenous proteases present in brain homogenate. To monitor PK efficiency, wild type FVB brain homogenate was digested under the same conditions to show PrP^{C} digestion. Samples were analysed by SDS-PAGE and immunoblotted for detection of PrP with an appropriate anti-PrP monoclonal antibody.

3.2.6 Bioassay of refolded hamster PrP

To assess prion infectivity derived from hamster Sc237 refolded PrP samples, samples from two separate batches of hamster PrP refolded in PBS, reduced pH 4 buffer and buffer

containing Cu^{2+} ions were sampled after 9 and 38 days of incubation at 4 °C and pelleted by centrifugation at 16,100 x g for 1 h. Samples were then diluted into D-PBS at appropriate volumes (see **Section 3.3.4**) and 30 µl inoculated intra cerebrally into groups of Syrian as described elsewhere (326). Inoculations from both batches of PrP were done on the same day and 12 control animals were similarly inoculated with 30 µl sterile D-PBS. Care of animals was performed according to institutional guidelines. Inoculated hamsters were observed over 623 days post inoculation for signs of clinical prion disease, and were then killed using a schedule 1 procedure. To investigate subclinical prion infection the brains from the culled animals were half fixed for immunohistochemistry, and half frozen prior to homogenisation at 10 % w/v in D-PBS. 250 µl aliquots of 10 % brain homogenates were processed via NaPTA precipitation and PK digestion and analysed by high sensitivity immunoblotting. Immunohistochemistry was performed by Jackie Linehan, within the MRC Prion Unit, to assess spongiosis, neuronal loss and PrP^{Sc} deposition as described elsewhere (213). Briefly, brains were fixed in 10 % v/v buffered formol saline and then immersed in 98 % v/v formic acid for 1 h. The fixed tissues were paraffin wax embedded and serial sections of 4 µm nominal thickness were cut and treated with 98 % formic acid for 5 min and then boiled in a low ionic strength buffer (2.1 mM Tris, 1.3 mM EDTA, 1.1 mM sodium citrate, pH 7.8) for 20 min to abolish the PrP^{C} signal. Abnormal PrP accumulation was examined using anti-PrP monoclonal antibody ICSM35 (D-Gen Ltd, London, UK). ICSM35 has been produced in *Prnp*$^{0/0}$ mice immunised with human recombinant PrP^{91-231} in its β form (322). ICSM35 is an IgG2b immunoglobulin and its epitope lies within the sequence 93-105 of human PrP (213;318). Gliosis was detected using a rabbit polyclonal antiserum. Immunodetection was accomplished on a Ventana automated immunostaining system (www.ventanamed.com).

3.2.7 In vitro assessment of prion infectivity in refolded mouse PrP samples

After optimisation of a cell based infectivity assay "scrapie cell assay" (SCA) (144), it was possible to assess the infectivity of refolded mouse PrP derived from 10 % RML brain homogenate within as little as 2 weeks. Infectivity was assessed using the assay performed by Dr Peter Klöhn and Dr Francesca Properzi in the MRC Prion Unit as described elsewhere (144). The scrapie cell assay is an *in vitro* replacement for bioassays, in which a cell line that expresses PrP^{C} is capable of propagating PrP^{Sc} and prion infectivity after infection by certain prion strains. A murine neuroblastoma cell line, N2a, is susceptible to the mouse strain RML, and subclones have been produced that have a sensitivity to report RML prion infection that is greater than bioassay in reporter mice (144).

After assessment of solubility of the RML derived purified PrP samples at time points of greater than 3 days, aliquots were sampled from each condition and pelleted by centrifugation at 16,100 x g for 30 min. To check the efficiency of sedimentation of PrP, supernatants were analysed by PrP immunoblotting with ICSM18 (see **Chapter 2**), and pellets were processed for examination in the SCA. A mouse bioassay titered RML standard brain homogenate and/or RML starting brain homogenate from which PrP samples were derived was serially diluted and run in parallel to the unknown samples as positive controls and in some cases a sample of denatured mouse PrP in GuHCl was used as a denatured control (usually equivalent to 1 ml starting 10 % RML brain homogenate).

N2aPK1 cells (a highly susceptible subclone of N2a cells) were plated at 20,000 cells per well on a 96 well plate 16 h prior to addition of samples. Samples were diluted in Opti-MEM-10 % v/v FCS (OFCS) media before application of at least 4 replicates in the assay at 300 µl per well. After addition of samples, cells were processed via one of two different methods. For the SCA, cells were passaged at 1:10 dilutions three times over a period of 12 days. For a more sensitive approach to detect infectivity with reduced background, cells were processed via a scrapie cell end point assay (SCEPA) in which cells were passaged at

1:3 dilutions three times and 1:10 dilutions four times over a period of 21 days. In both assay formats, at the end of the incubation period, 25,000 cells from each well were resuspended in 250 µl of D-PBS and transferred to a corresponding well on an ELISPOT plate (Multi Screen Immobilon-P 96-well Filtration Plates, sterile, Millipore). ELISPOT plates were activated with 70 % v/v EtOH and washed twice with D-PBS by suction prior to addition of cells. D-PBS was removed by suction and cells dried on membranes for 1 h at 50 °C. PK was added at 50 µl from 0.5 µg/ml stock in lysis buffer (50 mM Tris-HCl, 150 mM NaCl, 0.5 % w/v sodium deoxycholate, 0.5 % v/v Triton X-100, pH 8.0) to each well and incubated 90 min at 37 °C. Following removal of PK by suction, samples were washed with D-PBS, exposed to 2 mM PMSF for 10 min, and washed again with D-PBS. After incubation with 160 µl of 3 M guanidinium thiocyanate to expose PrP^{Sc} epitopes in 10 mM Tris-HCl, pH 8.0 for 10 min, the filters were washed four times with PBS and incubated with 160 µl of Superblock (tris buffered saline blocking buffer, Pierce) for 45 min. Anti-PrP antibody ICSM18 was added at a volume of 50 µl from a concentration of 0.6 µg/ml in TBST containing 1 % w/v non-fat milk powder. After 1 h the supernatant was suctioned off and the wells were washed seven times with TBST in succession. Alkaline phosphatase-conjugated anti-IgG1 (Southern Biotechnology Associates) was added at a volume of 50 µl at a dilution of 1:4,500 in TBST containing 1 % milk powder and incubated for 1 h. Wells were washed eight times repetitively with TBST, and 50 µl of alkaline phosphatase conjugate substrate (prepared as recommended by Bio-Rad) was added until a clear colour was seen and followed by two washes with H_2O. Plates were stored in the dark at -20 °C. PrP^{Sc}-positive cells were counted by using a Zeiss KS ELISPOT system (Stemi 2000-C stereo microscope equipped with a Hitachi HV-C20A colour camera and a KL 1500 LCD scanner and WELLSCAN software from Imaging Associates, Bicester, U.K.).

SCA – scrapie cell assay

Infectious units for samples analysed via SCA were calculated through use of a standard curve (generated from a serial dilution of an RML brain homogenate of known prion titre from bioassay in CD-1 mice), where the number of spots per well correspond to i.c. LD_{50} units in CD-1 mice (144). The assay can reliably report prion infection after exposure to an equivalent of an 10^{-7} dilution of 10 % RML brain homogenate (144).

SCEPA – Scrapie cell end point assay

As the SCEPA assay was processed slightly different to SCA, infectious units could not be calculated using the RML standard curve but instead the calculation is based upon the proportion of positive wells. Positive wells were calculated using a threshold of the mean of spot numbers in the non-infected controls plus 5 x standard deviation (Positive well threshold = mean of uninfected cells + (5 x SD)). Any wells above this threshold would be considered positive and those below considered negative. Positive wells are then calculated as a proportion of the total (P = ln (empty wells/total wells)). The infectious units (IU) present in the sample are calculated based on positive wells and dilution (IU = P x dilution x proportion loaded). The limit of detection of cell infectious doses (ID) using this method is 1 or less per well, equivalent to a 10^{-9} dilution of 10 % RML brain homogenate (144).

3.2.8 Bioassay of refolded mouse PrP

Although the SCA can detect infectivity to levels equivalent to *in vivo* bioassay, the N2aPK1 cells used can only propagate the RML prion strain (144). As PrP was refolded *in vitro*, and it is possible that there can be multiple pathogenic conformations of infectious PrP, denatured PrP could refold with prion strain properties different to that of RML

(115;297;327). To assess if there was any infectivity associated with refolded mouse PrP that would not be reported by the SCA, prion infectivity was also assessed in CD-1 mice (Charles River Laboratories, Wilmington, MA, USA). CD-1 mice are outbred and express *Prnp* allele a (328), commonly used to propagate RML prions (329) and should be capable of propagating multiple mouse prion strains. To assess infectivity derived from refolded mouse PrP samples, aliquots equivalent to 1 ml starting 10% RML brain homogenate were taken and pelleted by centrifugation at 16,100 x g for 1 h and diluted into sterile D-PBS (see results) and 30 µl inoculated intra cerebrally into CD-1 mice as described elsewhere (295;298).

3.2.9 PrP^{Sc} extraction from human vCJD and mouse RML 10 % brain homogenates

10 % w/v vCJD brain homogenates (*PRNP* 129MM with type 4 PrP^{Sc} (272)) were processed through NaPTA precipitation and PK digestion. Inhibition of PK activity was achieved by the addition of PMSF (from stock concentration of 200 mM in dimethylsulphoxide (DMSO) or methanol) to 10 mM final concentration in the sample then centrifuged at 16,100 x g for 30 min. Pellets were then processed further by differential extraction with various reagents, and centrifugation (16,100 x g for 30 min) after each treatment to yield pellets containing PrP^{Sc}. Full details of all conditions tested are not discussed in this thesis, however, two effective methods identified were treatment with 3 M KI in D-PBS containing 0.1 % v/v Tween 20 and 50 x complete protease inhibitors (Roche) for 16 h at 22 °C with gentle agitation, or treatment with 100 mM glycine pH 2 for 15 min at 22 °C. Samples were centrifuged at 16,100 x g for 30 min after each step. Samples, including starting homogenate and supernatants were analysed by SDS-PAGE and immunoblot or silver staining for PrP^{Sc} yield.

After the optimisation of the SCA and following the results obtained using human CJD brain homogenates experiments were repeated using certain optimal conditions with 10 %

w/v RML brain homogenate suitable for SCA infectivity analysis. All homogenates were processed as above but treated with a wider range of KI concentrations at 0, 0.5, 1, 2 and 3 M. Samples were centrifuged at 16,100 x g for 30 min, supernatants aliquoted into separate tubes and pellets resuspended in D-PBS containing 0.1 % w/v sarkosyl at a 10 fold higher concentration than the starting 10 % brain homogenate. Samples at all stages were analysed by PrP immunoblotting with ICSM18 or silver staining for total protein. After assessment of yield, purity and PK resistance, samples were processed by Dr Francesca Properzi and Natalie Gros in the MRC Prion Unit for infectivity analysis via the SCEPA. All samples were diluted into appropriate media (see **Section 3.2.7**) and applied to the assay with all samples equivalent to 30 nl starting 10 % RML brain homogenate.

3.3 Results

The aim of this study was to investigate the refolding of purified PrP under different solvent conditions and observe any changes in solubility, aggregation state, PK resistance and prion infectivity. For the first time these experiments use PrP derived from *ex-vivo* PrP^{Sc} with potential disease specific post-translational modifications. Additional experiments to extract PrP^{Sc} whilst maintaining its PK resistance were also undertaken to identify possible co-factors that may influence prion infectivity and if identified could be applied to PrP refolding studies.

3.3.1 Change in solubility of purified refolded PrP under chosen conditions

A distinct property of PrP^{Sc} is its ability to aggregate (21;22;330) due to a predominantly β-sheet structure (97). Accordingly, 1 M NaCl was used in the reduced pH 4 buffer to promote protein aggregation.

PrP samples (typically 10 µl) from each refolding condition using hamster Sc237 or mouse RML derived PrP were assessed for solubility analysis at various time points after incubation at 4 °C (solubility properties shown in **Figures 3.1** and **3.2** are representative of many samples tested). Centrifugation was performed at 16,100 x g for typically 30 min. Under these conditions hamster derived PrP incubated with the pH 4 reduced buffer or buffer containing Cu^{2+} ions were found to be insoluble. **Figure 3.1** shows that there has been a fundamental change in the conformation and aggregation state of refolded PrP in both of the chosen solvents. Mouse RML derived PrP also shows marked insolubility after incubation in the reduced pH 4 buffer (**Figure 3.2**) (mouse RML derived PrP was not refolded with the buffer containing Cu^{2+} ions). Mouse PrP incubated in the D-PBS control buffer was also found to be insoluble. To distinguish between the insolubility of PrP refolded under different conditions, PrP samples were incubated at room temperature with

1 % w/v SDS for 30 min before centrifugation at 16,100 x g. **Figure 3.2** shows the solubility of refolded mouse RML PrP in the presence or absence of SDS. After SDS treatment, mouse PrP refolded in D-PBS is shown to be partially soluble, whereas PrP refolded in pH 4 reduced buffer remains insoluble.

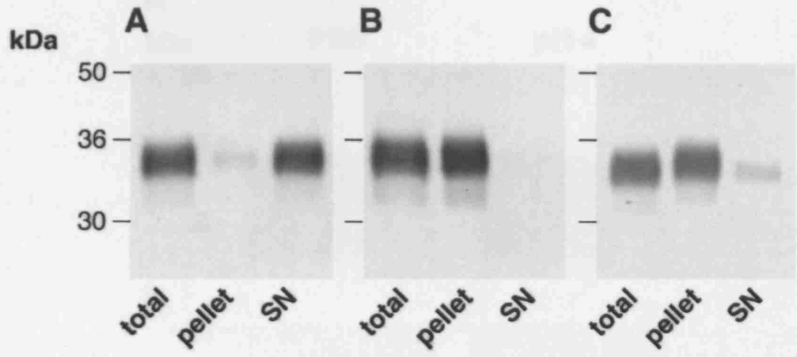

Figure 3.1: Solubility of hamster Sc237 derived PrP after refolding in different solvents

Each immunoblot shows 10 µl of each of the refolded PrP sample (total), (equivalent to 13 µl starting 10 % homogenate) or the pellet and supernatant (SN) fractions derived from identical 10 µl samples following centrifugation (16,100 x g for 30 min). Hamster Sc237 derived PrP refolded in D-PBS after 31 days of incubation is soluble (**A**), whereas PrP refolded in reduced pH 4 buffer after 31 days of incubation (**B**) or PrP refolded in the presence of Cu^{2+} ions after 12 days incubation (**C**) is insoluble. Immunoblots were labelled with anti-PrP monoclonal antibody 3F4 and developed using high sensitivity ECL.

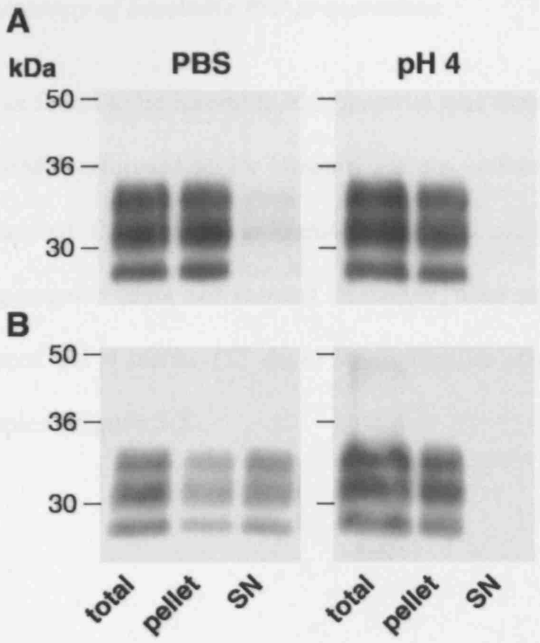

Figure 3.2: Solubility of mouse RML derived PrP after refolding in different solvents

Each immunoblot shows 10 µl of each of the refolded PrP sample (total, equivalent to 6.5 µl starting 10 % homogenate) in either D-PBS or reduced pH 4 buffer, or the pellet and supernatant (SN) fractions derived from identical 10 µl samples following centrifugation (16,100 x g for 1 h) after pretreatment with or without 1 % SDS for 30 min at 22 °C. Mouse RML derived PrP refolded in either D-PBS or pH 4 reduced buffer, after 20 days of incubation, is insoluble in the absence of SDS (**A**), However, after treatment with SDS prior to centrifugation, a proportion of PrP refolded in PBS becomes soluble, whereas all PrP refolded in reduced pH 4 buffer remains insoluble (**B**). Immunoblots were labelled with anti-PrP monoclonal antibody 3F4 and developed using high sensitivity ECL.

3.3.2 Electron microscopy of insoluble PrP preparations

As the refolded PrP was found to be insoluble, this material was examined by analysis with electron microscopy (EM) performed by Dr Howard Tattum, within the MRC Prion Unit. These experiments showed that insoluble hamster PrP and mouse PrP was typically comprised of small aggregates (data not shown). However, after prolonged incubation in either D-PBS or reduced pH 4 buffer (85 days) small fibrillar structures were found in RML derived PrP samples (**Figure 3.3**).

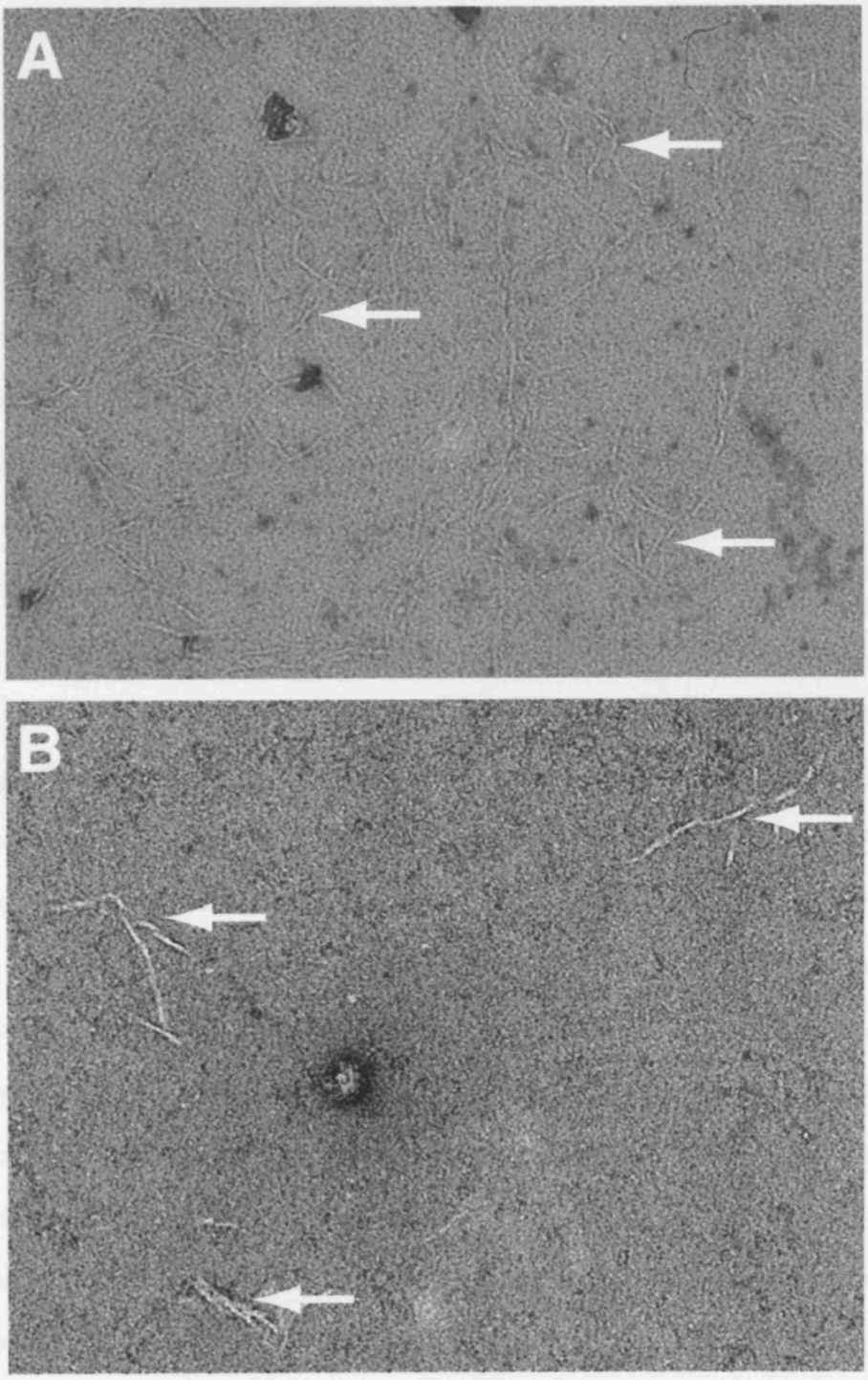

Figure 3.3: Electron microscopy of refolded mouse PrP

Fibrillar structures seen with mouse PrP refolded in PBS (**A**) or reduced pH 4 buffer (**B**) after incubation for 85 days at 4 °C. 10 µl of each PrP sample (equivalent to 16 µl starting 10 % brain homogenate) was diluted 5 fold in D-PBS before application on carbon coated, glow-discharged, 300-mesh copper grids. Recorded at 27,000 x magnification on a Tecnai T10 electron microscope (103).

3.3.3 Assessment of refolded hamster and mouse PrP for PK resistance

As PrP refolded in the chosen solvent conditions was found to be insoluble and consist of small aggregates, including fibrillar structures, it was investigated if these changes in conformation had conferred PK resistance to PrP.

PK sensitivity of refolded PrP was initially assessed using a protease concentration of 0.5-2 μg/ml over a time course of 0-60 min. Under these conditions, PrP signal was seen at short incubation periods but after prolonged incubation PrP was completely digested in all samples, with the exception of PrP refolded in buffer containing Cu^{2+} ions. As the protein levels in the samples were very low, this made the assessment of PK resistance difficult. To control for this the samples were subsequently supplemented with brain homogenate from *Prnp*$^{0/0}$ mice. These samples were then PK digested under conditions used to digest PrP in wild type FVB brain homogenate. Samples were centrifuged to collect insoluble PrP and pellets were resuspended in 1 % w/v FVB *Prnp*$^{0/0}$ brain homogenate and PK digested over time (see **Figure 3.4**). To control for variable PrP levels in the samples, a 10 fold higher volume was sampled from hamster PrP refolded in D-PBS compared to all other solvent conditions. To control for endogenous proteases in the FVB *Prnp*$^{0/0}$ brain homogenate, samples were also incubated without PK at the same time points to assess degradation of PrP. To control for PK activity, wild type FVB 1 % w/v brain homogenate was also digested at equivalent concentrations of protease for comparison. **Figure 3.4** shows the PK digestion of hamster Sc237 derived PrP, after incubation in the different solvent conditions, in the presence of 1 % FVB *Prnp*$^{0/0}$ brain homogenate. PrP refolded in the D-PBS control showed no PK resistance, but PrP in the reduced pH 4 buffer showed slight PK resistance at 10 min and in buffer containing Cu^{2+} ions PrP showed marked PK resistance even at 60 min. Control samples incubated without PK (**Figure 3.4B**) show that the degradation of PrP observed at earlier time points were not due to endogenous proteases, however some degradation was apparent after 60 min.

The PK resistance of PrP refolded in buffer containing Cu^{2+} ions was interesting as this could indicate that a PrP^{Sc}-like structure had been formed. To control for the high amount of Cu^{2+} ions compared to other samples it was necessary to digest them all in the same buffer. However a single centrifugation step would not be enough to reduce Cu^{2+} ions significantly below the original concentration. Because of the difficulties and potential loss of PrP associated with repetitive centrifugation and resuspension, Cu^{2+} ions were instead chelated by treatment with 10 mM EDTA. Under these conditions PrP was digested in all samples under the same PK conditions (data not shown). These data could be interpreted in two ways, either the PrP samples refolded in buffer containing Cu^{2+} ions had genuinely acquired PK resistance, but that this is reversed by Cu^{2+} ion chelation with EDTA or that Cu^{2+} ions have a direct inhibitory effect on PK itself. To control for the latter, BSA was used as a control protein, and PK digested under different Cu^{2+} ion concentrations and analysed via SDS-PAGE and silver staining. These experiments showed that as Cu^{2+} ion concentration increased so did the levels of detectable BSA (data not shown). These findings indicate that Cu^{2+} ions have a direct effect on the activity of PK and accordingly a detailed kinetic study was undertaken to assess this further. These findings are described in **Chapter 4**. As a consequence of these collective experiments it was concluded that no preparation of refolded hamster or mouse PrP had acquired significant PK resistance.

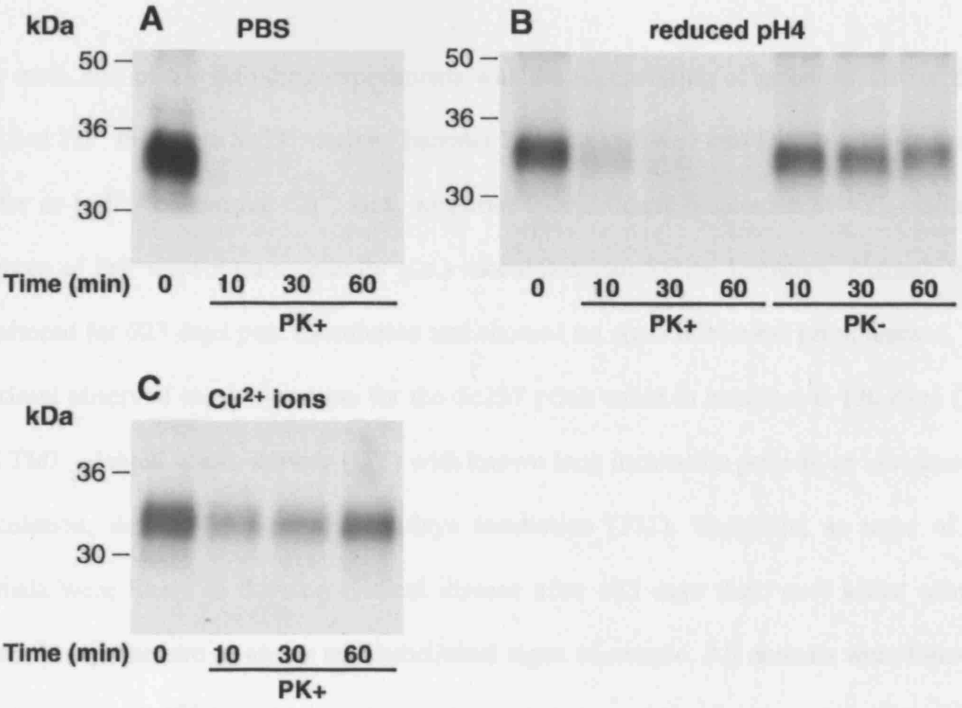

Figure 3.4: PK digestion of refolded hamster PrP

100 µl of PrP refolded in D-PBS buffer (**A**), or 10 µl of PrP refolded in reduced pH 4 buffer (**B**), or buffer containing Cu^{2+} ions (**C**), were sedimented by centrifugation (13,200 x g for 1 h) and pellets resuspended in 40 µl of 1 % FVB *Prnp*$^{0/0}$ brain homogenate. These samples were then PK digested (5 µg/ml PK at 37 °C) and 10 µl aliquots sampled at the time points of 0, 10, 30 and 60 min. Immunoblot labelled with mouse anti-PrP monoclonal antibody 3F4 and developed using high sensitivity ECL.

3.3.4 Bioassay of refolded hamster PrP

The main aim of the refolding experiments was the regeneration of prion infectivity from purified PrP. Insoluble Sc237 derived hamster PrP was refolded into D-PBS, reduced pH 4 buffer or buffer containing Cu^{2+} ions, and after 9 or 38 days incubation at 4°C, insoluble aliquots of PrP were intra-cerebrally (i.c.) inoculated into Syrian hamsters. Animals were monitored for 623 days post inoculation and showed no signs of clinical prion disease. The maximal observed incubation time for the Sc237 prion strain in hamsters is 130 days (24), and TME adapted strain, drowsy (DY) with known long incubation periods, at low dose i.c. inoculation, develop disease at 220 days incubation (331). Therefore, as none of the animals were likely to develop clinical disease after 623 days they were killed using a schedule 1 procedure to assess any subclinical signs of scrapie. All animals were found to be negative for PrP^{Sc} deposition and spongiosis via immunohistochemistry (see **Figure 3.5**) and PrP^{Sc} levels were undetectable using the most sensitive immunoblotting detection method (data not shown).

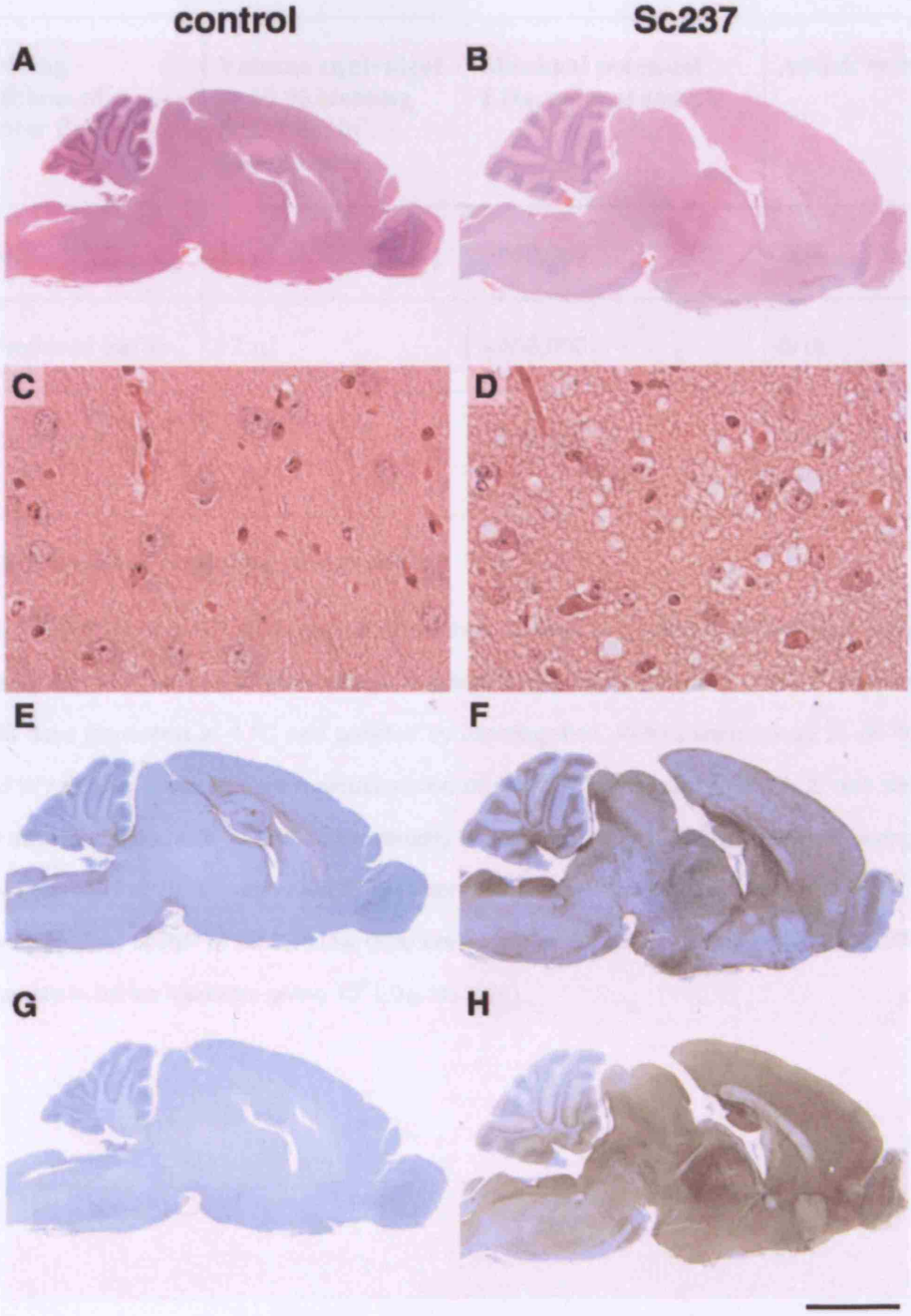

Figure 3.5: Immunohistochemistry of PrP^{Sc} deposition in Sc237 infected Syrian hamster brains

This figure demonstrates typical neuropathological features seen in clinically affected hamsters infected with the Sc237 prion strain. Hematoxylin and eosin (H&E) staining was used to detect spongiosis (**A**, **B**, **C** and **D**), GFAP staining to detect gliosis (**E** and **F**), and labelling with anti-PrP monoclonal antibody ICSM 35 to detect abnormal PrP deposition (**G** and **H**). Control panels of uninfected hamster brain show no spongiosis, gliosis or PrP deposition as expected. Bar for panels **A**, **B**, **E**, **F**, **G** and **H** is 4 mm, total width of panels **C** and **D** is 220 µm.

Refolding conditions of hamster PrP	Volume equivalent to 10 % starting Sc237 brain homogenate	Maximal potential LD_{50} units of sample	Attack rate
D-PBS	12 µl	~460,000	0/16
pH4 reduced buffer	12 µl	~460,000	0/16
Buffer containing Cu^{2+} ions	12 µl	~460,000	0/16

Table 3-1: Bioassay of refolded hamster PrP

Hamster Sc237 derived PrP samples from 2 batches refolded in 3 different buffers were inoculated intra-cerebrally in 8 Syrian hamsters (30 µl of refolded material per animal). Batch 1 was sampled after 38 days incubation at 4 °C and pelleted by centrifugation. Pellets were frozen at -80 °C and thawed to room temperature before resuspension on the day of inoculation. Batch 2, was sampled after 9 days incubation at 4 °C and pellets directly resuspended and inoculated without freezing. The volume equivalent of 10 % starting Sc237 hamster brain homogenate is based on the dilutions made and average yield of PrP of 50 %. LD_{50} units are based on titiration of hamster 10 % Sc237 brain homogenate in Syrian hamsters giving 10^8 LD_{50} /ml (326).

3.3.5 Assessment of prion infectivity of refolded mouse PrP in the scrapie cell assay

Samples usually equivalent to 1 ml starting homogenate (either as pellets of insoluble refolded PrP, or 5 µl of PrP in GuHCl as a control) were resuspended in media suitable for the scrapie cell assay in normal or end point format (see **Section 3.2.7**) and serially diluted to assess prion infectivity. For each experiment the starting 10 % RML brain homogenate was also serially diluted as a positive control. Infectious units were calculated either via a standard curve based on a correlation with a bioassay using a previously titrated stock RML homogenate (SCA) or using an equation based on number of positive wells for the more sensitive end point format assay (SCEPA) (see **Section 3.2.7**).

Despite application of relatively high quantities of refolded PrP all samples were found to be negative for detectable infectivity by both assays. **Table 3-2** shows that if all PrP molecules had folded into an infectious conformation then the maximal LD_{50} units would have been at least 10^6. Based on this data, it was concluded that if a pathogenic PrP conformer had been generated then this was at a concentration of < 1 part per million of total PrP.

RML derived purified PrP sample	Refolding conditions	Volume equivalent of 10 % RML brain homogenate (lowest dilution)	Maximal potential LD_{50} units of sample[a]	Positive wells (lowest dilution)
Truncated PrP	PBS	26 µl	~1.65 x 10^6	0/32[bc]
Truncated PrP	Reduced pH4	26 µl	~1.65 x 10^6	0/32[bc]
Truncated PrP	GuHCl	26 µl	~1.65 x 10^6	0/24[cd]
full length PrP	PBS	53 µl	~3.3 x 10^6	0/12[e]
full length PrP	Reduced pH4	53 µl	~3.3 x 10^6	0/12[e]
full length PrP	GuHCl	53 µl	~3.3 x 10^6	0/12[e]

Table 3-2: Scrapie cell assay of refolded mouse PrP

PrP samples were from several experiments and applied directly into the SCA. All samples had been incubated at 4 °C for at least 30 days and assessed for solubility prior to addition in the assay. Each well was loaded with 300 µl of refolded PrP pelleted by centrifugation at 16,100 x g for 1 h and resuspended in Opti-MEM containing 10 % FCS (OFCS) (Invitrogen) followed by a serial dilution. Samples were processed for either normal scrapie cell assay (SCA) or end point format (SCEPA). Positive wells were calculated based on spot number thresholds for each separate assay and infectious units based on calculations from mouse RML brain homogenate used in the SCA and SCEPA. LD_{50} units based on comparison to spot number from titred RML brain homogenate. As all samples were negative, only the lowest dilution is shown. Volumes of refolded PrP are given as the equivalent of 10 % starting RML brain homogenate based on the dilution made and an average yield of PrP of 50 %.

a) LD_{50} units based on comparison to bioassay of starting 10 % RML brain homogenate with $10^{8.8}$ LD_{50} units per g of brain (144) and 1 ml volume of a 10 % brain homogenate contains 100 mg wet weight brain

b) Results from 3 different batches of refolded PrP. One batch was plated at 8 wells per dilution for a normal SCA, 2 other batches were plated at 12 wells per dilution for the SCEPA assay

c) Batch 3 also used for *in vivo* bioassay, see below

d) Results from 2 different batches of refolded PrP plated at 12 wells per dilution for the SCEPA assay

e) Results from 1 batch of refolded PrP plated at 12 wells per dilution for the SCEPA assay

3.3.6 Bioassay of refolded mouse PrP

As the SCA can only report RML prions, it was necessary to use a mouse bioassay to investigate the generation of prion infectivity from refolded PrP that may have the properties of another prion strain. CD-1 mice were chosen for this purpose as they express *Prnp* allele a that can report multiple mouse PrP strains (328). Samples from mouse RML PrP refolded in D-PBS and reduced pH 4 buffer were sampled after incubation at 4 °C to assess solubility. Prior to bioassay the PrP samples had also been previously scored negative for prion infectivity in the SCA (see **Table 3-2**).

Each sample of purified PrP used to generate the inoculum represented the equivalent of 2 ml 10 % starting homogenate in 600 µl of reconstitution buffer. 300 µl of the sample (equivalent of 1 ml starting material) was taken after 89 days incubation at 4 °C and centrifuged at 16,100 x g for 1 h. A sample of original denatured purified PrP in GuHCl (5 µl aliquot equivalent to 1 ml starting homogenate) was also assayed. PrP pellets and the GuHCl sample were resuspended in 500 µl of D-PBS and 30 µl (equivalent of 24 µl starting 10 % brain homogenate) inoculated i.c. into CD-1 mice.

To date these mice have been observed over 350 days incubation without clinical signs of prion disease. Incubation time for RML inoculation of CD-1 mice is less than 350 days (326;332), indicating that is it unlikely the animals will succumb to clinical disease indicative of the RML prion strain thereby correlating with results from the SCA. However, as prolonged incubation times have been observed in other experiments, for example nearly 600 days with the synthetic PrP fibrils of Legname et al (124), mice are still being observed and will be assessed for possible subclinical infection in due course.

3.3.7 Investigations using purified full length mouse RML derived PrP

After the adaptation of the methods described in **Chapter 2** omitting PK digestion, full length mouse RML derived PrP was refolded under the conditions used for truncated PrP. Full length mouse PrP refolded under these conditions gave similar results to truncated PrP. Full length PrP samples showed complete insolubility after refolding in both D-PBS and reduced pH 4 buffer, and again D-PBS refolded PrP was observed to be partially soluble in the presence of 1% SDS. As with truncated PrP, refolded full length PrP showed no measurable PK resistance or infectivity in the SCA (data not shown). These data indicate that under the conditions tested the N-terminus of PrP has no additional effects in confering a PrP^{Sc}-like conformation.

3.3.8 Purification of human type 4 vCJD PrP^{Sc}

As yet it is unknown how PrP folds to an infectious conformation. The protein only hypothesis suggests that PrP^{Sc} is the sole infectious agent, but a variety of other co-factors could be needed to either target PrP^{Sc} into cells, play a part in the unfolding and refolding of PrP^{C} to the infectious conformation or stabilise infectious conformations. With the aim of identifying possible co-factors for use in the refolding studies described here, it was sought to purify PrP^{Sc} in a native PK resistant conformation by strategical rounds of extraction, similar to previous work reported (reviewed in (305)). Without a cost and time effective bioassay for human prions, assessment of PrP^{Sc} PK resistance rather than prion infectivity was initially used to screen appropriate conditions for purification.

Human type 4 vCJD 10 % brain homogenate was processed via NaPTA precipitation and PK digestion at 50 μg/ml followed by a panel of differential chemical extractions. Most methods were unable to solubilise and remove other proteins without also effecting PrP^{Sc} (data not shown). The best conditions discovered were overnight treatment with 3 M KI at

22 °C followed by treatment with 100 mM glycine at pH 2 for 15 min at 22 °C (see methods). The majority of PrP^{Sc} was found to remain in the pellet after centrifugation at 16,100 x g for 30 min and the majority of other proteins were solubilised into the supernatant (**Figure 3.6**). However, as these methods were acheived using vCJD material, there is no method to rapidly assess human prion infectivity (295;298).

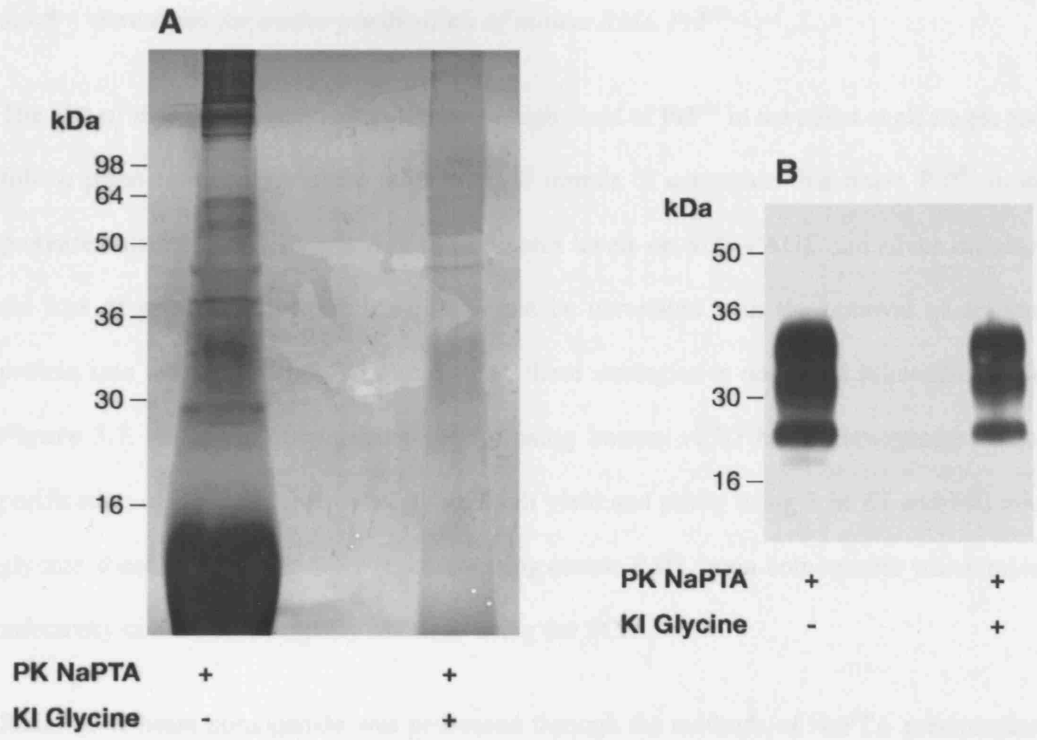

Figure 3.6: Potassium iodide and glycine treatment to purify PrP^{Sc} from type 4 vCJD brain homogenate

Human vCJD 10 % brain homogenate was processed via NaPTA precipitation and PK digestion at 50 µg/ml. The additional steps of incubation with 3 M KI followed by 100 mM glycine, with centrifugation at 16,100 x g for 30 min after each step, were applied for comparison of purity and yield. Total protein is shown via SDS-PAGE and silver staining (**A**) (2 ml equivalent of starting 10 % brain homogenate in each lane) and PrP yield by SDS-PAGE and immunoblotting (100 µl equivalent of starting 10 % brain homogenate in each lane) (**B**). The immunoblot was labelled with mouse anti-PrP monoclonal antibody 3F4 and developed using high sensitivity ECL.

3.3.9 Strategies for native purification of mouse RML PrP^{Sc}

The aim of these experiments was to have a high yield of PrP^{Sc} in the pellet at all stages and follow prion infectivity via the SCA through rounds of extraction that retain PrP^{Sc} in its protease resistant state. By viewing total protein levels on SDS-PAGE and silver staining, the loss of prion infectivity at any stage can be correlated with the removal of another protein into the supernatant. A summary of these strategies is described schematically in **Figure 3.7**. After the encouraging results using human vCJD brain homogenate where purification of PrP^{Sc} was achieved giving high yield and purity using 3 M KI and 100 mM glycine, these experiments were repeated using mouse RML brain homogenate where prion infectivity could also be rapidly assessed using the SCA.

RML 10 % brain homogenate was processed through the methods of NaPTA precipitation and PK digestion, yielding pellets enriched with PrP^{Sc} that can be further treated by differential methods of chemical extraction. Samples were centrifuged after each step at 16,100 x g for 30 min and both pellet and supernatant analysed in comparison with the starting material to examine PrP recovery, purity, prion infectivity and where appropriate a change in conformation of PrP by further PK digestion. Yield and purity was assessed via SDS-PAGE and immunoblotting or silver staining and infectivity was assessed using the SCA.

NaPTA precipitation and PK digestion of mouse RML brain homogenates gave a considerable increase in purity, shown by visualisation of distinct PrP bands and minimal contaminants on silver stain (**Figure 3.8B**). This finding was in contrast to vCJD brain homogenate processed via the same methods, where a much lower purity was observed (**Figure 3.6**). This study exemplifies the differences between prion strains and species. Comparison of immunoblot and silver stain shows a proportional removal of PrP with contaminants after exposure to increasing concentrations of KI (**Figure 3.8**) with no apparent further increase in the purity of PrP. Due to large sample volumes, it was difficult

to assess if PrP was solubilised into the supernatants or degraded. Accordingly, to investigate if treatment with KI had changed the PK resistant conformation of PrP^{Sc}, pellets were resuspended in D-PBS and treated with PK at 50 μg/ml for 1 h at 37 °C. **Figure 3.9** shows that approximately one third of the PrP^{Sc} has retained PK resistance. However, digestion of pellets not treated with KI also showed a similar decrease in protease resistance (data not shown) it is therefore likely that changes in protein:PK ratios have influenced these findings. These data are comparable to those of other researchers (333) showing that the majority of PrP^{Sc} can be degraded by prolonged protease treatment. Overall these findings established that partial PK resistance is retained by PrP^{Sc} exposed to KI, but this could not be accurately quantified.

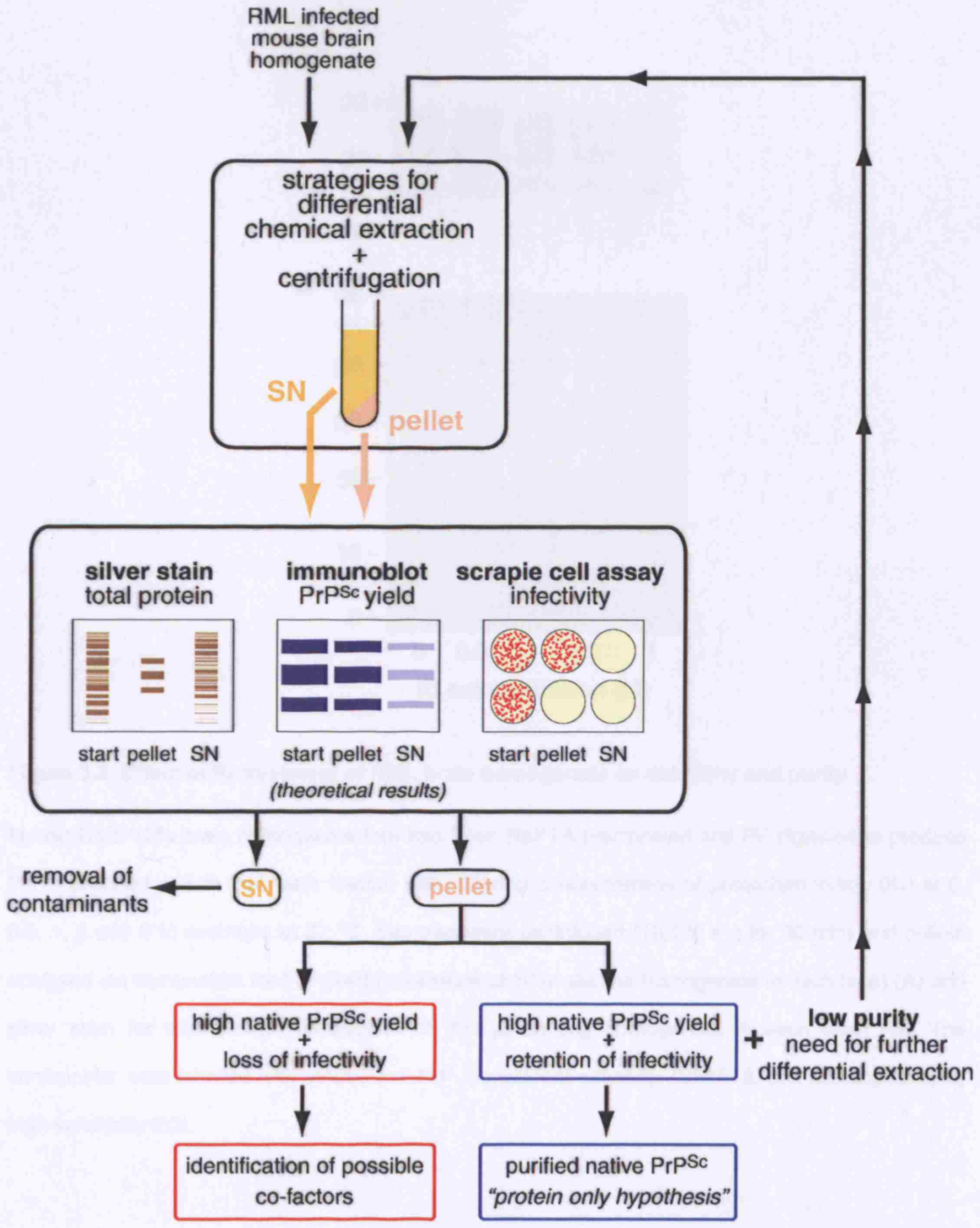

Figure 3.7: Strategical methods for purification of PrP^{Sc}

Rounds of chemical extraction and assessment of PrP^{Sc}, total protein (for contaminants and/or co-factors) and infectivity to analyse the structural components of an infectious prion.

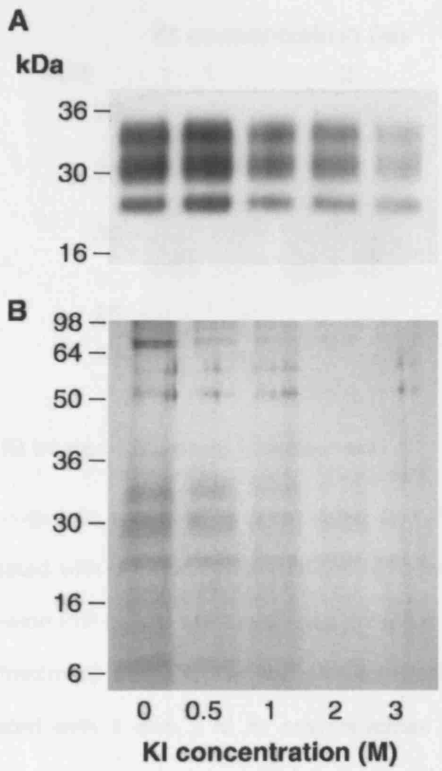

Figure 3.8: Effect of KI treatment of RML brain homogenate on solubility and purity

Mouse RML 10% brain homogenate that had been NaPTA precipitated and PK digested to produce PrP^{Sc} enriched pellets that were treated with differing concentrations of potassium iodide (KI) at 0, 0.5, 1, 2 and 3 M overnight at 22 °C. Samples were centrifuged (16,100 x g for 30 min) and pellets analysed via immunoblot for PrP yield (equivalent of 10 µl starting homogenate in each lane) (**A**) and silver stain for total protein (equivalent of 200 µl starting homogenate in each lane) (**B**). The immunoblot was labelled with mouse anti-PrP monoclonal antibody, ICSM-18, and developed using high sensitivity ECL.

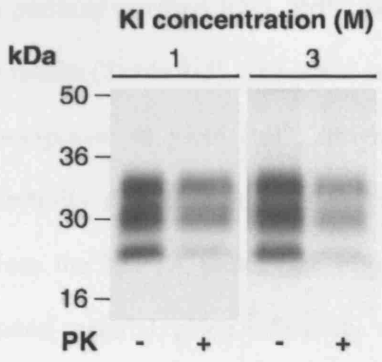

Figure 3.9: PK digestion of KI treated RML brain homogenate

Mouse RML 10 % brain homogenate was NaPTA precipitated and PK digested to produce PrP^{Sc} enriched pellets that were treated with differing concentrations of KI (centrifugation at 16,100 x g for 30 min after each step). KI treated PrP pellets were subjected to further PK digestion (50 µg/ml for 1 h at 37 °C) to see if the KI treatment had affected the protease resistant conformation of PrP^{Sc}. Representative samples treated with 1 and 3 M KI are presented (equivalent of 10 µl starting homogenate in each lane). Densitometry (using a Kodak Image Station 440 CF, Kodak, Hemel Hempstead, UK) shows that approximately one third of PrP^{Sc} signal remains after PK digestion.

Assessment of infectivity in partially purified RML PrP^{Sc} samples via the SCEPA assay yielded extremely interesting results (**Table 3-3**). The initial step of NaPTA precipitation of mouse RML 10% brain homogenate to yield PrP^{Sc} enriched pellets showed that this material retained 100 % infectivity (**Table 3-3**). This finding is consistent with highly efficient recovery of PrP^{Sc} into the NaPTA pellet (see **Figure 2.4**). However, after PK digestion of NaPTA precipitated material, prion infectivity was reduced to ~3 % of that present in an equivalent volume of starting RML homogenate. As PrP levels were not significantly different between these samples (see **Figure 2.4**) in relation to the protease resistant core of PrP^{Sc} (PrP^{27-30}) these data show that prion infectivity has changed dramatically without alteration of the concentration of PrP. This novel finding indicates the degradation of a component in the sample that has changed the specific infectivity of PrP^{Sc} (see **Section 3.4**). In contrast, subsequent treatment with KI showed no significant change in infectivity (**Table 3-3**) that could not be correlated with the amount of insoluble PrP^{27-30} retained in the pellet (**Figure 3.8**). Thus under these conditions prion infectivity correlates with PrP^{27-30} levels as extensively reported by others (27-29) (reviewed in (33)).

Unfortunately, this extremely interesting finding occurred at the end of the experimental work of this PhD. However studies are being continued in the MRC Prion Unit to investigate the component that is degraded in RML PrP^{Sc} infected brain homogenates resulting in the change in specific prion infectivity in these experiments.

Treatment	Log ID U/ml	ID retention (%)
Starting homogenate	7.248094	100 %
NaPTA treatment	7.272148	105.6 %
NaPTA and PK treatment	5.695172	2.79 %
O/N incubation	5.942361	4.95 %
0.5 M KI O/N incubation	5.637181	2.45 %
1 M KI O/N incubation	5.705569	2.87 %
2 M KI O/N incubation	5.658519	2.57 %
3 M KI O/N incubation	5.348383	1.26 %

Table 3-3: ID units of RML brain homogenate treated with NaPTA, PK and KI

Mouse RML 10% brain homogenate was processed through NaPTA precipitation and PK digestion (50 µg/ml for 1 h at 37 °C) (centrifugation at 16,100 x g for 30 min after each step) followed by incubation overnight (O/N) with various concentrations of potassium iodide (KI) 0-3 M. All samples were compared at equal volumes equivalent of 30 nl starting homogenate per well. Starting mouse 10 % RML brain homogenate contains $10^{7.248094}$ ID U/ml which are retained after NaPTA precipitation, but after PK digestion approximately infectivity is reduced to 3 %. ID units calculated via equations used for the SCEPA assay (see **Section 3.2.7**).

3.4 Discussion

Despite a wealth of research into prion structure, relatively little is known about PrP^{Sc} native conformation and whether PrP alone constitutes prion infectivity. As PrP^{Sc} is aggregated, isolation in a native state is extremely difficult. As a consequence most studies have concentrated on the refolding of rPrP to investigate the acquisition of PrP^{Sc}-like properties. However, important post-translational modifications may be essential for conferring prion infectivity and therefore studies with recombinant PrP may be inappropriate. Accordingly in this study the high yield purification of denatured PrP^{Sc} developed as described in **Chapter 2** has been exploited to provide a substrate for these experiments.

In accordance with reports in the literature, under the methods chosen, immunoaffinity purified PrP from both hamster Sc237 and mouse RML brain homogenates refolded into an insoluble conformation (94;122). Although the secondary structure could not be assessed for amount of β-sheet content due to low protein concentration, insoluble PrP was examined by electron microscopy. Over prolonged incubation periods RML derived mouse PrP was found to form fibrillar structures in addition to predominant amorphous aggregates. Detailed investigation of these may now be possible as described for fibrils derived from rPrP (103;334;335).

Although insoluble PrP aggregates were readily generated, none of the refolded PrP showed significant PK resistance, with the exception of hamster Sc237 derived material refolded in the presence of Cu^{2+} ions. However, this was found to be a false result due to direct inhibition of PK by Cu^{2+} ions (see **Chapter 4**). Although acquisition of protease resistance was not seen in insoluble PrP preparations, the assessment of this was difficult due to low PrP concentrations. However, as some pathogenic PrP conformations appear to be protease sensitive (241;336;337), the lack of acquisition of a protease resistant conformation may not necessarily imply that a pathogenic PrP conformation had not been

formed. Accordingly, insoluble PrP preparations were assessed for prion infectivity by bioassay and in the scrapie cell assay. Despite application of relatively large quantities of PrP no prion infectivity was detected.

The failure to generate infectivity under the conditions used to refold PrP could be due to a number of reasons, not just inappropriate conditions for refolding. A study by Telling et al in 1995 proposed that there may be a co-factor required for prion replication (338), while recently ferritin has shown to be co-transported with PrP^{Sc} into cells (339). Studies have also showed that PrP can enter cells via the laminin receptor (340).To date, however, no firm evidence has been reported for a co-factor that is essential for prion infectivity or PrP^{Sc} replication. Nevertheless, co-factors could be required to stabilise disease associated PrP conformations or mediate the targeting of PrP^{Sc} into cells.

The experiments designed to find possible co-factors required for specific prion infectivity produced extremely interesting results. Full prion infectivity was retained after NaPTA precipitation, showing correlation with efficient recovery of insoluble PrP^{Sc}. However, infectivity was reduced ~30 fold after PK digestion of NaPTA enriched pellets. The dramatic reduction in infectivity without loss of PrP^{27-30} concentration shows that the protease resistant core of PrP has lower specific prion infectivity. Although prion infectivity thereafter broadly correlated with PrP^{27-30} concentration during extraction with KI, these data show that an important factor influencing prion infection had been degraded. It could be that in this particular strain of prion, RML, the N-terminus is very important for the infectious conformation, or an important additional co-factor for specific infectivity could have been digested. These results could also, however, have exposed an experimental caveat of the SCA in that a prion co-factor that may be acquired *in vivo* is not present in this particular cell line.

The involvement of the protease sensitive N-terminal region of PrP^{Sc} in infectivity is unclear. Partially purified preparations of PrP^{Sc} have always utilised protease digestion at

an early stage and thus reported the infectivity of PrP^{27-30} (27-32). As precise (within 10 fold) infectious titre is hard to determine in bioassay it is difficult to compare PrP^{27-30} with total protein levels in whole brain homogenate. Thus it is unknown if protease treatment reduces specific prion infectivity when measured *in vivo*. Studies using transgenic mice have shown that inoculation of the RML prion strain into transgenic mice expressing a truncated form of PrP^{C} have a marked increase in incubation time compared with those expressing full length PrP (125;341). These studies suggest the N-terminus is an important part of the RML infectious prion. The N-terminus of the prion protein could be involved in stabilising PrP structure, targeting to specific cellular compartments (either directly or through interaction with co-factors) or prevention of clearance after inoculation. Recent studies have shown that the N-terminus of PrP facilitates entry into cells via macropinocytosis (342) suggesting one possible reason for the reduction in specific prion infectivity.

Although hamster PrP refolded in buffer containing Cu^{2+} ions did not acquire a protease resistant or infectious conformation, copper may still be important for prion infectivity. Other studies have shown that Cu^{2+} ions may genuinely change PrP^{Sc} conformation (119-121;279) and copper could be important in stabilising an infectious conformation of PrP. Copper is known to bind to the N-terminus of PrP (70), a region of the protein which is not contained in the protease resistant core of PrP^{Sc}, PrP^{27-30}. Thus, truncated PrP used in the refolding conditions may not reveal an essential Cu^{2+} mediated effect. Further experiments with full length PrP will be important in this regard.

Original studies calculated that ~ 10^5 PrP^{Sc} molecules constitute one infectious unit (28). These data suggested that either that a large oligomer of PrP^{Sc}, or minor subpopulation of PrP^{Sc} is actually infectious. However, the proposal that small PrP oligomers are the most infectious prions (147) do not support the idea of large PrP aggregates as originally suggested. Subsequent studies showed that the amount of PrP^{Sc} which reached the target for replication and infectivity was much less. In 2005 Safar and colleagues calculated that the

amount of PrP^{Sc} constituting one infectious unit was between 1000 and 4000 (145) due to clearance out of the brain in the first 24 hours (146). How PrP^{Sc} is cleared from cells is unknown, but some studies suggest that hydrolysis in acidic endosomes or lysosomes is likely (49;343).

The recent finding that fibrils synthesised from rPrP corresponding to the protease resistant core of PrP^{Sc} are infectious (124;125) again raises the issue of specific prion infectivity. Although the experimental evidence from Legname et al supports the protein only hypothesis and suggests that the protease resistant core of PrP^{Sc} is the infectious agent, there was a low infectious titre. 15 μg of PrP (equivalent to that present in ~10 ml 10 % brain homogenate) was inoculated into each animal and yet affected mice developed disease after at least 500 days, well beyond end point of all mouse adapted prion strains (124;304). Assuming all PrP molecules were in an infectious conformation, based on an RML-like, PrP:prion infectivity ratio then $>10^8$ infectious units were inoculated. Factors reducing specific prion infectivity in these experiments could be a clearance mechanism removing inoculated PrP (145;146), or that entry into cells could be limited (344-346). Also, the majority of inoculated PrP was of a fibrillar structure (93), and as the most infectious unit may be a much smaller oligomer of PrP^{Sc} (147), it is possible that only a few infectious oligomeric species are associated with the fibrillar material. A strain specific effect could also be the case, whereby an infectious conformation could have been produced, but due to conformational selection a low rate of prion replicication occurred with host PrP^{C}. A reduction in incubation time on subsequent passage supports the possibility of a strain specific effect (125;126). However, the low titre of synthetic prions generated precludes detailed structural analysis of an infectious prion. These experiments may also suggest the presence of a missing co-factor.

Studies have shown that scrapie brain microsomes have a higher efficiency for prion replication than purified PrP^{Sc} (346) which could indicate the presence of a co-factor that is contained in the microsome fraction. Evidence for the membrane itself being a co-factor is

shown by studies reconstituting purifed PrP into synthetic liposomes with phosphatidyl choline increasing specific prion infectivity (344;345). These membrane fractions were shown to internalise into cells (346), comparable with *in vivo* studies (347). Internalisation has also been shown to be mediated via the laminin receptor suggesting a co-factor could mediate internalisation (340). These data could imply that the studies of others and those reported in this thesis, could have generated infectious conformations of PrP, but in the absence of a co-factor are unable to infect cells.

Post translational modifications could also be an important part of an infectious PrP^{Sc} conformation. Although the amino acid sequence is known to be the same as PrP^{C} (36;37), little is known about any other differences between the molecules. In the Legname et al experiments, amino acid changes could have been acquired in the host animal or though chemical modifications (for example oxidation or deamidation) during the preparation that could have resulted in a minor population of modified PrP that is infectious (126). Analysis of purified *ex-vivo* PrP from different strains, processed through methods described in **Chapter 2**, may provide more information on possible post-translational modifications and will provide a substrate for further refolding studies.

3.4.1 Conclusions and future work

The most significant finding from the work described in this chapter is the effect of PK digestion dramatically reducing prion infectivity of RML prions. These important results have now been repeated and verified by other scientists within the MRC Prion Unit. The reduction in specific infectivity suggests that the $PrP^{27\text{-}30}$ is lacking a co-factor (which may be the PrP N-terminus) required for high specific infectivity. Further investigations may provide information on the nature of the co-factor which can then be applied to refolding studies using purified *ex-vivo* PrP to assess the structural components of an infectious prion.

Firstly, to analyse the reduction in specific infectivity shown in the scrapie cell assay with NaPTA precipitated and PK digested prion infected brain homogenate, it is important to show if this finding relates only to the *in vitro* assay. As a whole mammalian organism has many components that could be acquired for prion infectivity, which could be lacking in an *in vitro* system, experiments using NaPTA precipitated and PK digested prion infected brain homogenate are now being repeated for bioassay in CD-1 mice. Comparison of full length and PK truncated PrP^{Sc} infectious titres in bioassay and correlation with *in vitro* results may show that changes in specific prion infectivity seen *in vitro* are abrogated in a whole mammalian system.

Although bioassay results may be difficult to interpret, alongside these studies, potential prion co-factors could be sought by the partial purification methods described in **Figure 3.8** omitting proteolytic cleavage and following specific infectivity assessed by the scrapie cell assay. By assessing protein bands visualised on silver stain followed by amino acid sequence sequencing, specific proteins could be identified and added to PK digested material and/or purified PrP to assess changes in infectivity or acquisition of PrP^{Sc}-like properties and infectivity. The methods originally planned to include PK digestion, however this now seems inappropriate. Future studies should simply use potassium iodide and glycine treatment, among other methods of chemical extraction.

As well as following specific infectivity with native PrP^{Sc} purification, a more extensive refolding study using a range of solvent conditions should be undertaken. The solvent conditions chosen for the refolding studies described in this thesis, were examples of many similar conditions that have been reported. The methods for producing amyloid fibrils that gave Legname et al their synthetic prions include refolding in 5 M urea pH 3.7 followed by a further dilution in simple sodium acetate buffer to pH 5.5 (93). These methods are very similar to the low pH buffer used for refolding PrP as discussed in this thesis, with the omission of reducing agent, and should be applied to refold purified PrP in due course.

Although a simple solvent condition induced infectious prions for Legname et al, their low infectious titre and other studies suggest that other components may be necessary. Prion targeting is shown to be very important (344-346) and methods to reconstitute PrP into synthetic liposomes, or other membrane fractions that direct prions into cells is a priority to study.

Even though the conditions for refolding PrP with Cu^{2+} ions did not reconstitute prion infectivity using truncated hamster PrP, different results may be observed using full length PrP. As Cu^{2+} ions are known to bind to the octapeptide repeat region (70), stability of an infectious PrP conformation may be coordinated via this region, and assessment of truncated PrP may be unsuitable. Other co-factors may also be important for coordinating a stable infectious conformer by binding PrP, such as ferritin (339), and should be assessed in refolding conditions using full length purified PrP.

Although it is yet to be determined what the role of the N-terminus of PrP^{Sc} has in determining prion infectivity, so far refolding of full length purified PrP has not yielded any conformational differences to the truncated form. However, as it is now possible to purify full length, fully post-translationally modified PrP, all future refolding conditions should be performed using this substrate. If an infectious conformation is achieved from fully post-translationally modified PrP then investigations towards the strategic removal of the various post-translational modifications can be analysed to give further information as to the core component of an infectious prion.

4 Inhibition of proteinase K activity by Cu^{2+} ions

4.1 Introduction

Proteinase K (EC 3.4.21.14) is a typical member of the subtilisin family of proteinases (S8). The polypeptide chain consists of 278 amino acids, with molecular mass 28,930, and a pI of 8.9 (348). Proteinase K is an endopeptidase and carries at its active site the catalytic triad N^{39}, H^{69}, S^{224}. Proteinase K binds two Ca^{2+} ions, one tightly with a pK of 7.6×10^{-8} M^{-1}, and the other so loosely that its dissociation constant could not be determined (349). PK requires the Ca^{2+} ions for stability (348;349). If the Ca^{2+} ions are removed, a structural change is observed (350;351). Maximal activity is in the pH range 7.5–12.0 with a specific activity at about 300 U/mg, where one unit hydrolyzes 1 μ mole of N-Acetyl-L-Tyrosine ethyl ester (Ac-Tyr OEt) per minute at pH 9.3 at 30 °C in Tris-HCl buffer (352). Proteinase K remains active even at higher temperatures, until denaturation at 69 °C, and it is stable in 2 M urea, 0.5 % (w/v) SDS or 1% (w/v) Triton X, (352;353). Peptidyl chloromethanes (349;354-356) and Hg^{2+} ions (357-359) act as inhibitors. Several inhibitors of proteinase K have been isolated from wheat germ (360).

Proteinase K is relatively unspecific as shown by the cleavage of oxidized insulin B chain (361), but has a preference for aromatic and hydrophobic amino acids in P1, like other subtilisins (362). Besides peptide bonds, proteinase K also hydrolyzes esters (363). Studies on the crystal structure of proteinase K have illustrated the geometries of the catalytic site and the substrate recognition sites (355;356;364-366). The high resolution (0.98 Å) structure determined for proteinase K (367) showed several regions of the main chain and the side chains that had not been seen clearly in the earlier structures. Hydrogen bonds were clearly identified in the catalytic triad (Serine-Histidine-Aspartic acid), and electron density was observed for an unusual, short hydrogen bond between aspartic acid and histidine in the catalytic triad, designated the 'catalytic hydrogen bond'.

The 'chloromethyl-ketone' group of inhibitors attack the catalytic residues H^{69} and S^{224} to form two covalent links, one between H^{69}-N and the methylene group, and the other between S^{224}-Oγ and the ketone carbon atom. The ketonic oxygen carries a negative charge and is hydrogen bonded to N^{161}-Nδ and S^{224}-NH forming the 'oxyanion hole'. The peptide parts of these inhibitors are in extended conformations and fill subsites S1–S5 of the substrate-recognition site. Their backbones hydrogen bond with strands 100-104 and 132-136 of proteinase K to form three-stranded antiparallel β-pleated sheets. The complex between proteinase K and inhibitor PKI3 from wheat germ shows at 2.5 Å resolution that the inhibitor interacts with the active site and causes distortion of the active S^{224} such that it is no longer part of the catalytic triad (360). Proteinase K contains five cysteines, of which four form two disulfide bonds and one, C^{72}, is located close to H^{69} of the catalytic triad. This is where the inhibitor Hg^{2+} binds, and inhibits by distorting the active-site geometry (358).

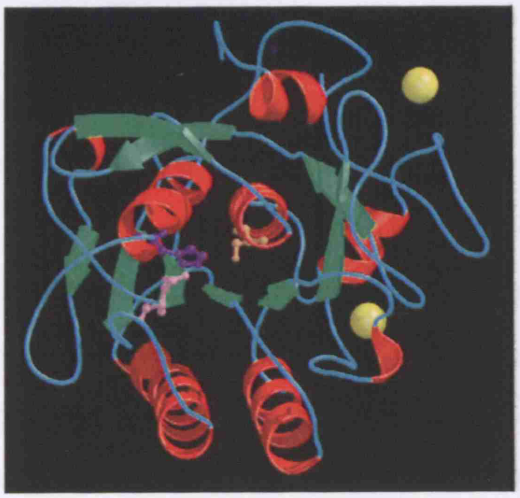

Figure 4.1: 3D model structure of proteinase K

Figure adapted from peptidase database (http://merops.sanger.ac.uk/) (365). α- helices are shown in red, β-sheet in green, catalytic residues are shown in ball-and-stick representation: N^{144} in pink, H^{174} in purple and S^{329} in orange. The structural calcium ions are shown as yellow spheres.

The formation of PrP^{Sc} from PrP^{C} is associated with an increase in the content of β-sheet structure in the protein, a decrease in solubility and acquisition of partial resistance to digestion by proteinase K (PK) (27). This characteristic is used widely as a diagnostic test for detecting PrP^{Sc} in both human and animal tissue (115;254;327). As well as *ex-vivo* diagnosis, PK is also used experimentally to analyse PrP samples processed via methods to acquire PrP^{Sc}-like properties. Due to the knowledge that the octapeptide repeat region can bind Cu^{2+} with high affinity (70;368) many studies have focussed on using transition metal ions to acquire PrP^{Sc}-like properties including PK resistance (72;119-122;369;370). During experiments assessing refolding PrP under ionic copper conditions (see **Chapter 3**) it was uncovered that a potential caveat of PK-resistant assessments could be the direct inhibition of the enzyme. By controlling for possible effects on proteinase K, inhibition was found to be due to the transition metal copper. While other researchers are aware of this possibility, and indeed have now demonstrated that PK activity is inhibited by high concentrations of Cu^{2+} ions (121), to-date there has been no comprehensive study of the sensitivity of PK activity to the binding of Cu^{2+} with respect to both concentration-dependence and time-dependence. Here, experiments were designed to mimic the conditions used in experiments that have sought to convert PrP to the PK-resistant form using either highly purified recombinant material or using the PrP^{C} present in brain homogenate.

4.1.1 Aims

After the work described in **Chapter 3** uncovered that copper ions inhibited PK it was important to establish the extent of inhibition so that assays using proteolytic digestion as a diagnostic for PrP^{Sc} wouldn't give false positives. It was sought to appropriately assess the inhibition providing results comparable for those working on prions.

4.2 Methods

4.2.1 Proteinase K

Proteinase K (EC 3.4.21.14) from the fungus *Tritirachium album limber* was obtained freeze-dried from Merck Biosciences, Ltd, Nottingham, UK. The specific enzymatic activity is approximately 30 Anson U/g, where 1 Anson unit is the amount of enzyme that liberates 1 mmol of Folin positive amino acids/minute at pH 7.5 and 35 °C using haemoglobin as substrate. A stock solution of 70 μM PK was prepared in 25 mM N-ethyl morpholoine buffer pH 7.4 (NEM buffer). Aliquots of this stock solution were used in all experiments and were stored frozen at -20 °C and thawed only once prior to use.

4.2.2 Measurement of proteinase K activity

To measure the maximum inhibitory effects of Cu^{2+} ions on PK in equilibrium, inhibition was measured after prolonged incubations. PK activity was measured using synthetic substrate p-nitrophenyl acetate (p-NA) (Sigma, Cat. N°. N-8130). Hydrolysis of p-NA by PK releases p-nitrophenol (p-NP) that can be monitored by a change in absorbance at 425 nm. For all experiments the final reaction volume was 1 ml with reactions performed in polystyrene cuvettes, (Sarstedt Ltd, Cat. N°. 67.742). For experiments performed at equilibrium, PK was diluted from stock solution into NEM buffer to give final protease concentrations of 0.7, 1.4 or 2.1 μM. Samples were adjusted with 1 mM $CuSO_4$ (prepared in H_2O), to give final concentrations of Cu^{2+} ions between 0 and 16 μM. Following equilibration at room temperature (~20 °C) for a minimum of 3 h or up to 20 h, samples were transferred to a Jasco V-530 spectrophotometer set to monitor absorbance at 425 nm. At time 0, samples were adjusted with a stock solution of 220 mM p-NA (prepared in MeOH) to give a final concentration of 2.5 mM p-NA. After rapid mixing the change in absorbance (A) at 425 nm was measured over the subsequent 120 seconds. The rate of

change in absorbance due to PK activity (ΔA/min) was determined following subtraction of the background rate of p-NA hydrolysis in buffer alone or buffer plus Cu^{2+} ions. To assess the specificity of inhibition, as other reported experiments refold PrP with other transition metal ions (72;370;371), equilibrium experiments were performed as above with zinc (Zn^{2+}) or manganese (Mn^{2+}) ions at 30 fold excess concentration of metal ions to PK.

4.2.3 Time resolved inhibition of PK activity

After observing maximal inhibitory effects of Cu^{2+} ions at equilibrium, it was important to assess the rate of inhibition. PK (35 μM) was incubated with a range of $CuSO_4$ concentrations (0.2 - 6 mM) in either the absence or presence of 10 % w/v normal hamster brain homogenate prepared in NEM buffer. 20 μl aliquots of sample were taken at various time points and diluted 50 fold in NEM buffer to give a final volume of 1 ml. Samples were then transferred to a Jasco V-530 spectrophotometer and PK activity was determined as described above. Rate constants are reported ± standard error (SEM) with a 95 % confidence limit.

4.2.4 PK digestion of brain homogenate

20 % w/v hamster brain homogenate prepared in NEM buffer was adjusted with NEM buffer lacking or containing $CuSO_4$ to 10 % w/v final concentration and final concentrations of Cu^{2+} ions of 0, 0.1, 0.5, 1, 2, 3, and 6 mM. Samples were digested with PK at a final protease concentration of 20 μg / ml for 30 min at 37 °C. Digestion was terminated by addition of an equal volume of 2 x SDS sample buffer (125 mM Tris-HCl, pH 6.8 containing 20 % v/v glycerol, 4 % w/v SDS, 4 % v/v 2-mercaptoethanol, 8 mM 4-(2-aminoethyl)-benzene sulfonyl fluoride and 0.02 % w/v bromophenol blue) and immediate transfer to a 100 °C heating block for 10 min. Samples were analysed by

electrophoresis on 16 % Tris-glycine gels (Invitrogen). Duplicate gels were were electroblotted onto PVDF membrane (Immobilon-P, Millipore) or silver stained. Immunoblotting with anti PrP monoclonal antibody 3F4 (274) using high sensitivity ECL and visualisation on Kodak BioMax MR film (Anachem, Luton UK) was performed as described in **Chapter 2**. Densitometry of silver stained gels or autoradiography film was performed using a Kodak Image Station 440 CF (Kodak, Hemel Hempstead, UK).

4.3 Results

It was sought to optimise conditions for analysis of enzymatic activity of proteinase K (PK) and inhibition by the transition metal copper. Conditions should use a suitable substrate that would give a measurable cleavage product with minimal interaction with all other assay components. Buffers used should optimise stability of enzyme, Cu^{2+} ions and substrate and all assessments should be comparable to conditions used for analysis of prions.

4.3.1 p-nitrophenyl acetate

The substrate used as a probe for the hydrolytic activity was p-nitrophenyl acetate (p-NA), this was chosen, rather than one based on polypeptide, for is its structural simplicity and its relatively poor ability to act as a chelator of transition metal ions. Consequently, the effects of Cu^{2+} that we see on the enzymatic activity of the system are due to effects on the enzyme itself rather than on the substrate. Also enzymatic activity would be easy to measure by a change of absorbance, as hydrolysis of p-NA by PK releases p-NP that can be monitored by a change in absorbance at 425 nm. The hydrolysis reaction is shown in **Figure 4.2**.

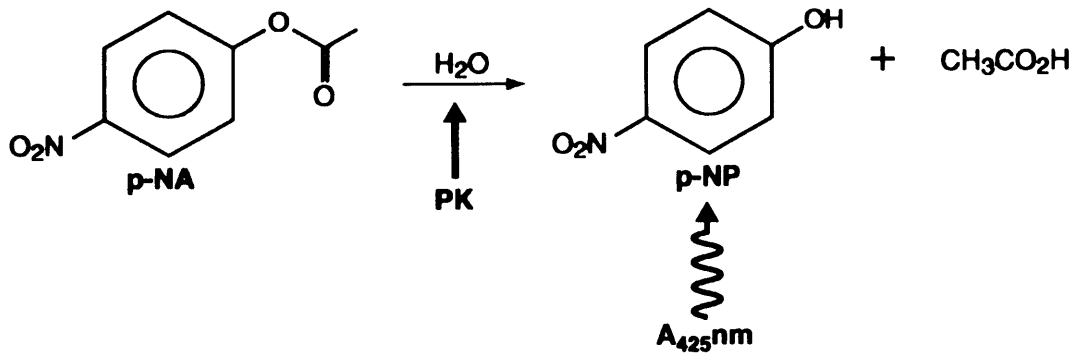

Figure 4.2: Hydrolysis of para-nitrophenyl acetate

Para-nitrophenyl acetate (p-NA) forms para-nitrophenol (p-NP) under hydrolysis. The hydrolysis reaction is catalysed by PK, the phenol giving a change in absorbance that correlates with the enzymatic rate.

4.3.2 Equilibrium inhibition of PK activity by Cu^{2+} ions

To assess the inhibitory effects of Cu^{2+} on PK activity at equilibrium, PK was incubated with a range of Cu^{2+} concentrations for 20 h. Experiments were performed in a non-chelating buffer (n-ethyl morpholine - NEM) so that that concentration-dependent effect of copper binding could be examined without undue complications. **Figure 4.3** shows that at a stoichiometry of < 1:1 there is little inhibition of PK activity by Cu^{2+} ions, however with increasing concentrations of Cu^{2+} ions a steep descent to zero activity is observed. The inset to **Figure 4.3** shows the extrapolated concentrations of Cu^{2+} ions required to abolish enzymatic activity. The slope of the inset plot indicates that a stoichiometry of 2-3 Cu^{2+} ions per enzyme molecule is required for complete inhibition of activity. These data are consistent with a system in which Cu^{2+} ions are initially bound through chelation or adsorption events to a high affinity site on PK that has no effect on enzyme activity. However, on further titration (to stoichiometries of > 1), further binding sites on the enzyme become occupied with Cu^{2+} ions leading to a complete inhibition of enzyme activity at a Cu^{2+} ion/enzyme ratio of 2-3. As the exact inhibitory effect upon binding of each Cu^{2+} ion is unknown, the system precludes precise quantitative analysis with respect to affinity, but the relative linearity of the response after initial titration of the non-inhibitory high affinity binding site would suggest that inhibitory Cu^{2+} ion binding is tight with a dissociation constant less the 1 μM. This inhibition appears specific to Cu^{2+} ions as no measurable decrease in PK activity was observed after a 20 h exposure to a 30 fold molar excess of either Zn^{2+} or Mn^{2+} ions (data not shown).

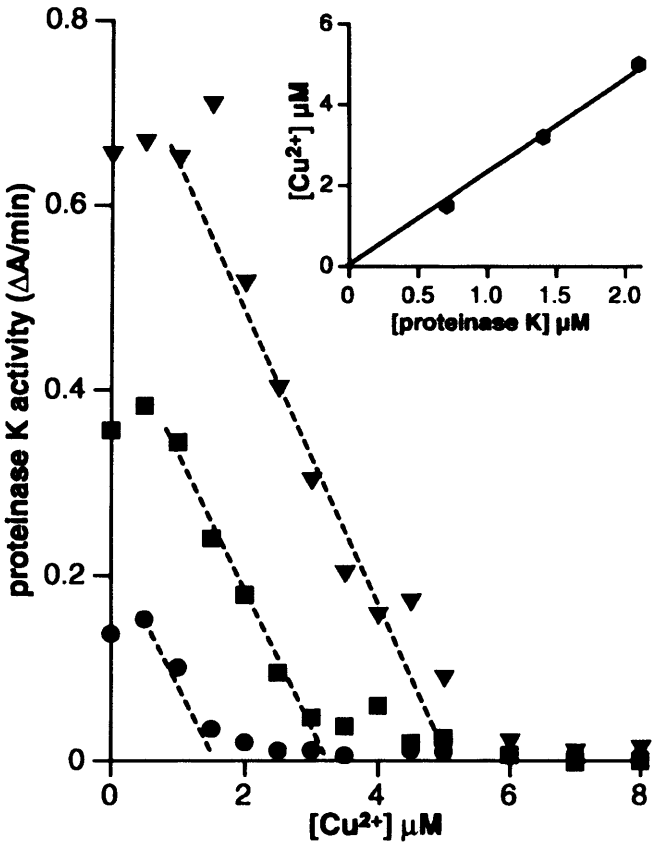

Figure 4.3: Equilibrium inhibition of PK activity by Cu^{2+} ions after prolonged incubation

The enzymatic activity of PK against p-NA was measured after incubation of the enzyme with the concentrations of Cu^{2+} ions indicated on the x-axis. The incubation period was 20 h and the experiment was carried out at 3 different concentrations of enzyme; 0.7 μM (circles), 1.4 μM (squares) and 2.1 μM (triangles). The dashed lines are extrapolations of the data points to zero activity and the concentrations of Cu^{2+} given by the intercepts are shown as a function of the PK concentration in the inset graph. Hence, the inset graph represents the copper-binding stoichiometry for complete abolition of enzyme activity.

4.3.3 Time-resolved inhibition of PK activity

The foregoing experiments demonstrate the effect of prolonged incubation of PK with Cu^{2+} ions, so that the system is at, or very near to, an equilibrium state. However, in practice, PK digestions are usually carried out for shorter times; typically over time periods of 30-60 min. In view of the variability of experimental incubation times, we measured the inhibition of PK activity by Cu^{2+} ions as a function of time. In these experiments Cu^{2+} ions were mixed with the enzyme and samples removed at a given time and assayed for the ability to hydrolyse p-NA. In order to make analysis of the system more straightforward, the experiment was performed under pseudo first-order conditions, i.e. with a large excess of copper over binding sites on the enzyme (35 μM PK with 0.5 or 1.5 mM Cu^{2+} ions).

Our findings demonstrate that the time-course of inhibition of PK activity is dependent on the concentration of Cu^{2+} ions and that the phenomenon occurs on two, well-separated time scales. Initially, there is rapid inhibition occurring on the same time-scale as that required to mix the components and withdraw the sample for assay, ~15 sec. This is then followed by a slower phase of inhibition that leads to a complete loss of proteolytic activity, see **Figure 4.4**.

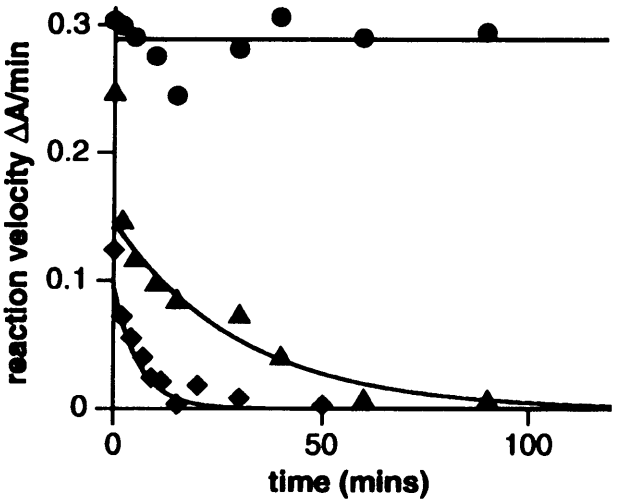

Figure 4.4: Time-resolved inhibition of PK activity by Cu^{2+} ions

PK was incubated with a series of concentrations of Cu^{2+} ions and aliquots removed at the times given on the x-axis for immediate assay. The dilution from incubation to assay was 50-fold. Three example progress curves representing residual activity as a function of time are shown at Cu^{2+} ion concentrations of 0 (circles), 0.5 mM (triangles) and 1.5 mM (diamonds). The data were fitted to a single-exponential decay function ($v = v_i.\exp(-k_{obs}.t)$) to determine the rate of irreversible loss of enzymatic activity. The observed rate constants (k_{obs}) are 0.042 (+/- 0.007) min^{-1} at 0.5 mM and 0.133 (+/- 0.025) min^{-1} at 0.5 mM and 1.5 mM Cu^{2+} ion concentration respectively.

The concentration-dependence of the initial rapid inhibition of PK activity by Cu^{2+} ions is analysed in **Figure 4.5A**, where the concentration of Cu^{2+} ions is shown on the x-axis. These data appear to fit to a hyperbolic inhibition phenomenon. However from this experiment alone it is difficult to tell whether this represents an irreversible inhibition of PK activity by Cu^{2+} ions with a measured $K_{0.5}$ of about 0.55 mM or a reversible but tighter inhibition that is still operating after the 50-fold dilution of the incubation mix into the assay buffer. To distinguish between these possibilities these experiments were repeated using the straightforward assay performed under dilute conditions rather than dilution of a concentrated incubation mixture. As shown in **Figure 4.5B**, the inhibition is indeed of a relatively high affinity and reversible. The apparent inhibition constant determined under dilute conditions is about 15 μM which compares very closely with 0.55 mM at 50-fold dilution (**A**) that gives an apparent inhibition constant of 11 μM.

Figure 4.5: Initial velocity of PK activity versus concentration of Cu^{2+} ions

The plot in (**A**) shows the result of an experiment in which PK was exposed to a series of concentrations of Cu^{2+} ions (shown on the x-axis) and aliquots removed immediately for assay. The dilution from incubation to assay was 50-fold. The y-axis therefore represents the rapid and reversible loss of activity (effectively it is the same as the y-axis intercept in **Figure 4.3**). The data were fitted to the function:

$$v = v_{max}.(1-([\ Cu^{2+}]/(K_d+[\ Cu^{2+}]))$$

where:

v - initial velocity

$\mathbf{v_{max}}$ - maximal velocity (in the absence of Cu^{2+} ions)

$\mathbf{K_d}$ - effective dissociation constant for binding

$[Cu^{2+}]$ - concentration of Cu^{2+} ions in the rapid incubation

The value for K_d given by the fit in (**A**) is 0.54 (+/- 0.3) mM. In (**B**) the assays were carried out at a 50-fold greater dilution than in (**A**) and the assay substrate added to initiate the reaction, i.e. there had been no pre-incubation at the higher concentrations of Cu^{2+} ions. The concentrations given on the y-axis are those present in the assay. The data were fitted to the same function as in (**A**) and the K_d reported for (**B**) is 15 (+/- 5) μM.

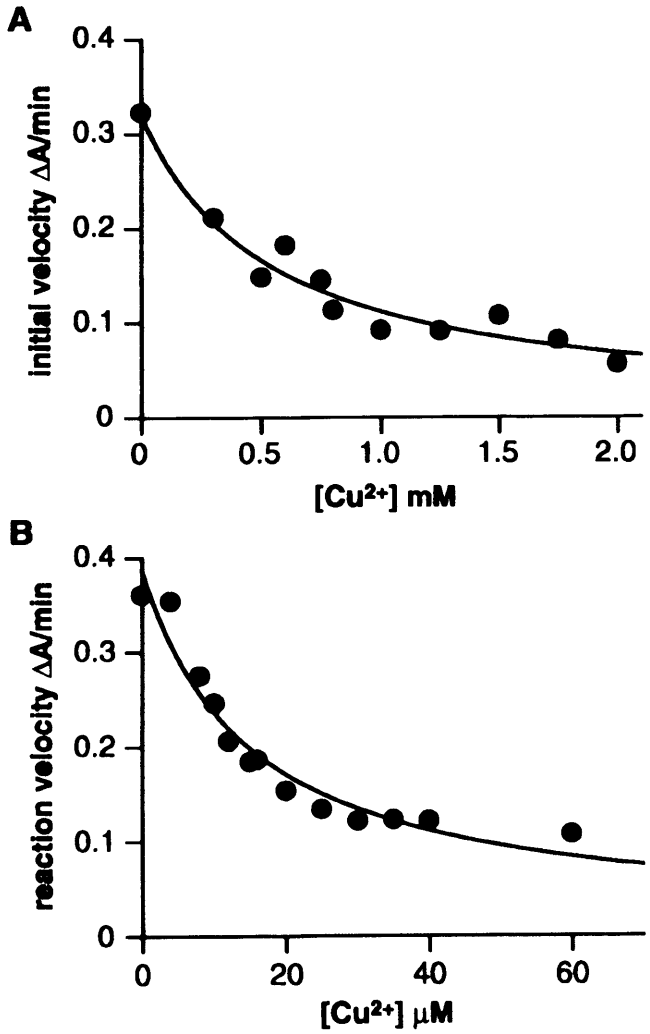
A
0.4
0.3
0.2
0.1
0
initial velocity ΔA/min
0
0.5
1.0
1.5
2.0
[Cu2+] mM
B
0.4
0.3
0.2
0.1
0
reaction velocity ΔA/min
0
20
40
60
[Cu2+] μM

Following this rapid and reversible phenomenon, the second phase of inhibition of PK activity by Cu^{2+} ions is slow and irreversible, having a half-time of about 6 min at a Cu^{2+} concentration of 2 mM. This phase is first-order, i.e. the activity of the enzyme decays in an exponential fashion. The decay reaches zero activity and is sufficiently slow that it can be properly resolved in time to provide a first-order rate constant. These observed rate constants are plotted as a function of the concentration of Cu^{2+} ions in **Figure 4.6**. Although the underlying molecular mechanisms of inhibition may be complicated, the data are consistent with an asymptotic increase in the rate constant with increasing Cu^{2+} ion concentration and conform to the following relationship:

$$k_{obs} = k._{max} \cdot [Cu^{2+}]/(K+[\ Cu^{2+}])$$

The fitted values for the constants are $3.7 \times 10^{-3}\ s^{-1}$ for k_{max} and 1.4×10^{-3} M for K. Both of these values can be considered as empirical constants that allow calculation of residual activity at given times and given concentrations of Cu^{2+} ions. The physical meaning of both k_{max} and K are dependent on the kinetic model.

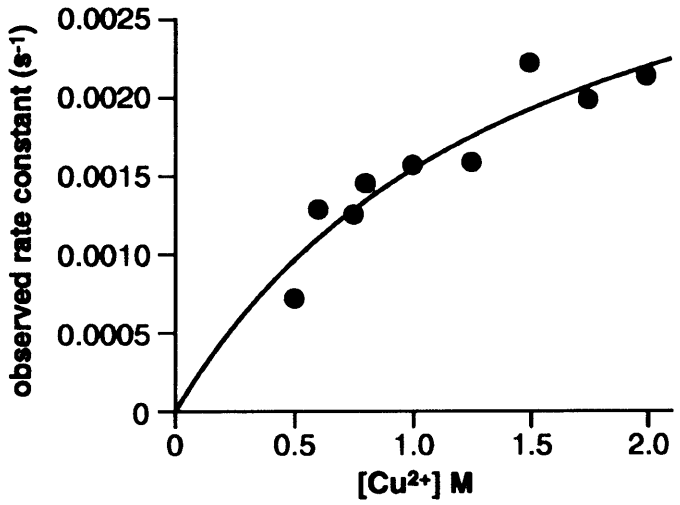

Figure 4.6: Transient kinetics of slow, irreversible inhibition of PK by Cu^{2+} ions

The observed rate constants for the slow, irreversible loss of enzyme activity on exposure to Cu^{2+} (see **Figure 4.4**) are plotted as a function of the metal ion concentration in the incubation and fitted to the equation:

$$k_{obs} = k_u \times [Cu^{2+}] / (K + [Cu^{2+}])$$

The value for k_u is 0.0038 (+/- 0.0008) s^{-1} and the value for K is ~1.5 (+/-0.5) mM.

4.3.4 Inhibition of PK activity in the presence of brain homogenate

Figure 4.7 exemplifies the inhibition of PK activity observed after its incubation with differing concentrations of Cu^{2+} in the presence of a 10 % brain homogenate. These results are not as straightforward to analyse or interpret as those collected in the absence of brain homogenate. Indeed, this is further complicated by the possibility of PK activity destroying endogenous proteases in the homogenate (or vice versa) and the possible effect of Cu^{2+} ions on homogenate hydrolases that are capable of cleaving p-NA. The interplay of these factors makes it impossible to produce an exact quantitative analysis, but some simplified conclusions can be drawn.

In initial experiments it was observed that brain homogenate alone has substantial hydrolytic activity when challenged with the assay substrate; but when PK is mixed with homogenate, within 30-60 seconds the level of activity is reduced to that observed in the presence of PK alone (data not shown). From these data it is concluded that PK is very effective in destroying endogenous proteases present in brain homogenate.

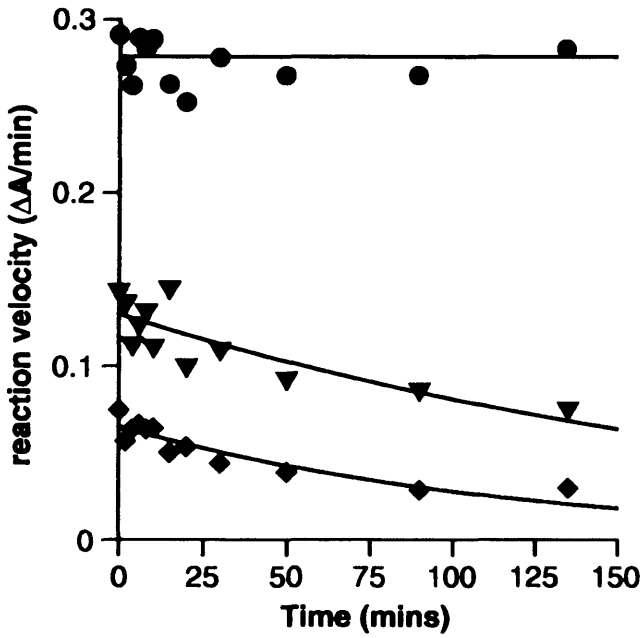

Figure 4.7: Time course of PK inhibition by Cu^{2+} ions in the presence of brain homogenate

Proteinase K was incubated with a series of concentrations of Cu^{2+} ions in 10 % hamster brain homogenate and aliquots removed at the times given on the x-axis for immediate assay. The dilution from incubation to assay was 50-fold. Three example progress curves representing residual activity as a function of time are shown at Cu^{2+} ion concentrations of 0 (circles), 2 mM (triangles) and 4 mM (diamonds). The data were fitted to a single-exponential decay function ($v = v_i.\exp(-k_{obs}.t)$) to determine the rate of irreversible loss of enzymatic activity. The observed rate constants (k_{obs}) are 0.0047 (+/- 0.0012) min^{-1} and 0.0086 (+/- 0.0019) min^{-1} at 2 mM and 4 mM Cu^{2+} ion concentrations respectively.

The inhibition of the PK activity by Cu^{2+} ions in the presence of brain homogenate occurred in two distinct phases, similar to that observed in the absence of brain homogenate. The rapid and reversible phase of inhibition is analysed in **Figure 4.8A** and shows the initial activity (after about a 30 second dead-time) as a function of the concentration of Cu^{2+} ions. The pattern of inhibition does not conform to a simple inverse hyperbola, rather there is a threshold below which there is little effect of Cu^{2+} ion concentration. It is likely this occurs because there is a relatively high concentration of tight Cu^{2+} ion-binding sites in the homogenate that have to be out-titrated before there is sufficient free metal ions to affect PK. The concentration of Cu^{2+} ions required to produce a significant (20 %) inhibition of PK activity is about 1 mM. The concentration of protein in a 10 % homogenate is approximately 10 mg/ml. With an average amino acid residue molecular mass of 110 this gives a residue concentration of about 90 mM, this means that, as a crude approximation, there is a one tight Cu^{2+} ion site per 90 amino acid residues. From this experiment alone it is difficult to tell whether this represents an irreversible inhibition with a measured $K_{0.5}$ of about 2 mM or a reversible but tighter inhibition that is still operating after the 50-fold dilution of the incubation mix into the assay buffer. To distinguish between these possibilities the experiment was again performed not with a concentrated incubation mixture, but by a straightforward assay in dilute conditions. This result is shown in **Figure 4.8B**, the analysis of which reveals that the inhibition is, indeed, of a relatively high affinity and reversible. The $K_{0.5}$ value is now about 30 μM which compares favorably with 2 mM divided by the 50-fold dilution which would provide an apparent inhibition constant of 40 μM.

Finally, the slow phase of inhibition is analysed in **Figure 4.8C**, which shows the first-order rate constant for the loss of enzymatic activity as a function of Cu^{2+} ion concentration. Again, as in the case of the rapid, reversible inhibition, there is no detectable, slow inhibition phase at concentrations Cu^{2+} ions below 1 mM, presumably because of adsorption onto components of the homogenate. At 2 mM Cu^{2+} ions the half-time for this

slow, irreversible inhibition is much longer than in the absence of homogenate being about 3 h as apposed to 6 min.

Figure 4.8: Analysis of the effects of Cu^{2+} ions on PK activity in the presence of brain homogenate: initial velocities and slow inhibition

The plot in (**A**) shows the result of an experiment in which PK was exposed to a series of concentrations of Cu^{2+} (shown on the x-axis) in the presence of 10 % brain tissue homogenate and aliquots removed immediately for assay. The dilution from incubation to assay was 50-fold. The y-axis therefore represents the rapid and reversible loss of activity (effectively it is the same as the y-axis intercept in **Figure 4.4**). The data were fitted to the phenomenological function

$$v = v_{max}.(1-([Cu^{2+}]^n/(K_{0.5}{}^n+[Cu^{2+}]^n))$$

where:

v - the initial velocity

$\mathbf{v_{max}}$ - maximal velocity (in the absence of Cu^{2+})

$[Cu^{2+}]$ - concentration of Cu^{2+} in the rapid incubation (prior to dilution into the assay cuvette)

$\mathbf{K_{0.5}}$ - concentration required for half-saturation

The value for $K_{0.5}$ in (**A**) given by the fit is 2.1 (+/- 0.3) mM and the Hill number (n) is 1.9. In plot (**B**) the assays were carried out at a 50-fold greater dilution than in (**A**) with respect to both the concentration of copper and brain homogenate. The assay substrate was added *in situ* to initiate the reaction, i.e. there had been no pre-incubation at the higher concentrations of Cu^{2+} ions. The concentrations given on the y-axis are those present in the assay. The data were fitted to the same function as in (**A**); the $K_{0.5}$ reported for (**B**) is 30 (+/- 8) μM and the Hill number (n) is 2.2. Shown in (**C**) are the rate constants for the slow inhibition phase in the presence of tissue homogenate (see **Figure 4.7** for primary data).

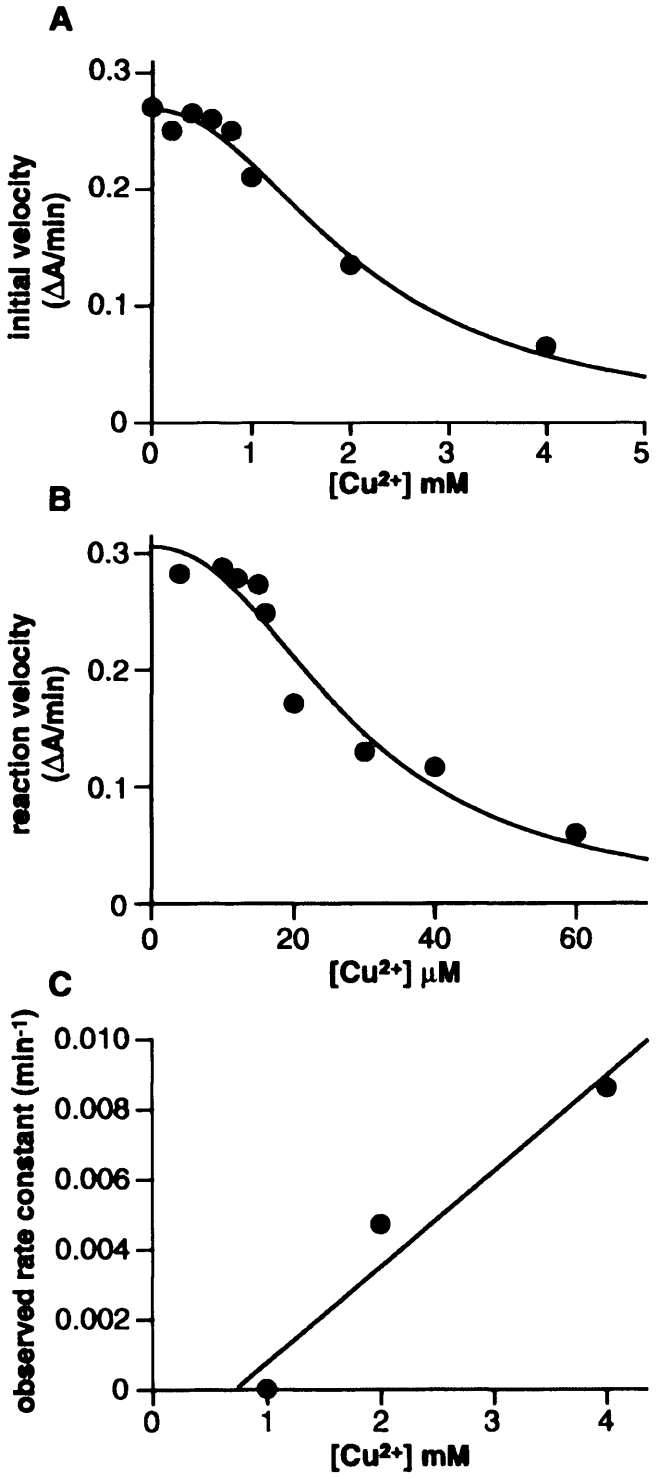
A
0.3
0.2
0.1
0
initial velocity (ΔA/min)
0
1
2
3
4
5
[Cu2+] mM
B
0.3
0.2
0.1
0
reaction velocity (ΔA/min)
0
20
40
60
[Cu2+] μM
C
0.010
0.008
0.006
0.004
0.002
0
observed rate constant (min-1)
0
1
2
3
4
[Cu2+] mM

4.3.5 PK inhibition by Cu^{2+} ions monitored by SDS-PAGE and PrP immunoblotting

To show direct comparison to experiments analysing a change in PrP conformation by protease resistance, PK digestion of PrP^C in hamster brain homogenate in the presence of increasing concentrations of Cu^{2+} ions was investigated. PrP^C was visualised by immunoblotting and total protein by silver staining. As shown in **Figure 4.9A**, PK digestion of PrP^C is inhibited in a concentration-dependent manner by Cu^{2+} ions at concentrations of 1 mM and above. This effect is not however unique to PrP^C as PK digestion of other proteins in the brain homogenate (visualised by silver stain) was similarly prevented at the same concentrations of Cu^{2+} ions (**Figure 4.9B**). Densitometry of PrP^C signal intensity and the intensity of three other selected silver-stained proteins showed a closely similar pattern of apparent resistance to PK digestion (**Figure 4.9C**). Importantly, the concentrations of 1-2 mM Cu^{2+} ions required to see significant inhibition of PK activity in the presence of brain homogenate using the p-NA assay (**Figure 4.8A**) correlates precisely with the concentration of Cu^{2+} ions that prevent PK digestion of PrP^C and other brain proteins. These data establish that Cu^{2+} ions are directly affecting PK activity rather than acting to selectively increase the apparent PK-resistance of PrP^C.

Figure 4.9: Analysis of the effects of Cu^{2+} ions on PK activity in the presence of brain homogenate by PrP immunoblot or SDS-PAGE silver stain

Normal hamster brain homogenate was prepared as a 20 % w/v in NEM buffer and diluted to 10 % in NEM buffer containing 0.1, 0.5, 1, 2, 3, and 6 mM $CuSO_4$. PK digestion was at 20 µg/ml final protease concentration for 30 min at 37°C and equivalent aliquots analysed by SDS-PAGE. (**A**) immunoblot probed with 3F4 showing that the signal intensity of PrP^C increases increasing $CuSO_4$ concentrations (equivalent of 1.25 µl starting 10 % homogenate in each lane). The lane denoted by the * symbol shows an identical volume of brain homogenate analysed in the absence of PK digestion. Densitometry of signal is shown in (**i**). (**B**) silver stain showing total homogenate protein (equivalent of 5 µl starting 10 % homogenate in each lane). Again the signal intensity increases with increasing $CuSO_4$ concentrations and three prominent bands, (**ii**), (**iii**) and (**iv**) were selected for densitometry as shown in (**C**).

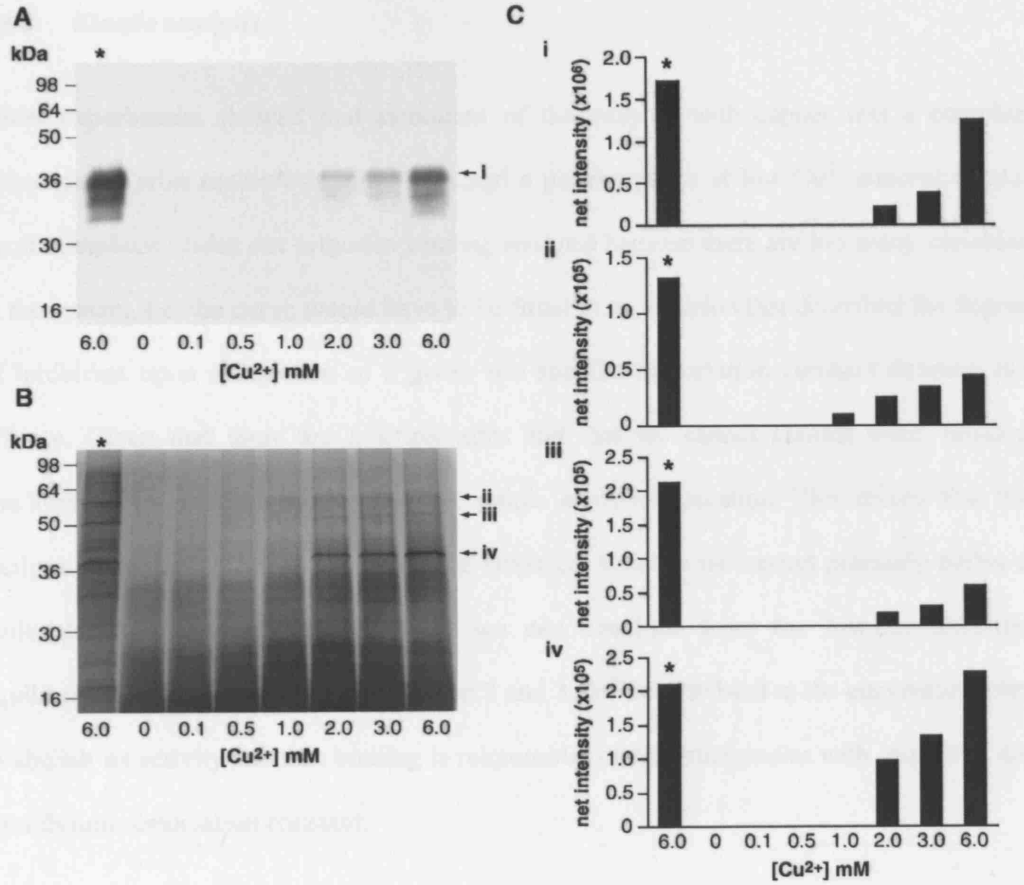
A
kDa
*
98
64
50
36
30
16
I
6.0 0 0.1 0.5 1.0 2.0 3.0 6.0
[Cu2+] mM
B
kDa
*
98
64
50
36
30
16
ii
iii
iv
6.0 0 0.1 0.5 1.0 2.0 3.0 6.0
[Cu2+] mM
C
i
ii
iii
iv
net intensity (x10⁶)
net intensity (x10⁵)
net intensity (x10⁵)
net intensity (x10⁵)
*
6.0 0 0.1 0.5 1.0 2.0 3.0 6.0
[Cu2+] mM

4.3.6 Kinetic analysis

Initial experiments showed that saturation of the enzyme with copper was a complex phenomenon with multiple binding sites and a plateau phase at low Cu^{2+} concentrations. Such complexity rules out orthodox binding analysis because there are too many variables in the system, i.e. the curve would have to be fitted to an equation that described the degree of inhibition upon occupation of a given site and the dissociation constant defining the affinity. Given that there are multiple sites and that we cannot assume weak binding conditions, this puts the system beyond simple analytical solution. This means that the analysis of inhibition has to be somewhat empirical because we cannot precisely define a molecular mechanism. However, what we can conclude from the low-concentration equilibrium data is that it requires between 2 and 3 Cu^{2+} ions to bind to the enzyme in order to abolish its activity and that binding is micromolar or sub-micromolar with respect to the equilibrium dissociation constant.

Part of the inhibition by copper is not instantaneous; there is a fast phase in which 80-85 % of the enzymatic activity is lost and a slow phase in which the remainder disappears. The fast phase represents reversible binding with an effective K_I of 10-20 μM. The slower phase, in which the rate constants are easily measurable, has a different mechanistic origin. The observed rate of this phase rises with the concentration of Cu^{2+} ions, but then reaches an asymptotic maximum. Although we cannot be certain of the mechanism, a reasonable physical model that can explain this kinetic pattern is described by the following scheme:

$$F = U \rightarrow U{:}\ Cu^{2+}$$

Where the folded state (**F**) can undergo slow and rate-limiting opening events to a more unfolded state (**U**) that can then form tight, irreversible interactions with the transition metal. If we define the rate constant for unfolding (F->U) as k_u, the rate constant for refolding or closing as k_c and the bimolecular rate of Cu^{2+} association as k_a then the

observed rate constant (k_{obs}) for the formation of the dead-end inhibited state (U: Cu^{2+}) is defined by the following equation:

$$\underline{\text{Equation 1}}: k_{obs} = k_u \times [Cu^{2+}] / (K + [Cu^{2+}])$$

Where the value of K is given by the ratio k_c/k_a and is measured in terms of the molarity (M) of Cu^{2+} ions in the incubation; it can also be defined as the concentration required to give half the maximal rate of irreversible Cu^{2+} inhibition. The data fits this empirical model well (see **Figure 4.6**), so that **Equation 1** serves as a useful tool in quantifying the effects of Cu^{2+} at a range of concentrations and incubation times.

The rapid reversible loss of activity shown in **Figure 4.5** can be quantified by the relationship:

$$\underline{\text{Equation 2}}: A = K_I/([Cu^{2+}] + K_I)$$

Where **A** is the fractional residual activity and $\mathbf{K_I}$ is the apparent inhibition constant.

Equation 1 gives the time-dependence of the slow, irreversible loss of activity so that the first order decay can be described by:

$$\underline{\text{Equation 3}}: A = \exp(-k_{obs}.t)$$

Where, again, **A** is the fractional residual activity and k_{obs} the observed first-order rate constant defined by **Equation 1**. Integrating **Equation 3** yields an expression for the total percentage activity (**A%**) over an incubation time ($\mathbf{t_i}$) for the slow phase of inhibition:

$$\underline{\text{Equation 4}}: A\% = 100.(1-\exp(-k_{obs}.t_i))/k_{obs}$$

Equations 2 and **4** can then be combined to describe the percentage of the uninhibited activity (**A%**) at any incubation time (**t**) at any concentration of Cu^{2+} ions:

$$\underline{\text{Equation 5}}: A\% = 100.\ (K_I/([\ Cu^{2+}] + K_I))\ (1-\exp(-k_{obs}.t_i))/k_{obs}$$

Where k_{obs} is defined by **Equation 1**.

The above quantitative arguments apply to systems in which there is no strong copper chelator in the system and no tissue homogenate, but essentially the same phenomena occur in the presence of a 10 % brain homogenate, i.e. there is a rapid reversible binding of copper that inhibits the enzyme activity and a slow irreversible phase. In these circumstances, PK is protected from Cu^{2+} inhibition by the presence of the proteolytic breakdown products of the tissue components and probably by other species present in this complex mixture. Thus in the presence of a 10 % brain homogenate it is not until a threshold of about 1 mM Cu^{2+} ions has been exceeded that we see significant inhibition of the proteolytic activity; either in the reversible or irreversible modes.

4.4 Discussion

PrP^{Sc} can be distinguished from its normal cellular precursor, PrP^{C}, by its detergent insolubility and partial resistance to proteolysis. Several studies have suggested that Cu^{2+} ions can convert PrP^{C} to a PK resistant conformation, however interpretation of these studies is complicated by potential inhibition of PK by Cu^{2+} ions. Here the kinetic and equilibrium effects of Cu^{2+} ions on PK activity have been examined using a simple synthetic substrate, p-NA.

In these experiments it was aimed to make a quantitative assessment of the concentration-dependence of PK inhibition by Cu^{2+} ions. The analysis has resolved this process into two distinct time domains; one phase of inhibition being reversible and occurring within seconds, the other being irreversible and occurring over longer time scales that could easily be resolved kinetically. One practical relevance of these findings is that inhibition occurs over the same metal concentrations and incubation periods as those used to distinguish PrP^{C} from PrP^{Sc} on the basis of their differential susceptibility to digestion by PK. As a consequence, if Cu^{2+} is investigated for its ability to convert the PrP^{C} conformation to the PrP^{Sc} form, then these effects must be considered.

However, the studies showed that inhibition of the enzyme with copper was a complex phenomenon. In most classical inhibition studies using small ligands, the time required for the inhibitory effect is very short. For instance, with freely diffusing ligands the time taken for interaction with a surface site is determined by the second-order rate constant describing the diffusion-collision process (typically 10^{7}-10^{8} $M^{-1}s^{-1}$) and the ligand concentration. Hence, even at a low ligand concentration, such as 1 mM, the binding event happens over a period of 10-100 ms. However, inhibition wrought by the binding of transition metals may occur more slowly if the metal has to penetrate the body of the protein rather than associate rapidly with a surface-exposed site. This type of 'burrowing' event may require the transient and infrequent opening of regions of the protein structure or, possibly, the global

unfolding of the molecule. Hence such processes may occur over slow time-scales. These phenomena are comparable to the inhibition of PK with mercury, Hg^{2+}, ions (358) and it may be likely that Cu^{2+} ions also covalently bind to the cysteine near the catalytic triad, distorting the structure of the active site.

Cu^{2+} ion binding to PrP is well researched, it is known that the binding is of high affinity and that PrP can apparently acquire many PrP^{Sc}-like properties after exposure to Cu^{2+} ions. However, some experiments reported in the literature have not controlled for direct effects on PK. Copper does indeed change PrP conformation as shown by acquisition of β-sheet structure (119;120) and effects on PrP^{Sc} digestion fragment sizes with metal ions (279). Also studies analysing protease resistance of PrP comparing time points of PrP incubation with Cu^{2+} ions (and other transition metals) show a differentiation over time with equivalent Cu^{2+} or Mn^{2+} and PK proportions verifying that inhibition of PK by Cu^{2+} ions is unlikely (120;121;369). However, other conclusions could be made aside from PrP acquisition of a genuine protease resistant structure. Large aggregates could have been formed preventing access of PK to digest internalised PrP embedded in such structures. Evidence for the presence for large aggregates can be supported by the visualisation of differing signal intensities of PrP at the same molecular weight on SDS-PAGE rather than a change in fragment size. An "all or nothing" digestion product is more likely to be indicative of PrP access to the enzyme than a change in conformation with Cu^{2+} ions conferring PK resistance to the entire amino acid length of the PrP used. Kuczius et al reported that they also saw inhibition of PK with Cu^{2+} ions, but didn't define the extent of the inhibition (121).

As it is possible that there could be a genuine acquisition of protease resistant structure of PrP under certain conditions containing Cu^{2+} ions, experiments looking at the refolding of PrP with Cu^{2+} ions should be analysed efficiently so that a genuine conformational change is observed and not inhibition of PK. The kinetics of inhibition shown here can now analyse the activity of PK under free ionic Cu^{2+} concentrations to establish a threshold at which

genuine resistance takes place. Other simple ways to show if a protease resistant structure has been acquired in conditions containing Cu^{2+} ions can also be addressed, such as comparison to other proteins, removal of Cu^{2+} by chelation or dialysis, showing an increase in resistance over time or digestion with other enzymes not effected by copper. It is to be noted that the inhibitory effects were not seen with Zn^{2+} or Mn^{2+}, which have also been shown to acquire a protease resistant structure of PrP (369;370).

As shown in **Chapter 3**, refolding PrP under ionic conditions did not acquire a protease resistant conformation. The false positive seen initially was reversed after chelation and conditions used were shown to inhibit PK by comparison with a control protein. To simply demonstrate this in relation to PrP, the comparison of the effects of Cu^{2+} ions on PK activity using homogenate containing PrP^{C} was shown using SDS-PAGE and immunoblot or silver staining for PrP and total protein levels. Looking at total protein effects by using a simple method such as silver stain shows whether Cu^{2+} ions specifically affect PrP or act directly on the enzyme itself. Under circumstances involving a purified sample of PrP that cannot be compared with other proteins, the mathematical equations to subtract the levels of inhibition of PK produced by Cu^{2+} ions have been provided here.Those working on the acquisition of protease resistance and infectivity in the prion field should in the future consider a protease not effected by Cu^{2+} ions, or simply address prion infectivity itself, as it has not been shown that there is a direct correlation between Cu^{2+} ion coordinated PrP conformation and prion infectivity.

5 General discussion

Prion diseases are fatal neurodegenerative diseases and due to their transmissibility pose a great risk to human health. Since the UK population exposure to BSE infected bovine offals there have been 159 cases of vCJD so far (www.cjd.ed.ac.uk). From the assessment of another acquired human prion disease, kuru, where there is no species barrier, it has been shown that the incubation period can be up to 40 years (90). Clinical cases of vCJD so far have had relatively short incubation times, and with the knowledge that incubation times increase in the presence of a species/transmission barrier (182), bovine BSE transmission to humans are expected to present with a larger mean incubation period than that of kuru (90;181). Thus a greater number of clinical vCJD cases will arise in the future and asymptomatic carriers pose a risk of subsequent infection to the population via iatrogenic routes. Variant CJD has already been transmitted via blood (259;372). Extensive research is therefore needed to understand the molecular biology of prions, improve diagnostics and prevent disease. To date, a critical understanding of PrP^{C} function, the structure of the infectious agent, the mechanism of PrP^{C} to PrP^{Sc} conversion and the mechanism of neurodegeneration are lacking and there are currently no methods for preclinical diagnosis and treatment of prion disease.

This thesis describes work geared toward determining the structure of the infectious agent and further characterisation of PrP^{Sc}. This has involved development of a method for purification of PrP^{Sc} to allow investigation of covalent post-translational modifications including its oligosaccharides and GPI anchor. This purification method provides a novel substrate for refolding studies to analyse a change in PrP properties under different solvent conditions. Partial purification methods for PrP^{Sc}, retaining its protease resistant conformation and following infectivity were developed for the identification of possible prion co-factors. Included in these studies was a kinetic analysis of inhibition of the enzyme proteinase K (PK) by Cu^{2+} ions. A distinct property of PrP^{Sc} is its protease resistance to PK

and knowledge of mechanisms of inhibition of this protease are extremely important to exclude false positives in physicochemical characterisation of PrP.

To date, the infectious agent in prion disease is thought to comprise the disease associated protein, PrP^{Sc} and many lines of evidence suggest that PrP^{Sc} is the sole infectious agent supporting the protein only hypothesis of prion propagation:

- Prion infectivity correlates with PrP^{Sc} levels shown by partial purification methods (27-30;32)
- Anti-PrP antibodies are known to prevent PrP^{Sc} replication (313) and show retardation of prion disease *in vivo* (373;374) and cure infection *in vitro* (375)
- Mutations of PrP are known to cause disease in familial forms of prion disease (208;216;376;377) (reviewed in (77;210;254))
- Certain amino acid polymorphisms of PrP have a dramatic effect on prion disease incubation times, susceptibility to disease and strain specific effects (77;91;295;328)
- Congenital or conditional *Prnp* knockout mice are resistant to disease (148;149;151;152;378;379) (reviewed in (150;380))
- The protein only hypothesis of prion propagation in mammals is strongly supported by yeast prion biology (381-384)
- Prion infectivity has been generated from purified refolded rPrP (124;125).

Although prion infectivity in mammals has been generated from synthetic prions, the infectious PrP species has not been determined and infectivity was of an extremely low titre. Although factors, such as clearance or targeting, could remove the fibrils generated from rPrP (93) a $>10^8$ reduction in infectious titre compared to RML prions indicates that

the fibrils are unlikely to be the infectious agent. Previous studies suggest that PrP^{Sc} oligomers have the highest infectious titre (147) thus a small amount of infectious oligomeric PrP species maybe associated with PrP fibrils *in vitro* or the fibrils maybe broken down *in vivo* to generate a small amount of oligomeric PrP. It can also not be ruled out that a co-factor or post translational modifications were acquired *in vivo* post-inoculation or during the preparation of the fibrils. Even though the Legname et al findings were pioneering in showing that infectious prions can be generated *in vitro* the nature of the infectious PrP isoform remains unknown.

The detailed characterisation of the infectious conformation and properties of PrP^{Sc} is extremely important for evaluating therapeutic targets. The generation of *in vitro* prions by Legname et al have not furthered the understanding of the infectious properties of PrP^{Sc} and there are remaining questions to be answered. Not only is the infectious PrP conformation unknown (either as a single PrP^{Sc} molecule or as an oligomeric structure) the post-translational modifications of PrP^{Sc} that could confer prion strain specific properties are still unknown, as are the identity any other factors required for prion infectivity.

It is therefore fundamental to know the properties of PrP^{Sc}, how it is derived and how it differs from PrP^{C}. To date the following information is known about the differing properties of PrP^{C} and PrP^{Sc}:

- PrP^{C} and PrP^{Sc} have the same amino acid sequence (36;37)
- PrP^{Sc} has a markedly different conformation to PrP^{C}, with a substantial increase in β-sheet structure (96;97;101)
- PrP^{C} is protease sensitive and PrP^{Sc} partially resistant (27-29)
- The GPI anchor is readily cleaved by PIPLC in PrP^{C} but not in PrP^{Sc} (48-50)

- There is an increase of bi- tri- and tetra-antennary complex sugar chains in PrP^{Sc} oligosaccharides compared with PrP^{C} (54-57).

What is not known about PrP^{Sc} is the exact conformation, composition of the oligosaccharides and GPI anchor, and if there are any other post-translational modifications that distinguish it from PrP^{C}. Changes in amino acid sequence are known to generate infectious PrP conformations by knowledge of inherited forms of prion disease, and the effect of the codon 129 polymorphism on disease susceptibility shows the importance of amino acid sequence on infectious PrP^{Sc} conformations (reviewed in (77)). There are many post-translational modifications that would not significantly change molecular mass migration as analysed by SDS-PAGE (385). Post-translational modifications could confer amino acid changes to PrP *in vivo* (or *in vitro* generated prions (124-126)) rendering the PrP conformation infectious.

One of the most interesting amino acid modifications is ubiquitination. Ubiquitin is a 76 residue peptide that is linked via its C-terminal end to lysine groups on other proteins as a tag for degradation by the proteasome (386;387). The proteasome is well documented in a variety of protein misfolding neurodegenerative disorders (388-392) including prion disease (157;393;394) the latter suggesting that PrP^{Sc} accumulation causes proteasome impairment which leads to neurodegeneration by a caspase mediated mechanism. PrP has many lysine residues that can be ubiquitinated, the majority being in the unstructured N-terminus (41)(see **Figures 1.1** and **1.2**). As the N-terminal structure of PrP^{Sc} is unknown, it may be possible that these residues are inaccessible to ubiquitination and prevented from degradation. Although studies have investigated ubiquitination of PrP (395;396), to date differences between PrP^{C} and PrP^{Sc} regarding ubiquitination is unknown. Notably because methods used to isolate PrP^{Sc} include proteolytic digestion, ubiquitin chains attached to lysine residues of PrP^{Sc} are likely to be removed.

The possibility of chemical modification to an amino acid (or the converse) conferring a disease associated change has been seen in other neurodegenerative disorders. Studies on Huntington's disease, have shown that the normal huntingtin protein is palmitoylated for essential trafficking and function (397). The mutated form of huntingtin had a marked reduction in palmitoylation. This shows that changes in post-translational modifications can have fundamental effects on protein function. Such modifications of PrP could mediate a change in targeting for degradation or effect conformational stability.

For the first time full length *ex-vivo* PrP^{Sc} with GPI anchor and oligosaccharides has been purified efficiently for further analysis (see **Chapter 2**). By further processing of this purified material by HPLC, and other methods, post translational modifications can now be examined in detail. This study is now ongoing in the MRC Prion Unit and may identify disease associated differences between PrP^{Sc} and PrP^{C} and differences that distinguish PrP^{Sc} isoforms associated with distinct prion strains.

Although post-translational modifications of PrP^{Sc} may be important in prion disease a wealth of evidence suggests that prion infectivity is encoded by PrP^{Sc} conformation alone (5;33;295;300;302). None of the conditions tested described in **Chapter 3** for refolding PrP generated prion infectivity or protease resistant PrP, but a change in conformation was observed by marked changes in insolubility. Failure to generate infectivity could be due to the omission of a co-factor required for PrP stability or PrP targeting, but as the exact conformational properties associated with the generation of an infectious prion are still unknown, the lack of prion infectivity could be due to inappropriate solvent conditions. As there is a huge conformational difference between PrP^{C} and PrP^{Sc}, it is important to understand how the disease associated conformational change arises *in vivo*.

Studies examining the equilibrium states of PrP have shown that a multitude of stable conformations can arise from the same primary PrP sequence (113). This supports the protein only hypothesis including the existence of multiple prion strains as they show

differing PrP^{Sc} conformations. However, the spectrum of multiple PrP conformations that can be pathogenic or non-pathogenic appear to overlap with those that can be partially protease resistant or protease sensitive complicating identification of each isoform by methods that diagnose PrP^{Sc} by partial resistance to proteolysis. It has been shown that some infectious PrP isoforms are protease sensitive (228;336;337;241;273;398;399) (reviewed in (400)). There are also strain specific differences in protease resistance (333). At high concentrations of PK further digestion of PrP^{Sc} is observed and the rate of digestion depends on the prion strain (333). Brain samples from some inherited prion diseases produce smaller PrP fragments between 8-15 kDa after PK digestion showing a marked difference in the conformation of the parent abnormal PrP isoform from PrP conformers generating PrP^{27-30} (76;210;213).

A variety of studies show that the generation of a protease resistant conformation is not necessarily indicative of an infectious PrP conformation *in vivo* (401;402). Also studies generating protease resistant conformations of rPrP *in vitro* have shown that they are not infectious (94;403-405). Amplification models using PrP^{Sc} as a seed in brain homogenate containing PrP^{C}, have shown replication of PrP^{Sc} by definition of protease resistance, but subsequently the concentration of this material has shown no correlation with infectivity (127-129;131-133;136;406). Studies generating *de novo* prions such as those from Legname et al or Soto et al show that an increase in protease resistant PrP with a disproportionate lower infectivity titre may not just be explained by lower specific prion infectivity relating to prevention of cell targeting or increased clearance. It is possible that in these studies more than one conformation of PrP that is protease resistant has been generated containing only a minute sub-population of PrP that is infectious (124;125;137;407).

Without a greater understanding of the relationship between pathogenic PrP conformations and PrP protease resistance, infectious prions may be overlooked by certain methods of detection and noninfectious forms of PrP misdiagnosed. As shown in **Chapter 3**, inhibition

of PK by Cu^{2+} ions can be misinterpreted as acquisition of protease resistance of PrP. However, Cu^{2+} ions may still be a possible co-factor for acquisition of PrP protease resistance and infectivity. Analysis of the experimental design of studies investigating the refolding of PrP in the presence of Cu^{2+} ions suggest that in some cases inhibition of PK cannot explain the results (119-121). As Cu^{2+} ions have shown to have a genuine effect on PrP conformation (279) the knowledge that Cu^{2+} ions can inhibit PK should not deter the future use of Cu^{2+} in refolding studies.

As well as understanding post-translational modifications of PrP itself that could generate an infectious conformation, knowledge of what other components may modulate the specific infectivity of prions is required. As shown in the work described in **Chapter 3**, protease digestion of PrP^{Sc} had a marked effect on specific prion infectivity when assessed by an *in vitro* assay. This suggests that the protease resistant core of PrP^{Sc}, PrP^{27-30}, has lower specific prion infectivity. Co-factors that contribute to specific prion infectivity (including the N-terminus) could do this by targeting PrP into cells (340;342;344-346), stabilising the infectious PrP conformation or preventing the clearance of PrP (145). Notably these co-factors may be acquired *in vivo* after inoculation. This would explain the lack of data to show a change in specific prion infectivity, after protease digestion, by bioassay.

Continuation of the work set out in **Chapter 3** could assess possible co-factors required for specific prion infectivity by partial purification methods and following PrP^{Sc} in a protease resistant and infectious conformation. With further characterisation of the reduction in specific prion infectivity by proteolytic digestion of brain homogenates and correlation with co-factors, specific components that modify prion infectivity may be identified. If identified, these co-factors will be applied to refolding studies using purified PrP to generate prion infectivity, or alter the specific prion infectivity of PK treated brain homogenate. This will facilitate analysis of the mechanism by which the co-factor contributes to the prion infectivity of PrP^{Sc} either by stabilising an infectious conformation,

targeting PrP^{Sc} into cells, or prevention of PrP^{Sc} clearance. These studies may further substantiate the protein only hypothesis of prion propogation by establishing that PrP^{Sc} is the sole infectious agent, and that a co-factor only facilitates its efficient delivery.

5.1 Conclusion

Although the exact conformation of infectious PrP^{Sc} and the structure of infectious prions are still unknown, the work reported in this thesis has provided important new methods to aid in prion research. The development of a purification method that is applicable to multiple species and prion strains yielding full length PrP with post-translational modifications will further our knowledge of PrP^{Sc} structure and may reveal changes confering prion infectivity and prion strain specific properties. Kinetic analysis of PK inhibition by Cu^{2+} ions now allows futher investigation of the refolding of PrP in the presense of Cu^{2+} ions to generate a PrP^{Sc}-like conformation under conditions that exclude false positives due to inhibition of the enzyme. It is now known that a protease sensitive co-factor modifies specific prion infectivity. Further investigations may reveal what the co-factor is, if there is more than one, and how it interacts with PrP^{Sc} in the infectious process. Such information may provide further evidence for the protein only hypothesis of prion propagation and identify novel targets for prion therapeutics.

6 References

(1) Sigurdsson B. Observations on three slow infections of sheep. The British Vet J 1954; 110:341-354.

(2) Alper T, Haig DA, Clarke MC. The exceptionally small size of the scrapie agent. Biochem Biophys Res Commun 1966; 22:278-284.

(3) Alper T, Cramp WA, Haig DA, Clarke MC. Does the agent of scrapie replicate without nucleic acid? Nature 1967; 214:764-766.

(4) Diener TO, McKinley MP, Prusiner SB. Viroids and prions. Proc Natl Acad Sci U S A 1982; 79(17):5220-5224.

(5) Prusiner SB. Novel proteinaceous infectious particles cause scrapie. Science 1982; 216(4542):136-144.

(6) Cho HJ. Requirement of a protein component for scrapie infectivity. Intervirology 1980; 14:213-216.

(7) Hunter GD, Gibbons RA, Kimberlin RH, Millson GC. Further studies of the infectivity and stability of extracts and homogenates derived from scrapie affected mouse brains. J Comp Pathol 1969; 79(1):101-108.

(8) Millson GC, Hunter GD, Kimberlin RH. The physico-chemical nature of the scrapie agent. Front Biol 1976; 44:243-266.

(9) Griffith JS. Self-replication and scrapie. Nature 1967; 215(105):1043-1044.

(10) Weissmann C. Birth of a prion: spontaneous generation revisited. Cell 2005; 122(2):165-168.

(11) Chandler RL. Encephalopathy in mice produced by inoculation with scrapie brain material. Lancet 1961;1378-1379.

(12) Mould DL, Smith W, Dawson AM. Centrifugation studies on the infectivities of cellular fractions derived frommouse brain infected with scrapie (Suffolk strain). J Gen Microbiol 1965; 40(1):71-79.

(13) Kimberlin RH. Experimental scrapie in the mouse: a review of an important model disease. Sci Prog 1976; 63(252):461-481.

(14) Gibbons RA, Hunter GD. Nature of the scrapie agent. Nature 1967; 215:1041-1043.

(15) Hunter GD, Millson GC. Attempts to release the scrapie agent from tissue debris. J Comp Pathol 1967; 77(3):301-307.

(16) Hunter GD, Kimberlin RH, Millson GC, Gibbons RA. An experimental examination of the scrapie agent in cell membrane mixtures. I. Stability and physicochemical properties of the scrapie agent. J Comp Pathol 1971; 81(1):23-32.

(17) Semancik JS, Marsh RF, Geelen JL, Hanson RP. Properties of the scrapie agent-endomembrane complex from hamster brain. J Virol 1976; 18:693-700.

(18) Malone TG, Marsh RF, Hanson RP, Semancik JS. Membrane-free scrapie activity. J Virol 1978; 25(3):933-935.

(19) Siakotos AN, Gajdusek DC, Gibbs CJJr, Traub RD, Bucana C. Partial purification of the scrapie agent from mouse brain by pressure disruption and zonal centrifugation in sucrose-sodium chloride gradients. Virology 1976; 70:230-237.

(20) Brown P, Green EM, Gajdusek DC. Effect of different gradient solutions on the buoyant density of scrapie infectivity. Proc Soc Exp Biol Med 1978; 158(4):513-516.

(21) Prusiner SB, Hadlow WJ, Eklund CM, Race RE, Cochran SP. Sedimentation characteristics of the scrapie agent from murine spleen and brain. Biochemistry 1978; 17(23):4987-4992.

(22) Prusiner SB, Garfin DE, Cochran SP, McKinley MP, Groth DF, Hadlow WJ et al. Experimental scrapie in the mouse: electrophoretic and sedimentation properties of the partially purified agent. J Neurochem 1980; 35:574-582.

(23) Prusiner SB, Hadlow WJ, Eklund CM, Race RE. Sedimentation properties of the scrapie agent. Proc Natl Acad Sci U S A 1977; 74(10):4656-4660.

(24) Prusiner SB, Groth DF, Cochran SP, Masiarz FR, McKinley MP, Martinez HM. Molecular properties, partial purification, and assay by incubation period measurements of the hamster scrapie agent. Biochemistry 1980; 19:4883-4891.

(25) Prusiner SB, Groth DF, Cochran SP, McKinley MP, Masiarz FR. Gel electrophoresis and glass permeation chromatography of the hamster scrapie agent after enzymatic digestion and detergent extraction. Biochemistry 1980; 19:4892-4898.

(26) Prusiner SB, McKinley MP, Groth DF, Bowman K, Mock NI, Cochran SP et al. Scrapie agent contains a hydrophobic protein. Proc Natl Acad Sci U S A 1981; 78:6675-6679.

(27) Prusiner SB, Bolton DC, Groth DF, Bowman K, Cochran SP, Mc Kinley MP. Further purification and characterization of scrapie prions. Biochemistry 1982; 21:6942-6950.

(28) Bolton DC, McKinley MP, Prusiner SB. Identification of a protein that purifies with the scrapie prion. Science 1982; 218:1309-1311.

(29) McKinley MP, Bolton DC, Prusiner SB. A protease-resistant protein is a structural component of the scrapie prion. Cell 1983; 35:57-62.

(30) Hope J, Morton LJ, Farquhar CF, Multhaup G, Beyreuther K, Kimberlin RH. The major polypeptide of scrapie-associated fibrils (SAF) has the same size, charge distribution and N-terminal protein sequence as predicted for the normal brain protein (PrP). EMBO J 1986; 5:2591-2597.

(31) Turk E, Teplow DB, Hood LE, Prusiner SB. Purification and properties of the cellular and scrapie hamster prion proteins. Eur J Biochem 1988; 176:21-30.

(32) Safar J, Wang W, Padgett MP, Ceroni M, Piccardo P, Zopf D et al. Molecular mass, biochemical composition, and physicochemical behavior of the infectious form of the scrapie precursor protein monomer. Proc Natl Acad Sci U S A 1990; 87:6373-6377.

(33) Prusiner SB. Molecular Biology of Prion Diseases. Science 1991; 252(14 June):1515-1522.

(34) Prusiner SB, Groth DF, Bolton DC, Kent SB, Hood LE. Purification and structural studies of a major scrapie prion protein. Cell 1984; 38:127-134.

(35) Bendheim PE, Barry RA, DeArmond SJ, Stites DP, Prusiner SB. Antibodies to a scrapie prion protein. Nature 1984; 310:418-421.

(36) Chesebro B, Race R, Wehrly K, Nishio J, Bloom M, Lechner D et al. Identification of scrapie prion protein-specific mRNA in scrapie- infected and uninfected brain. Nature 1985; 315:331-333.

(37) Oesch B, Westaway D, Walchli M, McKinley MP, Kent SB, Aebersold R et al. A cellular gene encodes scrapie PrP 27-30 protein. Cell 1985; 40:735-746.

(38) Basler K, Oesch B, Scott M, Westaway D, Walchli M, Groth DF et al. Scrapie and cellular PrP isoforms are encoded by the same chromosomal gene. Cell 1986; 46:417-428.

(39) Locht C, Chesebro B, Race R, Keith JM. Molecular cloning and complete sequence of prion protein cDNA from mouse brain infected with the scrapie agent. Proc Natl Acad Sci U S A 1986; 83:6372-6376.

(40) Van Rheede T, Smolenaars MM, Madsen O, De Jong WW. Molecular evolution of the Mammalian prion protein. Mol Biol Evol 2003; 20(1):111-121.

(41) Wopfner F, Weidenhöfer G, Schneider R, Von Brunn A, Gilch S, Schwarz TF et al. Analysis of 27 mammalian and 9 avian PrPs reveals high conservation of flexible regions of the prion protein. Journal of Molecular Biology 1999; 289(5):1163-1178.

(42) Collinge J, Palmer.M.S. Prion Diseases. 1st ed. Oxford: Oxford University Press, 1997.

(43) Stahl N, Borchelt DR, Hsiao K, Prusiner SB. Scrapie prion protein contains a phosphatidylinositol glycolipid. Cell 1987; 51:229-240.

(44) Baldwin MA, Stahl N, Hecker R, Pan KM, Burlingame AL, Prusiner SB. Glycosylinositol Phospholipid Anchors of Prion Proteins. In: Prusiner SB, Collinge J, Powell J, Anderton B, editors. Prion Diseases of Humans and Animals. London: Ellis Horwood, 1992.

(45) Chatterjee S, Mayor S. The GPI-anchor and protein sorting. Cell Mol Life Sci 2001; 58(14):1969-1987.

(46) Baldwin MA, Stahl N, Reinders LG, Gibson BW, Prusiner SB, Burlingame AL. Permethylation and tandem mass spectrometry of oligosaccharides having free hexosamine: analysis of the glycoinositol phospholipid anchor glycan from the scrapie prion protein. Anal Biochem 1990; 191:174-182.

(47) Stahl N, Baldwin MA, Teplow D, Hood L, Beavis R, Chait B et al. Cataloging Post-Translational Modifications of the scrapie prion protein by mass spectrometry. In: Prusiner SB, Collinge J, Powell J, Anderton B, editors. Prion Diseases of Humans and Animals. London: Ellis Horwood, 1992.

(48) Stahl N, Borchelt DR, Prusiner SB. Differential release of cellular and scrapie prion proteins from cellular membranes by phosphatidylinositol-specific phospholipase. Biochemistry 1990; 29:5405-5412.

(49) Caughey B, Neary K, Buller R, Ernst D, Perry LL, Chesebro B et al. Normal and scrapie-associated forms of prion protein differ in their sensitivities to phospholipase and proteases in intact neuroblastoma cells. J Virol 1990; 64:1093-1101.

(50) Borchelt DR, Rogers M, Stahl N, Telling G, Prusiner SB. Release of the cellular prion protein from cultured cells after loss of its glycoinositol phospholipid anchor. Glycobiology 1993; 3:319-329.

(51) Lewis PA, Properzi F, Prodromidou K, Clarke AR, Collinge J, Jackson GS. Removal of the glycosylphosphatidylinositol anchor from PrP(Sc) by cathepsin D does not reduce prion infectivity. Biochem J 2006; 395(2):443-448.

(52) Chesebro B, Trifilo M, Race R, Meade-White K, Teng C, LaCasse R et al. Anchorless prion protein results in infectious amyloid disease without clinical scrapie. Science 2005; 308(5727):1435-1439.

(53) Baldwin MA. Analysis of glycosylphosphatidylinositol protein anchors: the prion protein. Methods Enzymol 2005; 405:172-187.

(54) Endo T, Groth D, Prusiner SB, Kobata A. Diversity of oligosaccharide structures linked to asparagines of the scrapie prion protein. Biochemistry 1989; 28:8380-8388.

(55) Somerville RA, Ritchie LA. Differential glycosylation of the protein (PrP) forming scrapie- associated fibrils. J Gen Virol 1990; 71:833-839.

(56) Rudd PM, Wormald MR, Wing DR, Prusiner SB, Dwek RA. Prion glycoprotein: Structure, dynamics, and roles for the sugars. Biochemistry 2001; 40(13):3759-3766.

(57) Rudd PM, Endo T, Colominas C, Groth D, Wheeler SF, Harvey DJ et al. Glycosylation differences between the normal and pathogenic prion protein isoforms. Proc Natl Acad Sci USA 1999; 96(23):13044-13049.

(58) Riek R, Hornemann S, Wider G, Billeter M, Glockshuber R, Wuthrich K. NMR structure of the mouse prion protein domain PrP (121-231). Nature 1996; 382:180-182.

(59) Zahn R, Liu AZ, Lührs T, Riek R, Von Schroetter C, García FL et al. NMR solution structure of the human prion protein. Proc Natl Acad Sci USA 2000; 97(1):145-150.

(60) Liu H, Farr-Jones S, Ulyanov NB, Llinas M, Marqusee S, Groth D et al. Solution structure of syrian hamster prion protein (90-231). Biochemistry 1999; 38(17):5362-5377.

(61) Hosszu LLP, Baxter NJ, Jackson GS, Power A, Clarke AR, Waltho JP et al. Structural mobility of the human prion protein probed by backbone hydrogen exchange. Nature Struct Biol 1999; 6(8):740-743.

(62) Lysek DA, Schorn C, Nivon LG, Esteve-Moya V, Christen B, Calzolai L et al. Prion protein NMR structures of cats, dogs, pigs, and sheep. Proc Natl Acad Sci U S A 2005; 102(3):640-645.

(63) Calzolai L, Lysek DA, Perez DR, Guntert P, Wuthrich K. Prion protein NMR structures of chickens, turtles, and frogs. Proc Natl Acad Sci U S A 2005; 102(3):651-655.

(64) Gossert AD, Bonjour S, Lysek DA, Fiorito F, Wuthrich K. Prion protein NMR structures of elk and of mouse/elk hybrids. Proc Natl Acad Sci U S A 2005; 102(3):646-650.

(65) Hosszu LL, Jackson GS, Trevitt CR, Jones S, Batchelor M, Bhelt D et al. The residue 129 polymorphism in human prion protein does not confer susceptibility to CJD by altering the structure or global stability of PrPC. J Biol Chem 2004; 279(27):28515-28521.

(66) Hornemann S, Schorn C, Wuthrich K. NMR structure of the bovine prion protein isolated from healthy calf brains. EMBO Rep 2004; 5(12):1159-1164.

(67) Eghiaian F, Grosclaude J, Lesceu S, Debey P, Doublet B, Treguer E et al. Insight into the PrPC -> PrPSc conversion from the structures of antibody-bound ovine prion scrapie-susceptibility variants. Proc Natl Acad Sci U S A 2004; 101(28):10254-10259.

(68) Haire LF, Whyte SM, Vasisht N, Gill AC, Verma C, Dodson EJ et al. The crystal structure of the globular domain of sheep prion protein. J Mol Biol 2004; 336(5):1175-1183.

(69) Knaus KJ, Morillas M, Swietnicki W, Malone M, Surewicz WK, Yee VC. Crystal structure of the human prion protein reveals a mechanism for oligomerization. Nat Struct Biol 2001; 8(9):770-774.

(70) Jackson GS, Murray I, Hosszu LLP, Gibbs N, Waltho JP, Clarke AR et al. Location and properties of metal-binding sites on the human prion protein. Proc Natl Acad Sci U S A 2001; 98(15):8531-8535.

(71) Riek R, Wider G, Billeter M, Hornemann S, Glockshuber R, Wuthrich K. Prion protein NMR structure and familial human spongiform encephalopathies. Proc Natl Acad Sci U S A 1998; 95(20):11667-11672.

(72) Nishina K, Jenks S, Supattapone S. Ionic strength and transition metals control PrP^{Sc} protease resistance and conversion-inducing activity. J Biol chem 2004; 279(39):40788-40794.

(73) Brown LR, Harris DA. Copper and zinc cause delivery of the prion protein from the plasma membrane to a subset of early endosomes and the Golgi. J Neurochem 2003; 87(2):353-363.

(74) Taylor DR, Hooper NM. The prion protein and lipid rafts (Review). Mol Membr Biol 2006; 23(1):89-99.

(75) Taylor DR, Watt NT, Perera WS, Hooper NM. Assigning functions to distinct regions of the N-terminus of the prion protein that are involved in its copper-stimulated, clathrin-dependent endocytosis. J Cell Sci 2005; 118(Pt 21):5141-5153.

(76) Hill AF, Joiner S, Beck JA, Campbell TA, Dickinson A, Poulter M et al. Distinct glycoform ratios of protease resistant prion protein associated with PRNP point mutations. Brain 2006; 129(Pt 3):676-685.

(77) Mead S. Prion disease genetics. Eur J Hum Genet 2006; 14(3):273-281.

(78) Kovacs GG, Voigtlander T, Gelpi E, Budka H. Rationale for diagnosing human prion disease. World J Biol Psychiatry 2004; 5(2):83-91.

(79) Kovacs GG, Kalev O, Budka H. Contribution of neuropathology to the understanding of human prion disease. Folia Neuropathol 2004; 42 Suppl A:69-76.

(80) Mead S, Poulter M, Beck J, Webb TE, Campbell TA, Linehan JM et al. Inherited prion disease with six octapeptide repeat insertional mutation--molecular analysis of phenotypic heterogeneity. Brain 2006; 129(Pt 9):2297-2317.

(81) Stewart RS, Harris DA. Mutational analysis of topological determinants in PrP, and measurement of transmembrane and cytosolic PrP during prion infection. J Biol Chem 2003; 278(46):45960-45968.

(82) Glover KJ, Whiles JA, Wood MJ, Melacini G, Komives EA, Vold RR. Conformational dimorphism and transmembrane orientation of prion protein residues 110-136 in bicelles. Biochemistry 2001; 40(44):13137-13142.

(83) Forloni G, Angeretti N, Chiesa R, Monzani E, Salmona M, Bugiani O et al. Neurotoxicity of a prion protein fragment. Nature 1993; 362:543-546.

(84) Gasset M, Baldwin MA, Lloyd DH, Gabriel JM, Holtzman DM, Cohen F et al. Predicted alpha-helical regions of the prion protein when synthesized as peptides form amyloid. Proc Natl Acad Sci U S A 1992; 89:10940-10944.

(85) Goldfarb LG, Brown P, Haltia M, Ghiso J, Frangione B, Gajdusek DC. Synthetic peptides corresponding to different mutated regions of the amyloid gene in familial Creutzfeldt-Jakob disease show enhanced in vitro formation of morphologically different amyloid fibrils. Proc Natl Acad Sci U S A 1993; 90:4451-4454.

(86) Selvaggini C, de Gioia L, Cantu L, Ghibaudi E, Diomede L, Passerini F et al. Molecular characteristics of a protease-resistant, amyloidogenic and neurotoxic peptide homologous to residues 106-126 of the prion protein. Biochem Biophys Res Commun 1993; 194:1380-1386.

(87) Owen F, Poulter M, Collinge J, Crow TJ. Codon 129 changes in the prion protein gene in Caucasians. Am J Hum Genet 1990; 46:1215-1216.

(88) Mead S, Stumpf MP, Whitfield J, Beck JA, Poulter M, Campbell T et al. Balancing Selection at the Prion Protein Gene Consistent with Prehistoric Kurulike Epidemics. Science 2003; 300(5619):640-648.

(89) Palmer MS, Collinge J. Mutations and Polymorphisms in the Prion Protein Gene. Human Mutation 1993; 2:168-173.

(90) Collinge J, Whitfield J, McKintosh E, Beck J, Mead S, Thomas DJ et al. Kuru in the 21st century--an acquired human prion disease with very long incubation periods. Lancet 2006; 367(9528):2068-2074.

(91) Collinge J, Palmer MS, Dryden AJ. Genetic predisposition to iatrogenic Creutzfeldt-Jakob disease. Lancet 1991; 337:1441-1442.

(92) Palmer MS, Dryden AJ, Hughes JT, Collinge J. Homozygous prion protein genotype predisposes to sporadic Creutzfeldt-Jakob disease. Nature 1991; 352:340-342.

(93) Baskakov IV, Legname G, Baldwin MA, Prusiner SB, Cohen FE. Pathway complexity of prion protein assembly into amyloid. J Biol Chem 2002; 277(24):21140-21148.

(94) Jackson GS, Hill AF, Joseph C, Hosszu LLP, Clarke AR, Collinge J. Multiple folding pathways for heterologously expressed human prion protein. Biochimica et Biophysica Acta 1999; 1431(1):1-13.

(95) Lewis PA, Tattum MH, Jones S, Bhelt D, Batchelor M, Clarke AR et al. Codon 129 polymorphism of the human prion protein influences the kinetics of amyloid formation. J Gen Virol 2006; 87(Pt 8):2443-2449.

(96) Gasset M, Baldwin MA, Fletterick RJ, Prusiner SB. Perturbation of the secondary structure of the scrapie prion protein under conditions that alter infectivity. Proc Natl Acad Sci U S A 1993; 90:1-5.

(97) Pan K-M, Baldwin MA, Nguyen J, Gasset M, Serban A, Groth D et al. Conversion of α-helices into β-sheets features in the formation of the scrapie prion proteins. Proc Natl Acad Sci USA 1993; 90:10962-10966.

(98) Thomzig A, Spassov S, Friedrich M, Naumann D, Beekes M. Discriminating scrapie and BSE isolates by infrared spectroscopy of pathological prion protein. J Biol Chem 2004; 279(32):33847-33854.

(99) Caughey B, Raymond GJ, Bessen RA. Strain-dependent differences in β-sheet conformations of abnormal prion protein. Journal of Biological Chemistry 1998; 273(48):32230-32235.

(100) Spassov S, Beekes M, Naumann D. Structural differences between TSEs strains investigated by FT-IR spectroscopy. Biochim Biophys Acta 2006; 1760(7):1138-1149.

(101) Bessen RA, Marsh RF. Biochemical and physical properties of the prion protein from two strains of the transmissible mink encephalopathy agent. J Virol 1992; 66:2096-2101.

(102) Budka H. Neuropathology of prion diseases. Br Med Bull 2003; 66(1):121-130.

(103) Tattum MH, Cohen-Krausz S, Khalili-Shirazi A, Jackson GS, Orlova EV, Collinge J et al. Elongated Oligomers Assemble into Mammalian PrP Amyloid Fibrils. J Mol Biol 2006; 357:975-985.

(104) Lasmezas CI. Putative functions of PrP(C). Br Med Bull 2003; 66(1):61-70.

(105) Swietnicki W, Petersen R, Gambetti P, Surewicz WK. pH-dependent stability and conformation of the recombinant human prion protein PrP(90-231). J Biol Chem 1997; 272(44):27517-27520.

(106) Mehlhorn I, Groth D, Stöckel J, Moffat B, Reilly D, Yansura D et al. High-level expression and characterization of a purified 142-residue polypeptide of the prion protein. Biochemistry 1996; 35:5528-5537.

(107) Weissmann C, Bueler H, Fischer M, Bluethmann H, Aguet M. Molecular biology of prion diseases. Dev Biol Stand 1993; 80:53-54.

(108) Baskakov IV, Legname G, Prusiner SB, Cohen FE. Folding of prion protein to its native α-helical conformation is under kinetic control. Journal of Biological Chemistry 2001; 276(23 PT 1):19687-19690.

(109) Jackson GS, Hosszu LLP, Power A, Hill AF, Kenney J, Saibil H et al. Reversible Conversion of Monomeric Human Prion Protein Between Native and Fibrilogenic Conformations. Science 1999; 283:1935-1937.

(110) Khalili-Shirazi A, Summers L, Linehan J, Mallinson G, Anstee D, Hawke S et al. PrP glycoforms are associated in a strain-specific ratio in native PrP^{Sc}. J Gen Virol 2005; 86(Pt 9):2635-2644.

(111) Lu BY, Beck PJ, Chang JY. Oxidative folding of murine prion mPrP(23-231). Eur J Biochem 2001; 268(13):3767-3773.

(112) Apetri AC, Surewicz WK. Kinetic intermediate in the folding of human prion protein. J Biol Chem 2002; 277(47):44589-44592.

(113) Hosszu LL, Wells MA, Jackson GS, Jones S, Batchelor M, Clarke AR et al. Definable Equilibrium States in the Folding of Human Prion Protein. Biochemistry 2005; 44(50):16649-16657.

(114) Wildegger G, Liemann S, Glockshuber R. Extremely rapid folding of the C-terminal domain of the prion protein without kinetic intermediates. Nature Struct Biol 1999; 6(6):550-553.

(115) Collinge J. Prion diseases of humans and animals: their causes and molecular basis. Annu Rev Neurosci 2001; 24:519-550.

(116) Jackson GS, Clarke AR. Mammalian prion proteins. Curr Opin Struct Biol 2000; 10(1):69-74.

(117) Prusiner SB, Groth D, Serban A, Stahl N, Gabizon R. Attempts to restore scrapie prion infectivity after exposure to protein denaturants. Proc Natl Acad Sci U S A 1993; 90:2793-2797.

(118) Stöckel J, Safar J, Wallace AC, Cohen FE, Prusiner SB. Prion protein selectively binds copper(II) ions. Biochemistry 1998; 37:7185-7193.

(119) Wong BS, Vénien-Bryan C, Williamson RA, Burton DR, Gambetti P, Sy MS et al. Copper refolding of prion protein. Biochemical and Biophysical Research Communications 2000; 276(3):1217-1224.

(120) Qin K, Yang DS, Yang Y, Chishti MA, Meng LJ, Kretzschmar HA et al. Copper(II)-induced conformational changes and protease resistance in recombinant and cellular PrP. Effect of protein age and deamidation. J Biol Chem 2000; 275(25):19121-19131.

(121) Kuczius T, Buschmann A, Zhang W, Karch H, Becker K, Peters G et al. Cellular prion protein acquires resistance to proteolytic degradation following copper ion binding. Biol Chem 2004; 385(8):739-747.

(122) McKenzie D, Bartz J, Mirwald J, Olander D, Marsh R, Aiken J. Reversibility of scrapie inactivation is enhanced by copper. Journal of Biological Chemistry 1998; 273(40):25545-25547.

(123) Giese A, Levin J, Bertsch U, Kretzschmar H. Effect of metal ions on de novo aggregation of full-length prion protein. Biochem Biophys Res Commun 2004; 320(4):1240-1246.

(124) Legname G, Baskakov IV, Nguyen HO, Riesner D, Cohen FE, DeArmond SJ et al. Synthetic mammalian prions. Science 2004; 305(5684):673-676.

(125) Legname G, Nguyen HO, Baskakov IV, Cohen FE, DeArmond SJ, Prusiner SB. Strain-specified characteristics of mouse synthetic prions. Proc Natl Acad Sci U S A 2005; 102(6):2168-2173.

(126) Baskakov IV, Breydo L. Converting the prion protein: What makes the protein infectious. Biochim Biophys Acta 2006.

(127) Kocisko DA, Come JH, Priola SA, Chesebro B, Raymond GJ, Lansbury PT et al. Cell-free formation of protease-resistant prion protein. Nature 1994; 370:471-474.

(128) Kocisko DA, Priola SA, Raymond GJ, Chesebro B, Lansbury PT, Jr., Caughey B. Species specificity in the cell-free conversion of prion protein to protease-resistant forms: a model for the scrapie species barrier. Proc Natl Acad Sci U S A 1995; 92(9):3923-3927.

(129) Bessen RA, Kocisko DA, Raymond GJ, Nandan S, Lansbury PT, Caughey B. Non-genetic propagation of strain-specific properties of scrapie prion protein. Nature 1995; 375:698-700.

(130) Raymond GJ, Hope J, Kocisko DA, Priola SA, Raymond LD, Bossers A et al. Molecular assessment of the potential transmissibilities of BSE and scrapie to humans. Nature 1997; 388:285-288.

(131) Caughey WS, Raymond LD, Horiuchi M, Caughey B. Inhibition of protease-resistant prion protein formation by porphyrins and phthalocyanines. Proc Natl Acad Sci USA 1998; 95:12117-12122.

(132) Chabry J, Caughey B, Chesebro B. Specific inhibition of *in vitro* formation of protease-resistant prion protein by synthetic peptides. J Biol chem 1998; 273(21):13203-13207.

(133) Demaimay R, Harper J, Gordon H, Weaver D, Chesebro B, Caughey B. Structural aspects of Congo red as an inhibitor of protease-resistant prion protein formation. J Neurochem 1998; 71(6):2534-2541.

(134) Caughey B. Prion protein conversions: insight into mechanisms, TSE transmission barriers and strains. Br Med Bull 2003; 66(1):109-120.

(135) Sarafoff NI, Bieschke J, Giese A, Weber P, Bertsch U, Kretzschmar HA. Automated PrP^{res} amplification using indirect sonication. J Biochem Biophys Methods 2005; 63(3):213-221.

(136) Bieschke J, Weber P, Sarafoff N, Beekes M, Giese A, Kretzschmar H. Autocatalytic self-propagation of misfolded prion protein. Proc Natl Acad Sci U S A 2004; 101(33):12207-12211.

(137) Castilla J, Saa P, Hetz C, Soto C. In vitro generation of infectious scrapie prions. Cell 2005; 121(2):195-206.

(138) Saborio GP, Permanne B, Soto C. Sensitive detection of pathological prion protein by cyclic amplification of protein misfolding. Nature 2001; 411(6839):810-813.

(139) Supattapone S. Prion protein conversion in vitro. J Mol Med 2004; 82(6):348-356.

(140) Rubenstein R, Carp RI, Callahan SM. In vitro replication of scrapie agent in a neuronal model: infection of PC12 cells. J Gen Virol 1984; 65:2191-2198.

(141) Butler DA, Scott MR, Bockman JM, Borchelt DR, Taraboulos A, Hsiao KK et al. Scrapie-infected murine neuroblastoma cells produce protease- resistant prion proteins. J Virol 1988; 62:1558-1564.

(142) Schatzl HM, Laszlo L, Holtzman DM, Tatzelt J, DeArmond SJ, Weiner RI et al. A hypothalamic neuronal cell line persistently infected with scrapie prions exhibits apoptosis. J Virol 1997; 71(11):8821-8831.

(143) Bosque PJ, Prusiner SB. Cultured cell sublines highly susceptible to prion infection. Journal of Virology 2000; 74(9):4377-4386.

(144) Klohn PC, Stoltze L, Flechsig E, Enari M, Weissmann C. A quantitative, highly sensitive cell-based infectivity assay for mouse scrapie prions. Proc Natl Acad Sci U S A 2003; 100(20):11666-11671.

(145) Safar JG, Kellings K, Serban A, Groth D, Cleaver JE, Prusiner SB et al. Search for a prion-specific nucleic Acid. J Virol 2005; 79(16):10796-10806.

(146) Safar JG, DeArmond SJ, Kociuba K, Deering C, Didorenko S, Bouzamondo-Bernstein E et al. Prion clearance in bigenic mice. J Gen Virol 2005; 86(Pt 10):2913-2923.

(147) Silveira JR, Raymond GJ, Hughson AG, Race RE, Sim VL, Hayes SF et al. The most infectious prion protein particles. Nature 2005; 437(7056):257-261.

(148) Bueler H, Aguzzi A, Sailer A, Greiner RA, Autenried P, Aguet M et al. Mice devoid of PrP are resistant to scrapie. Cell 1993; 73:1339-1347.

(149) Sailer A, Bueler H, Fischer M, Aguzzi A, Weissmann C. No propagation of prions in mice devoid of PrP. Cell 1994; 77:967-968.

(150) Weissmann C, Flechsig E. PrP knock-out and PrP transgenic mice in prion research. Br Med Bull 2003; 66(1):43-60.

(151) Mallucci GR, Ratté S, Asante EA, Linehan J, Gowland I, Jefferys JGR et al. Post-natal knockout of prion protein alters hippocampal CA1 properties, but does not result in neurodegeneration. EMBO J 2002; 21(3):202-210.

(152) Mallucci G, Dickinson A, Linehan J, Klohn PC, Brandner S, Collinge J. Depleting neuronal PrP in prion infection prevents disease and reverses spongiosis. Science 2003; 302(5646):871-874.

(153) Mallucci G, Collinge J. Rational targeting for prion therapeutics. Nat Rev Neurosci 2005; 6(1):23-34.

(154) Asante E, Collinge J. Transgenic studies of the influence of the PrP structure on TSE diseases. Advances in Protein Chemistry. Academic Press, 2000: 273-311.

(155) Giese A, Groschup MH, Hess B, Kretzschmar HA. Neuronal cell death in scrapie-infected mice is due to apoptosis. Brain Pathol 1995; 5:213-221.

(156) Cronier S, Laude H, Peyrin JM. Prions can infect primary cultured neurons and astrocytes and promote neuronal cell death. Proc Natl Acad Sci U S A 2004; 101(33):12271-12276.

(157) Kristiansen M, Messenger MJ, Klohn PC, Brandner S, Wadsworth JD, Collinge J et al. Disease-related prion protein forms aggresomes in neuronal cells leading to caspase-activation and apoptosis. J Biol chem 2005; 280(46):38851-38861.

(158) Hetz C, Russelakis-Carneiro M, Maundrell K, Castilla J, Soto C. Caspase-12 and endoplasmic reticulum stress mediate neurotoxicity of pathological prion protein. EMBO J 2003; 22(20):5435-5445.

(159) Ma JY, Lindquist S. Wild-type PrP and a mutant associated with prion disease are subject to retrograde transport and proteasome degradation. Proc Natl Acad Sci USA 2001; 98(26):14955-14960.

(160) Ma J, Lindquist S. Conversion of PrP to a Self-Perpetuating PrP^{Sc}-like Conformation in the Cytosol. Science 2002; 298(5599):1785-1788.

(161) Ciechanover A, Brundin P. The ubiquitin proteasome system in neurodegenerative diseases. Sometimes the chicken, sometimes the egg. Neuron 2003; 40(2):427-446.

(162) Verhoef LG, Lindsten K, Masucci MG, Dantuma NP. Aggregate formation inhibits proteasomal degradation of polyglutamine proteins. Hum Mol Genet 2002; 11(22):2689-2700.

(163) Bence NF, Sampat RM, Kopito RR. Impairment of the ubiquitin-proteasome system by protein aggregation. Science 2001; 292(5521):1552-1555.

(164) Journal of the House of Commons 1755; 27:87.

(165) Brown P, Bradley R. 1755 and all that: a historical primer of transmissible spongiform encephalopathy. BMJ 1998; 317(7174):1688-1692.

(166) Besnoit MM, Morel Ch. Note sur les lesions nerveuses de la tremblante du mouton. Revue Veterinaire, T 1898; XXIII (LV):27-400.

(167) Cuillé J, Chelle PL. La maladie dite tremblante du mouton est-elle inocuable? C R Acad Sci 1936; 203:1552-1554.

(168) Gordon WS. Advances in veterinary research. Vet Rec 1946; 58:518-525.

(169) Brown P, Cathala F, Raubertas RF, Gajdusek DC, Castaigne P. The epidemiology of Creutzfeldt-Jakob disease: conclusion of a 15-year investigation in France and review of the world literature. Neurology 1987; 37:895-904.

(170) Williams ES, Young S. Chronic wasting disease of captive mule deer: a spongiform encephalopathy. J Wildl Dis 1980; 16:89-98.

(171) Williams ES, Miller MW. Chronic wasting disease in deer and elk in North America. Rev Sci Tech 2002; 21(2):305-316.

(172) Miller MW, Williams ES. Chronic wasting disease of cervids. Curr Top Microbiol Immunol 2004; 284:193-214.

(173) Miller MW, Conner MM. Epidemiology of chronic wasting disease in free-ranging mule deer: spatial, temporal, and demographic influences on observed prevalence patterns. J Wildl Dis 2005; 41(2):275-290.

(174) Miller MW. Environmental sources of prion transmission in mule deer. Emerg Infect Dis 2004; 10(6):1003-1006.

(175) Marsh RF, Bessen RA, Lehmann S, Hartsough GR. Epidemiological and experimental studies on a new incident of transmissible mink encephalopathy. J Gen Virol 1991; 72:589-594.

(176) Kimberlin RH, Marsh RF. Comparison of scrapie and transmissible mink encephalopathy in hamsters. I. Biochemical studies of brain during development of disease. J Infect Dis 1975; 131:97-103.

(177) Marsh RF, Bessen RA. Epidemiologic and experimental studies on transmissible mink encephalopathy. Dev Biol Stand 1993; 80:111-118.

(178) Weissmann C, Aguzzi A. Bovine spongiform encephalopathy and early onset variant Creutzfeldt-Jakob disease. Curr Opin Neurobiol 1997; 7:695-700.

(179) Donnelly CA, Ferguson NM, Ghani AC, Anderson RM. Implications of BSE infection screening data for the scale of the British BSE epidemic and current European infection levels. Proc R Soc Lond B Biol Sci 2002; 269(1506):2179-2190.

(180) Ferguson NM, Ghani AC, Donnelly CA, Hagenaars TJ, Anderson RM. Estimating the human health risk from possible BSE infection of the British sheep flock. Nature 2002; 415(6870):420-424.

(181) Collinge J. Variant Creutzfeldt-Jakob disease. Lancet 1999; 354(9175):317-323.

(182) Pattison IH. Experiments with scrapie with special reference to the nature of the agent and the pathology of the disease. In: Gajdusek CJ, Gibbs CJ, Alpers MP, editors. Slow, Latent and Temperate Virus Infections, NINDB Monograph 2. Washington DC: US Government Printing, 1965: 249-257.

(183) Will RG, Ironside JW, Zeidler M, Cousens SN, Estibeiro K, Alperovitch A et al. A new variant of Creutzfeldt-Jakob disease in the UK. Lancet 1996; 347:921-925.

(184) Hill AF, Desbruslais M, Joiner S, Sidle KCL, Gowland I, Collinge J. The same prion strain causes vCJD and BSE. Nature 1997; 389:448-450.

(185) Collinge J. Assessing Risks of BSE Transmission to Humans. In: Goebel K, editor. International Seminar on Nuclear War and Planetary Emergencies. Singapore: World Scientific, 1997: 54.

(186) Bruce ME, Will RG, Ironside JW, McConnell I, Drummond D, Suttie A et al. Transmissions to mice indicate that 'new variant' CJD is caused by the BSE agent. Nature 1997; 389:498-501.

(187) Collinge J, Rossor M. A new variant of prion disease. Lancet 1996; 347:916-917.

(188) Sugiura K, Ito K, Yokoyama R, Kumagai S, Onodera T. A model to assess the risk of the introduction into Japan of the bovine spongiform encephalopathy agent through imported animals, meat and meat-and-bone meal. Rev Sci Tech 2003; 22(3):777-794.

(189) Coulthart MB, Mogk R, Rancourt JM, Godal DL, Czub S. Prion protein gene sequence of Canada's first non-imported case of bovine spongiform encephalopathy (BSE). Genome 2003; 46(6):1005-1009.

(190) Agerholm JS, Tegtmeier CL, Nielsen TK. Survey of laboratory findings in suspected cases of bovine spongiform encephalopathy in Denmark from 1990 to 2000. APMIS 2002; 110(1):54-60.

(191) Calavas D, Ducrot C, Baron TG. Past, present and future of bovine spongiform encephalopathy in France. Curr Top Microbiol Immunol 2004; 284:51-63.

(192) Cohen-Sabas CH, Heim D, Zurbriggen A, Stark KD. Age-period-cohort analysis of the Bovine Spongiform Encephalopathy (BSE) epidemic in Switzerland. Prev Vet Med 2004; 66(1-4):19-33.

(193) Cunningham AA, Kirkwood JK, Dawson M, Spencer YI, Green RB, Wells GAH. Distribution of Bovine Spongiform Encephalopathy Infectivity in Greater Kudu (Tragelaphus strepsiceros). Emerg Infect Dis 2004; 10(6):1011-1049.

(194) Kirkwood JK, Cunningham AA. Epidemiological observations on spongiform encephalopathies in captive wild animals in the British Isles. Vet Rec 1994; 135:296-303.

(195) Cunningham AA. Bovine Spongiform Encephalopathy and British Zoos. Journal of Zoo and Wildlife Medicine 1991; 22(3):304-308.

(196) Creutzfeldt HG. Uber eine eigenartige herdfoermige Erkrankung des Zentralnervensystems. Z Gesamte Neurol Psychiatry 1920; 57:1-18.

(197) Jakob A. Uber eigenartige Erkrankungen des Zentralnervensystems mit bemerkenswertem anatomischem Befund. Z Gesamte Neurol psychiatry 1921; 64:147-228.

(198) Jakob A. Uber eine der multiplen Sklerose klinisch nahestehende Erkrankung des Zentralnervensystems (spastische Pseudosklerose) mit bemerkenswertem anatomischen Befund. Med Klin 1921; 13:372-376.

(199) Caramelli M, Ru G, Acutis P, Forloni G. Prion diseases: current understanding of epidemiology and pathogenesis, and therapeutic advances. CNS Drugs 2006; 20(1):15-28.

(200) Brown P, Cathala F, Castaigne P, Gajdusek DC. Creutzfeldt-Jakob disease: clinical analysis of a consecutive series of 230 neuropathologically verified cases. Ann Neurol 1986; 20:597-602.

(201) Brown P, Rodgers-Johnson P, Cathala F, Gibbs CJJr, Gajdusek DC. Creutzfeldt-Jakob disease of long duration: clinicopathological characteristics, transmissibility, and differential diagnosis. Annals of Neurology 1984; 16:295-304.

(202) Gambetti P, Kong Q, Zou W, Parchi P, Chen SG. Sporadic and familial CJD: classification and characterisation. Br Med Bull 2003; 66(1):213-239.

(203) Gomori AJ, Partnow MJ, Horoupian DS, Hirano A. The ataxic form of Creutzfeldt-Jakob disease. Arch Neurol 1973; 29:318-323.

(204) Kropp S, Schulz-Schaeffer WJ, Finkenstaedt M, Riedemann C, Windl O, Steinhoff BJ et al. The Heidenhain variant of Creutzfeldt-Jakob disease. Arch Neurol 1999; 56(1):55-61.

(205) Schroter A, Zerr I, Henkel K, Tschampa HJ, Finkenstaedt M, Poser S. Magnetic resonance imaging in the clinical diagnosis of Creutzfeldt-Jakob disease. Arch Neurol 2000; 57(12):1751-1757.

(206) Giraud P, Biacabe AG, Chazot G, Later R, Joyeux O, Moene Y et al. Increased Detection of 14-3-3 Protein in Cerebrospinal Fluid in Sporadic Creutzfeldt-Jakob Disease during the Disease Course. Eur Neurol 2002; 48(4):218-221.

(207) Zerr I, Schulz-Schaeffer WJ, Giese A, Bodemer M, Schroeter A, Henkel K et al. Current Clinical Diagnosis in Creutzfeldt-Jakob Disease: Identification of Uncommon Variants. Ann Neurol 2000; 48(3):323-329.

(208) Hsiao K, Baker HF, Crow TJ, Poulter M, Owen F, Terwilliger JD et al. Linkage of a prion protein missense variant to Gerstmann- Straussler syndrome. Nature 1989; 338:342-345.

(209) Doh ura K, Tateishi J, Sasaki H, Kitamoto T, Sakaki Y. Pro----leu change at position 102 of prion protein is the most common but not the sole mutation related to Gerstmann-Straussler syndrome. Biochem Biophys Res Commun 1989; 163:974-979.

(210) Kovacs GG, Trabattoni G, Hainfellner JA, Ironside JW, Knight RS, Budka H. Mutations of the prion protein gene phenotypic spectrum. J Neurol 2002; 249(11):1567-1582.

(211) Barbanti P, Fabbrini G, Salvatore M, Petraroli R, Cardone F, Maras B et al. Polymorphism at codon 129 or codon 219 of *PRNP* and clinical heterogeneity in a previously unreported family with Gerstmann- Straussler-Scheinker disease (PrP-P102L mutation). Neurology 1996; 47:734-741.

(212) Chapman J, Brown P, Goldfarb LG, Arlazoroff A, Gajdusek DC, Korczyn AD. Clinical heterogeneity and unusual presentations of Creutzfeldt- Jakob disease in Jewish patients with the PRNP codon 200 mutation. J Neurol Neurosurg Psychiatry 1993; 56:1109-1112.

(213) Wadsworth JD, Joiner S, Linehan JM, Cooper S, Powell C, Mallinson G et al. Phenotypic heterogeneity in inherited prion disease (P102L) is associated with

differential propagation of protease-resistant wild-type and mutant prion protein. Brain 2006; 129(Pt 6):1557-1569.

(214) Goldfarb LG, Brown P, McCombie WR, Goldgaber D, Swergold GD, Wills PR et al. Transmissible familial Creutzfeldt-Jakob disease associated with five, seven, and eight extra octapeptide coding repeats in the *PRNP* gene. Proc Natl Acad Sci USA 1991; 88:10926-10930.

(215) Beck JA, Mead S, Campbell TA, Dickinson A, Wientjens DPMW, Croes EA et al. Two-octapeptide repeat deletion of prion protein associated with rapidly progressive dementia. Neurology 2001; 57(2):354-356.

(216) Owen F, Poulter M, Lofthouse R, Collinge J, Crow TJ, Risby D et al. Insertion in prion protein gene in familial Creutzfeldt-Jakob disease. Lancet 1989; 1:51-52.

(217) Prusiner SB. Inherited prion diseases. Proc Natl Acad Sci USA 1994; 91:4611-4614.

(218) Mitrova E, Belay G. Creutzfeldt-Jakob disease with E200K mutation in Slovakia: characterization and development. Acta Virol 2002; 46(1):31-39.

(219) Collinge J, Palmer MS, Campbell TA, Sidle KCL, Carroll D, Harding AE. Inherited prion disease (PrP lysine 200) in Britain: two case reports. BMJ 1993; 306:301-302.

(220) Goldfarb LG, Brown P, Mitrova E, Cervenakova L, Goldin L, Korczyn AD et al. Creutzfeldt-Jacob disease associated with the PRNP codon 200Lys mutation: an analysis of 45 families. Eur J Epidemiol 1991; 7:477-486.

(221) Simon ES, Kahana E, Chapman J, Treves TA, Gabizon R, Rosenmann H et al. Creutzfeldt-Jakob disease profile in patients homozygous for the PRNP E200K mutation. Annals of Neurology 2000; 47(2):257-260.

(222) Bertoni JM, Brown P, Goldfarb LG, Rubenstein R, Gajdusek DC. Familial Creutzfeldt-Jakob disease (codon 200 mutation) with supranuclear palsy. JAMA 1992; 268:2413-2415.

(223) Inoue I, Kitamoto T, Doh-ura K, Shii H, Goto I, Tateishi J. Japanese family with Creutzfeldt-Jakob disease with codon 200 point mutation of the prion protein gene. Neurology 1994; 44:299-301.

(224) Collinge J, Brown J, Hardy J, Mullan M, Rossor MN, Baker H et al. Inherited prion disease with 144 base pair gene insertion: II: Clinical and pathological features. Brain 1992; 115:687-710.

(225) Jarius C, Kovacs GG, Belay G, Hainfellner JA, Mitrova E, Budka H. Distinctive cerebellar immunoreactivity for the prion protein in familial (E200K) Creutzfeldt-Jakob disease. Acta Neuropathol (Berl) 2003; 105(5):449-454.

(226) Vital C, Gray F, Vital A, Parchi P, Capellari S, Petersen RB et al. Prion encephalopathy with insertion of octapeptide repeats: the number of repeats determines the type of cerebellar deposits. Neuropathol & Appl Neurobiol 1998; 24:125-130.

(227) King A, Doey L, Rossor M, Mead S, Collinge J, Lantos P. Phenotypic variability in the brains of a family with a prion disease characterized by a 144-base pair insertion in the prion protein gene. Neuropathol Appl Neurobiol 2003; 29(2):98-105.

(228) Collinge J, Owen F, Poulter M, Leach M, Crow TJ, Rossor MN et al. Prion dementia without characteristic pathology. Lancet 1990; 336:7-9.

(229) Parchi P, Chen SG, Brown P, Zou W, Capellari S, Budka H et al. Different patterns of truncated prion protein fragments correlate with distinct phenotypes in P102L Gerstmann-Sträussler-Scheinker disease. Proc Natl Acad Sci USA 1998; 95:8322-8327.

(230) Kitamoto T, Amano N, Terao Y, Nakazato Y, Isshiki T, Mizutani T et al. A new inherited prion disease (PrP-P105L mutation) showing spastic paraparesis. Ann Neurol 1993; 34:808-813.

(231) Mastrianni JA, Curtis MT, Oberholtzer JC, Da Costa MM, DeArmond S, Prusiner SB et al. Prion disease (PrP-A117V) presenting with ataxia instead of dementia. Neurology 1995; 45:2042-2050.

(232) Piccardo P, Seiler C, Dlouhy SR, Young K, Farlow MR, Prelli F et al. Proteinase-K-resistant prion protein isoforms in Gerstmann- Straussler-Scheinker disease (Indiana kindred). J Neuropathol Exp Neurol 1996; 55:1157-1163.

(233) Lugaresi E, Medori R, Baruzzi PM, Cortelli P, Lugaresi A, Tinuper P et al. Fatal familial insomnia and dysautonomia, with selective degeneration of thalamic nuclei. N Engl J Med 1986; 315:997-1003.

(234) Montagna P, Gambetti P, Cortelli P, Lugaresi E. Familial and sporadic fatal insomnia. Lancet Neurol 2003; 2(3):167-176.

(235) Goldfarb LG, Haltia M, Brown P, Nieto A, Kovanen J, McCombie WR et al. New mutation in scrapie amyloid precursor gene (at codon 178) in Finnish Creutzfeldt-Jakob kindred. Lancet 1991; 337:425.

(236) Collins S, McLean CA, Masters CL. Gerstmann-Straussler-Scheinker syndrome,fatal familial insomnia, and kuru: a review of these less common human transmissible spongiform encephalopathies. J Clin Neurosci 2001; 8(5):387-397.

(237) Medori R, Tritschler HJ, LeBlanc AC, Villare F, Manetto V, Montagna P et al. Fatal Familial Insomnia, a prion disease with a mutation in codon 178 of the prion protein gene: study of two kindreds. In: Prusiner SB, Collinge J, Powell J, Anderton B, editors. Prion Diseases of Humans and Animals. London: Ellis Horwood, 1992: 180-187.

(238) Taratuto AL, Piccardo P, Reich EG, Chen SG, Sevlever G, Schultz M et al. Insomnia associated with thalamic involvement in E200K Creutzfeldt-Jakob disease. Neurology 2002; 58(3):362-367.

(239) Chapman J, Arlazoroff A, Goldfarb LG, Cervenakova L, Neufeld MY, Werber E et al. Fatal insomnia in a case of familial Creutzfeldt-Jakob disease with the codon 200^{Lys} mutation. Neurology 1996; 46:758-761.

(240) Goldfarb LG, Petersen RB, Tabaton M, Brown P, LeBlanc AC, Montagna P et al. Fatal familial insomnia and familial Creutzfeldt-Jakob disease: disease phenotype determined by a DNA polymorphism. Science 1992; 258:806-808.

(241) Collinge J, Palmer MS, Sidle KCL, Gowland I, Medori R, Ironside J et al. Transmission of fatal familial insomnia to laboratory animals. Lancet 1995; 346:569-570.

(242) Gajdusek DC, Zigas V. Degenerative disease of the central nervous system in New Guinea. New Eng J Med 1957; 257:974-978.

(243) Gajdusek DC, Gibbs CJJr, Alpers MP. Experimental transmission of a kuru-like syndrome to chimpanzees. Nature 1966; 209(5025):794-796.

(244) Zigas V, Gajdusek DC. Kuru: clinical study of a new syndrome resembling paralysis agitans in natives of the Eastern Highlands of Australian New Guinea. Med J Aust 1957; 2:745-754.

(245) Kretzschmar HA. Neuropathology of human prion diseases (spongiform encephalopathies). Dev Biol Stand 1993; 80:71-90.

(246) Alpers MP, Gajdusek EC. Changing patterns of kuru: epidemiological changes in the period of increasing contact of the Fore people with Western civilization. American Journal of Tropical Medicine and Hygiene 1965; 14:852-879.

(247) Alpers M, Rail L. Kuru and Creutzfeldt-Jakob disease: clinical and aetiological aspects. Proc Aust Assoc Neurol 1971; 8:7-15.

(248) Alpers M. Kuru: Age and Duration Studies. Department of Medicine, University of Adelaide 1964.

(249) Alpers M. Kuru: clinical and aetiological aspects. In: Whitty CWM, Hughes JT, MacCallum FO, editors. Virus diseases and the nervous system. Oxford & Edinburgh: Blackwell Scientific Publications, 1969: 83-97.

(250) Alpers M. Epidemiological changes in kuru, 1957 to 1963. NINDB Monograph No. 2, Slow, Latent and Temperate Virus Infections. Bethesda: 1964: 65-82.

(251) Alpers MP. Epidemiology and Clinical Aspects of Kuru. In: Prusiner SB, McKinley MP, editors. Prions: Novel infectious pathogens causing scrapie and Creutzfeldt-Jakob disease. San Diego: Academic Press, 1987: 451-465.

(252) Lee HS, Brown P, Cervenáková L, Garruto RM, Alpers MP, Gajdusek DC et al. Increased susceptibility to Kuru of carriers of the *PRNP* 129 methionine/methionine genotype. Journal of Infectious Diseases 2001; 183(2):192-196.

(253) Will RG, Zeidler M, Stewart GE, Macleod MA, Ironside JW, Cousens SN et al. Diagnosis of new variant Creutzfeldt-Jakob disease. Annals of Neurology 2000; 47(5):575-582.

(254) Wadsworth JD, Hill AF, Beck JA, Collinge J. Molecular and clinical classification of human prion disease. Br Med Bull 2003; 66(1):241-254.

(255) Zeidler M. 14-3-3 cerebrospinal fluid protein and Creutzfeldt-Jakob disease. Annals of Neurology 2000; 47(5):683-684.

(256) Zeidler M, Sellar RJ, Collie DA, Knight R, Stewart G, Macleod MA et al. The pulvinar sign on magnetic resonance imaging in variant Creutzfeldt-Jakob disease. Lancet 2000; 355(9213):1412-1418.

(257) Lasmezas CI, Fournier JG, Nouvel V, Boe H, Marce D, Lamoury F et al. Adaptation of the bovine spongiform encephalopathy agent to primates and comparison with Creutzfeldt-- Jakob disease: implications for human health. Proc Natl Acad Sci U S A 2001; 98(7):4142-4147.

(258) Zeidler M, Stewart G, Cousens SN, Estebeiro K, Will RG. Codon 129 genotype and new variant CJD. Lancet 1997; 350:668.

(259) Peden AH, Head MW, Ritchie DL, Bell JE, Ironside JW. Preclinical vCJD after blood transfusion in a PRNP codon 129 heterozygous patient. Lancet 2004; 364(9433):527-529.

(260) Bruce ME. TSE strain variation. Br Med Bull 2003; 66(1):99-108.

(261) Meyer N, Rosenbaum V, Schmidt B, Gilles K, Mirenda C, Groth D et al. Search for a putative scrapie genome in purified prion fractions reveals a paucity of nucleic acids. J Gen Virol 1991; 72:37-49.

(262) Kellings K, Meyer N, Mirenda C, Prusiner SB, Riesner D. Further analysis of nucleic acids in purified scrapie prion preparations by improved return refocusing gel electrophoresis. J Gen Virol 1992; 73:1025-1029.

(263) Riesner D, Kellings K, Meyer N, Mirenda C, Prusiner SB. Nucleic Acids and Scrapie Prions. In: Prusiner SB, Collinge J, Powell J, Anderton B, editors. Prion Diseases of Humans and Animals. London: Ellis Horwood, 1992.

(264) Weissmann C. A 'unified theory' of prion propagation. Nature 1991; 352:679-683.

(265) Bessen RA, Marsh RF. Identification of two biologically distinct strains of transmissible mink encephalopathy in hamsters. J Gen Virol 1992; 73 (Pt 2):329-334.

(266) Bessen RA, Marsh RF. Distinct PrP properties suggest the molecular basis of strain variation in transmissible mink encephalopathy. Journal of Virology 1994; 68:7859-7868.

(267) Bartz JC, Bessen RA, McKenzie D, Marsh RF, Aiken JM. Adaptation and selection of prion protein strain conformations following interspecies transmission of transmissible mink encephalopathy. Journal of Virology 2000; 74(12):5542-5547.

(268) Lawson VA, Collins SJ, Masters CL, Hill AF. Prion protein glycosylation. J Neurochem 2005; 93(4):793-801.

(269) Caughey B, Raymond GJ. The scrapie-associated form of PrP is made from a cell surface precursor that is both protease- and phospholipase-sensitive. J Biol Chem 1991; 266 No 27:18217-18223.

(270) Somerville RA, Chong A, Mulqueen OU, Birkett CR, Wood SCER, Hope J. Biochemical typing of scrapie strains. Nature 1997; 386:564.

(271) DeArmond SJ, Sánchez H, Yehiely F, Qiu Y, Ninchak-Casey A, Daggett V et al. Selective neuronal targeting in prion disease. Neuron 1997; 19:1337-1348.

(272) Hill AF, Joiner S, Wadsworth JD, Sidle KC, Bell JE, Budka H et al. Molecular classification of sporadic Creutzfeldt-Jakob disease. Brain 2003; 126(Pt 6):1333-1346.

(273) Safar J, Wille H, Itri V, Groth D, Serban H, Torchia M et al. Eight prion strains PrP^{Sc} molecules with different conformations. Nat Med 1998; 4(10):1157-1165.

(274) Kascsak RJ, Rubenstein R, Merz PA, Tonna DeMasi M, Fersko R, Carp RI et al. Mouse polyclonal and monoclonal antibody to scrapie-associated fibril proteins. J Virol 1987; 61:3688-3693.

(275) Peretz D, Williamson RA, Matsunaga Y, Serban H, Pinilla C, Bastidas RB et al. A conformational transition at the N terminus of the prion protein features in formation of the scrapie isoform. J Mol Biol 1997; 273:614-622.

(276) Lloyd SE, Uphill JB, Targonski PV, Fisher EM, Collinge J. Identification of genetic loci affecting mouse-adapted bovine spongiform encephalopathy incubation time in mice. Neurogenetics 2002; 4(2):77-81.

(277) Jackson GS, Beck JA, Navarrete C, Brown J, Sutton PM, Contreras M et al. HLA-DQ7 antigen and resistance to variant CJD. Nature 2001; 414(6861):269-270.

(278) Collinge J, Sidle KCL, Meads J, Ironside J, Hill AF. Molecular analysis of prion strain variation and the aetiology of 'new variant' CJD. Nature 1996; 383:685-690.

(279) Wadsworth JDF, Hill AF, Joiner S, Jackson GS, Clarke AR, Collinge J. Strain-specific prion-protein conformation determined by metal ions. Nature Cell Biology 1999; 1:55-59.

(280) Parchi P, Castellani R, Capellari S, Ghetti B, Young K, Chen SG et al. Molecular basis of Phenotypic Variability in Sporadic Creutzfeldt-Jakob Disease. Annals of Neurology 1996; 39(5):669-680.

(281) Parchi P, Capellari S, Chen SG, Petersen RB, Gambetti P, Kopp N et al. Typing prion isoforms. Nature 1997; 386:232-233.

(282) Parchi P, Giese A, Capellari S, Brown P, Schulz-Schaeffer W, Windl O et al. Classification of sporadic Creutzfeldt-Jakob Disease based on molecular and phenotypic analysis of 300 subjects. Annals of Neurology 1999; 46(2):224-233.

(283) Zanusso G, Farinazzo A, Fiorini M, Gelati M, Castagna A, Righetti PG et al. pH-dependent prion protein conformation in classical Creutzfeldt-Jakob disease. Journal of Biological Chemistry 2001; 276(44 PT 1):40377-40380.

(284) Notari S, Capellari S, Giese A, Westner I, Baruzzi A, Ghetti B et al. Effects of different experimental conditions on the PrPSc core generated by protease digestion: Implications for strain typing and molecular classification of CJD. J Biol Chem 2004.

(285) Lewis V, Hill AF, Klug GM, Boyd A, Masters CL, Collins SJ. Australian sporadic CJD analysis supports endogenous determinants of molecular-clinical profiles. Neurology 2005; 65(1):113-118.

(286) Polymenidou M, Verrghese-Nikolakaki S, Groschup M, Chaplin MJ, Stack MJ, Plaitakis A et al. A short purification process for quantitative isolation of PrPSc from

naturally occurring and experimental transmissible spongiform encephalopathies. BMC Infect Dis 2002; 2(1):23.

(287) Polymenidou M, Stoeck K, Glatzel M, Vey M, Bellon A, Aguzzi A. Coexistence of multiple PrP(Sc) types in individuals with Creutzfeldt-Jakob disease. Lancet Neurol 2005; 4(12):805-814.

(288) Yull HM, Ritchie DL, Langeveld JP, van Zijderveld FG, Bruce ME, Ironside JW et al. Detection of type 1 prion protein in variant Creutzfeldt-Jakob disease. Am J Pathol 2006; 168(1):151-157.

(289) Zanusso G, Farinazzo A, Prelli F, Fiorini M, Gelati M, Ferrari S et al. Identification of distinct N-terminal truncated forms of prion protein in different Creutzfeldt-Jakob disease subtypes. J Biol chem 2004; 279(37):38936-38942.

(290) Parchi P, Zou WQ, Wang W, Brown P, Capellari S, Ghetti B et al. Genetic influence on the structural variations of the abnormal prion protein. Proc Natl Acad Sci USA 2000; 97(18):10168-10172.

(291) Bruce M, Chree A, McConnell I, Foster J, Pearson G, Fraser H. Transmission of bovine spongiform encephalopathy and scrapie to mice: Strain variation and the species barrier. Philos Trans R Soc Lond [Biol] 1994; 343:405-411.

(292) Kimberlin RH, Walker CA. Characteristics of a Short Incubation Model of Scrapie in the Golden Hamster. J Gen Virol 1977; 34:295-304.

(293) Kimberlin RH, Cole S, Walker CA. Temporary and permanent modifications to a single strain of mouse scrapie on transmission to rats and hamsters. J Gen Virol 1987; 68:1875-1881.

(294) Scott MR, Peretz D, Nguyen HO, DeArmond SJ, Prusiner SB. Transmission barriers for bovine, ovine, and human prions in transgenic mice. J Virol 2005; 79(9):5259-5271.

(295) Wadsworth JD, Asante EA, Desbruslais M, Linehan JM, Joiner S, Gowland I et al. Human Prion Protein with Valine 129 Prevents Expression of Variant CJD Phenotype. Science 2004; 306(5702):1793-1796.

(296) Peretz D, Williamson RA, Legname G, Matsunaga Y, Vergara J, Burton DR et al. A change in the conformation of prions accompanies the emergence of a new prion strain. Neuron 2002; 34(6):921-932.

(297) Hill AF, Collinge J. Subclinical prion infection in humans and animals. Br Med Bull 2003; 66(1):161-170.

(298) Asante EA, Linehan JM, Desbruslais M, Joiner S, Gowland I, Wood A et al. BSE prions propagate as either variant CJD-like or sporadic CJD-like prion strains in transgenic mice expressing human prion protein. EMBO J 2002; 21 (23):6358-6366.

(299) Asante EA, Linehan JM, Gowland I, Joiner S, Fox K, Cooper S et al. Dissociation of pathological and molecular phenotype of variant Creutzfeldt-Jakob disease in transgenic human prion protein 129 heterozygous mice. Proc Natl Acad Sci U S A 2006; 103(28):10759-10764.

(300) Lloyd SE, Linehan JM, Desbruslais M, Joiner S, Buckell J, Brandner S et al. Characterization of two distinct prion strains derived from bovine spongiform encephalopathy transmissions to inbred mice. J Gen Virol 2004; 85(Pt 8):2471-2478.

(301) Asante EA, Gowland I, Linehan JM, Mahal SP, Collinge J. Expression Pattern of a Mini Human PrP Gene Promoter in Transgenic Mice. Neurobiol Dis 2002; 10(1):1-7.

(302) Hill AF, Collinge J. Subclinical prion infection. Trends Microbiol 2003; 11(12):578-584.

(303) Prusiner SB, McKinley MP, Bowman K, Bolton DC, Bendheim PE, Groth DF et al. Scrapie prions aggregate to form amyloid-like birefringent rods. Cell 1983; 35:349-358.

(304) Pan KM, Stahl N, Prusiner SB. Purification and properties of the cellular prion protein from Syrian hamster brain. Protein Sci 1992; 1:1343-1352.

(305) Prusiner SB, Bowman K, Groth DF. Purification of Scrapie Prions. In: Prusiner SB, McKinley MP, editors. Prions: Novel Infectious pathogens causing scrapie and Creutzfeldt-Jakob disease. San Diego: Academic Press, 1987: 149-171.

(306) Diringer H, Hilmert H, Simon D, Werner E, Ehlers B. Towards purification of the scrapie agent. Eur J Biochem 1983; 134:555-560.

(307) Hilmert H, Diringer H. A rapid and efficient method to enrich SAF-protein from scrapie brains of hamsters. Biosci Rep 1984; 4:165-170.

(308) Castle BE, Dees C, German TL, Marsh RF. Effects of different methods of purification on aggregation of scrapie infectivity. J Gen Virol 1987; 68:225-231.

(309) Bolton DC, Bendheim PE, Marmorstein AD, Potempska A. Isolation and structural studies of the intact scrapie agent protein. Arch Biochem Biophys 1987; 258:579-590.

(310) Bolton DC, Rudelli RD, Currie JR, Bendheim PE. Copurification of Sp33-37 and scrapie agent from hamster brain prior to detectable histopathology and clinical disease. J Gen Virol 1991; 72 (Pt 12):2905-2913.

(311) Takahashi K, Shinagawa M, Doi S, Sasaki S, Goto H, Sato G. Purification of scrapie agent from infected animal brains and raising of antibodies to the purified fraction. Microbiol Immunol 1986; 30:123-131.

(312) Hope J, Multhaup G, Reekie LJ, Kimberlin RH, Beyreuther K. Molecular pathology of scrapie-associated fibril protein (PrP) in mouse brain affected by the ME7 strain of scrapie. Eur J Biochem 1988; 172:271-277.

(313) Gabizon R, McKinley MP, Groth D, Prusiner SB. Immunoaffinity purification and neutralization of scrapie prion infectivity. Proc Natl Acad Sci U S A 1988; 85:6617-6621.

(314) Gabizon R, McKinley MP, Groth D, Westaway D, DeArmond SJ, Carlson GA et al. Immunoaffinity purification and neutralization of scrapie prions. Prog Clin Biol Res 1989; 317:583-600.

(315) Bendheim PE, Potempska A, Kascsak RJ, Bolton DC. Purification and partial characterization of the normal cellular homologue of the scrapie agent protein. J Infect Dis 1988; 158:1198-1208.

(316) Wadsworth JDF, Joiner S, Hill AF, Campbell TA, Desbruslais M, Luthert PJ et al. Tissue distribution of protease resistant prion protein in variant CJD using a highly sensitive immuno-blotting assay. Lancet 2001; 358(9277):171-180.

(317) Smith BJ. SDS Polyacrylamide Gel Electrophoresis for N-Terminal Protein Sequencing. In: Smith BJ, editor. Protein Sequencing Protocols. Totowa, New Jersey 07512: Humana Press, 1997: 17-24.

(318) Khalili-Shirazi A, Quaratino S, Londei M, Summers L, Tayebi M, Clarke AR et al. Protein conformation significantly influences immune responses to prion protein. J Immunol 2005; 174(6):3256-3263.

(319) Heukeshoven J, Dernick R. Simplified method for silver staining of proteins in polyacrylamide gels and the mechanism of silver staining. Electrophoresis 1985; 6:103-112.

(320) Harlow E, Lane D. Immunoaffinity Purification. In: Harlow E, Lane D, editors. Antibodies: A Laboratory Manual. Cold Spring Harbor: Cold Spring Harbor Laboratories, 1988: 511-552.

(321) Peterson GL. Determination of total protein. Methods Enzymol 1983; 91:95-119.

(322) Beringue V, Mallinson G, Kaisar M, Tayebi M, Sattar Z, Jackson G et al. Regional heterogeneity of cellular prion protein isoforms in the mouse brain. Brain 2003; 126(9):2065-2073.

(323) Gersten DM, Marchalonis JJ. A rapid, novel method for the solid-phase derivatization of IgG antibodies for immune-affinity chromatography. J Immunol Methods 1978; 24(3-4):305-309.

(324) Alvarez-Martinez MT, Torrent J, Lange R, Verdier JM, Balny C, Liautard JP. Optimized overproduction, purification, characterization and high-pressure sensitivity of the prion protein in the native (PrP(C)-like) or amyloid (PrP(Sc)-like) conformation. Biochim Biophys Acta 2003; 1645(2):228-240.

(325) Bueler H, Fischer M, Lang Y, Bluethmann H, Lipp H-P, DeArmond SJ et al. Normal development and behaviour of mice lacking the neuronal cell-surface PrP protein. Nature 1992; 356:577-582.

(326) Hill AF, Joiner S, Linehan J, Desbruslais M, Lantos PL, Collinge J. Species barrier independent prion replication in apparently resistant species. Proc Natl Acad Sci (USA) 2000; 97(18):10248-10253.

(327) Prusiner SB. Prions. Proc Natl Acad Sci U S A 1998; 95(23):13363-13383.

(328) Lloyd SE, Thompson SR, Beck JA, Linehan JM, Wadsworth JD, Brandner S et al. Identification and characterization of a novel mouse prion gene allele. Mamm Genome 2004; 15(5):383-389.

(329) Tatzelt J, Groth DF, Torchia M, Prusiner SB, DeArmond SJ. Kinetics of prion protein accumulation in the CNS of mice with experimental scrapie. Journal of Neuropathology and Experimental Neurology 1999; 58(12):1244-1249.

(330) Caughey B, Raymond GJ, Kocisko DA, Lansbury PT. Scrapie infectivity correlates with converting activity, protease resistance, and aggregation of scrapie-associated prion protein in guanidine denaturation studies. J Virology 1997; 71(5):4107-4110.

(331) Bartz JC, Aiken JM, Bessen RA. Delay in onset of prion disease for the HY strain of transmissible mink encephalopathy as a result of prior peripheral inoculation with the replication-deficient DY strain. J Gen Virol 2004; 85(Pt 1):265-273.

(332) Thackray AM, Klein MA, Aguzzi A, Bujdoso R. Chronic subclinical prion disease induced by low-dose inoculum. J Virol 2002; 76(5):2510-2517.

(333) Kuczius T, Groschup MH. Differences in proteinase K resistance and neuronal deposition of abnormal prion proteins characterize bovine spongiform encephalopathy (BSE) and scrapie strains. Mol Med 1999; 5(6):406-418.

(334) Torrent J, Alvarez-Martinez MT, Harricane MC, Heitz F, Liautard JP, Balny C et al. High Pressure Induces Scrapie-like Prion Protein Misfolding and Amyloid Fibril Formation. Biochemistry 2004; 43(22):7162-7170.

(335) Makarava N, Bocharova OV, Salnikov VV, Breydo L, Anderson M, Baskakov IV. Dichotomous versus palm-type mechanisms of lateral assembly of amyloid fibrils. Protein Sci 2006; 15(6):1334-1341.

(336) Lasmezas CI, Deslys J-P, Robain O, Jaegly A, Beringue V, Peyrin J-M et al. Transmission of the BSE agent to mice in the absence of detectable abnormal prion protein. Science 1997; 275:402-405.

(337) Tremblay P, Ball HL, Kaneko K, Groth D, Hegde RS, Cohen FE et al. Mutant PrP(Sc) Conformers Induced by a Synthetic Peptide and Several Prion Strains. J Virol 2004; 78(4):2088-2099.

(338) Telling GC, Scott M, Mastrianni J, Gabizon R, Torchia M, Cohen FE et al. Prion propagation in mice expressing human and chimeric PrP transgenes implicates the interaction of cellular PrP with another protein. Cell 1995; 83:79-90.

(339) Mishra RS, Basu S, Gu Y, Luo X, Zou WQ, Mishra R et al. Protease-resistant human prion protein and ferritin are cotransported across Caco-2 epithelial cells: implications for species barrier in prion uptake from the intestine. J Neurosci 2004; 24(50):11280-11290.

(340) Gauczynski S, Nikles D, El Gogo S, Papy-Garcia D, Rey C, Alban S et al. The 37-kDa/67-kDa Laminin Receptor Acts as a Receptor for Infectious Prions and Is Inhibited by Polysulfated Glycanes. J Infect Dis 2006; 194(5):702-709.

(341) Flechsig E, Shmerling D, Hegyi I, Raeber AJ, Fischer M, Cozzio A et al. Prion protein devoid of the octapeptide repeat region restores susceptibility to scrapie in PrP knockout mice. Neuron 2000; 27(2):399-408.

(342) Magzoub M, Sandgren S, Lundberg P, Oglecka K, Lilja J, Wittrup A et al. N-terminal peptides from unprocessed prion proteins enter cells by macropinocytosis. Biochem Biophys Res Commun 2006; 348(2):379-385.

(343) Taraboulos A, Raeber A, Borchelt DR, Serban D, Prusiner SB. Synthesis and trafficking of prion proteins in cultured cells. Mol Biol of the Cell 1992; 3:851-863.

(344) Gabizon R, McKinley MP, Prusiner SB. Purified prion proteins and scrapie infectivity copartition into liposomes. Proc Natl Acad Sci U S A 1987; 84:4017-4021.

(345) Gabizon R, McKinley MP, Groth DF, Kenaga L, Prusiner SB. Properties of scrapie prion protein liposomes. J Biol Chem 1988; 263:4950-4955.

(346) Baron GS, Magalhaes AC, Prado MA, Caughey B. Mouse-adapted scrapie infection of SN56 cells: greater efficiency with microsome-associated versus purified PrP-res. J Virol 2006; 80(5):2106-2117.

(347) Magalhaes AC, Baron GS, Lee KS, Steele-Mortimer O, Dorward D, Prado MA et al. Uptake and neuritic transport of scrapie prion protein coincident with infection of neuronal cells. J Neurosci 2005; 25(21):5207-5216.

(348) Ebeling W, Hennrich N, Klockow M, Metz H, Orth HD, Lang H. Proteinase K from Tritirachium album Limber. Eur J Biochem 1974; 47(1):91-97.

(349) Bajorath J, Hinrichs W, Saenger W. The enzymatic activity of proteinase K is controlled by calcium. Eur J Biochem 1988; 176(2):441-447.

(350) Bajorath J, Raghunathan S, Hinrichs W, Saenger W. Long-range structural changes in proteinase K triggered by calcium ion removal. Nature 1989; 337(6206):481-484.

(351) Muller A, Hinrichs W, Wolf WM, Saenger W. Crystal structure of calcium-free proteinase K at 1.5-A resolution. J Biol Chem 1994; 269(37):23108-23111.

(352) Sweeney PJ, Walker JM. Proteinase K (EC 3.4.21.14). Methods Mol Biol 1993; 16:305-311.

(353) Goldenberger D, Perschil I, Ritzler M, Altwegg M. A simple "universal" DNA extraction procedure using SDS and proteinase K is compatible with direct PCR amplification. PCR Methods Appl 1995; 4(6):368-370.

(354) Betzel C, Pal GP, Struck M, Jany KD, Saenger W. Active-site geometry of proteinase K. Crystallographic study of its complex with a dipeptide chloromethyl ketone inhibitor. FEBS Lett 1986; 197(1-2):105-110.

(355) Betzel C, Bellemann M, Pal GP, Bajorath J, Saenger W, Wilson KS. X-ray and model-building studies on the specificity of the active site of proteinase K. Proteins 1988; 4(3):157-164.

(356) Wolf WM, Bajorath J, Muller A, Raghunathan S, Singh TP, Hinrichs W et al. Inhibition of proteinase K by methoxysuccinyl-Ala-Ala-Pro-Ala-chloromethyl ketone. An x-ray study at 2.2-A resolution. J Biol Chem 1991; 266(26):17695-17699.

(357) Bagger S, Breddam K, Byberg BR. Binding of mercury(II) to protein thiol groups: a study of proteinase K and carboxypeptidase Y. J Inorg Biochem 1991; 42(2):97-103.

(358) Muller A, Saenger W. Studies on the inhibitory action of mercury upon proteinase K. J Biol Chem 1993; 268(35):26150-26154.

(359) Saxena AK, Singh TP, Peters K, Fittkau S, Visanji M, Wilson KS et al. Structure of a ternary complex of proteinase K, mercury, and a substrate-analogue hexa-peptide at 2.2 A resolution. Proteins 1996; 25(2):195-201.

(360) Pal GP, Kavounis CA, Jany KD, Tsernoglou D. The three-dimensional structure of the complex of proteinase K with its naturally occurring protein inhibitor, PKI3. FEBS Lett 1994; 341(2-3):167-170.

(361) Kraus E, Kiltz HH, Femfert UF. The specificity of proteinase K against oxidized insulin B chain. Hoppe Seylers Z Physiol Chem 1976; 357(2):233-237.

(362) Bromme D, Peters K, Fink S, Fittkau S. Enzyme-substrate interactions in the hydrolysis of peptide substrates by thermitase, subtilisin BPN', and proteinase K. Arch Biochem Biophys 1986; 244(2):439-446.

(363) Borhan B, Hammock B, Seifert J, Wilson BW. Methyl and phenyl esters and thioesters of carboxylic acids as surrogate substrates for microassay of proteinase K esterase activity. Anal Bioanal Chem 1996; 354(4):490-492.

(364) Pahler A, Banerjee A, Dattagupta JK, Fujiwara T, Lindner K, Pal GP et al. Three-dimensional structure of fungal proteinase K reveals similarity to bacterial subtilisin. EMBO J 1984; 3(6):1311-1314.

(365) Betzel C, Pal GP, Saenger W. Three-dimensional structure of proteinase K at 0.15-nm resolution. Eur J Biochem 1988; 178(1):155-171.

(366) Betzel C, Pal GP, Saenger W. Synchrotron X-ray data collection and restrained least-squares refinement of the crystal structure of proteinase K at 1.5 A resolution. Acta Crystallogr B 1988; 44 (Pt 2):163-172.

(367) Betzel C, Gourinath S, Kumar P, Kaur P, Perbandt M, Eschenburg S et al. Structure of a serine protease proteinase K from Tritirachium album limber at 0.98 A resolution. Biochemistry 2001; 40(10):3080-3088.

(368) Hornshaw MP, McDermott JR, Candy JM, Lakey JH. Copper binding to the N-terminal tandem repeat region of mammalian and avian prion protein: Structural studies using synthetic peptides. Biochem Biophys Res Commun 1995; 214:993-999.

(369) Brown DR, Hafiz F, Glasssmith LL, Wong BS, Jones IM, Clive C et al. Consequences of manganese replacement of copper for prion protein function and proteinase resistance. EMBO J 2000; 19(6):1180-1186.

(370) Kim NH, Choi JK, Jeong BH, Kim JI, Kwon MS, Carp RI et al. Effect of transition metals (Mn, Cu, Fe) and deoxycholic acid (DA) on the conversion of PrPC to PrPres. FASEB J 2005; 19(7):783-785.

(371) Levin J, Bertsch U, Kretzschmar H, Giese A. Single particle analysis of manganese-induced prion protein aggregates. Biochem Biophys Res Commun 2005; 329(4):1200-1207.

(372) Llewelyn CA, Hewitt PE, Knight RS, Amar K, Cousens S, Mackenzie J et al. Possible transmission of variant Creutzfeldt-Jakob disease by blood transfusion. Lancet 2004; 363(9407):417-421.

(373) Sigurdsson EM, Sy MS, Li R, Scholtzova H, Kascsak RJ, Kascsak R et al. Anti-prion antibodies for prophylaxis following prion exposure in mice. Neurosci Lett 2003; 336(3):185-187.

(374) White AR, Enever P, Tayebi M, Mushens R, Linehan J, Brandner S et al. Monoclonal antibodies inhibit prion replication and delay the development of prion disease. Nature 2003; 422(6927):80-83.

(375) Enari M, Flechsig E, Weissmann C. Scrapie prion protein accumulation by scrapie-infected neuroblastoma cells abrogated by exposure to a prion protein antibody. Proc Natl Acad Sci USA 2001; 98(16):9295-9299.

(376) Carlson GA, Hsiao K, Oesch B, Westaway D, Prusiner SB. Genetics of prion infections. Trends Genet 1991; 7:61-65.

(377) Collinge J, Harding AE, Owen F, Poulter M, Lofthouse R, Boughey AM et al. Diagnosis of Gerstmann-Straussler syndrome in familial dementia with prion protein gene analysis. Lancet 1989; 2:15-17.

(378) Prusiner SB, Groth D, Serban A, Koehler R, Foster D, Torchia M et al. Ablation of the prion protein (PrP) gene in mice prevents scrapie and facilitates production of anti-PrP antibodies. Proc Natl Acad Sci USA 1993; 90:10608-10612.

(379) Weissmann C, Büeler H, Fischer M, Sailer A, Aguzzi A, Aguet M. PrP-deficient mice are resistant to scrapie. Ann NY Acad Sci 1994; 724:235-240.

(380) Aguzzi A, Brandner S, Marino S, Steinbach JP. Transgenic and knockout mice in the study of neurodegenerative diseases. J Molecular Medicine 1996; 74:111-126.

(381) Tuite MF, Cox BS. The [PSI(+)] prion of yeast: A problem of inheritance. Methods 2006; 39(1):9-22.

(382) Wickner RB. [URE3] as an altered *URE2* protein: Evidence for a prion analog in *Saccharomyces cerevisiae*. Science 1994; 264:566-569.

(383) Uptain SM, Lindquist S. Prions as Protein-Based Genetic Elements. Annu Rev Microbiol 2002; 56:703-741.

(384) Wickner RB, Edskes HK, Ross ED, Pierce MM, Baxa U, Brachmann A et al. Prion Genetics: New Rules for a New Kind of Gene. Annu Rev Genet 2004; 38:681-707.

(385) Smith BJ, Turner JP. Letter codes, Structures, Masses, and derivatives of amino acids. In: Smith BJ, editor. Protein Sequencing Protocols. Totowa, New Jersey 07512: Humana Press, 1997: 329-356.

(386) Hershko A, Ciechanover A. The ubiquitin system for protein degradation. Annu Rev Biochem 1992; 61:761-807.

(387) Rechsteiner M. Ubiquitin-mediated pathways for intracellular proteolysis. Annu Rev Cell Biol 1987; 3:1-30.

(388) Dawson TM, Dawson VL. Molecular pathways of neurodegeneration in Parkinson's disease. Science 2003; 302(5646):819-822.

(389) Petrucelli L, Dawson TM. Mechanism of neurodegenerative disease: role of the ubiquitin proteasome system. Ann Med 2004; 36(4):315-320.

(390) Ding Q, Keller JN. Does proteasome inhibition play a role in mediating neuropathology and neuron death in Alzheimer's disease? J Alzheimers Dis 2003; 5(3):241-245.

(391) Forloni G, Terreni L, Bertani I, Fogliarino S, Invernizzi R, Assini A et al. Protein misfolding in Alzheimer's and Parkinson's disease: genetics and molecular mechanisms. Neurobiol Aging 2002; 23(5):957-976.

(392) Snyder H, Wolozin B. Pathological proteins in Parkinson's disease: focus on the proteasome. J Mol Neurosci 2004; 24(3):425-442.

(393) Dimcheff DE, Portis JL, Caughey B. Prion proteins meet protein quality control. Trends Cell Biol 2003; 13(7):337-340.

(394) Yedidia Y, Horonchik L, Tzaban S, Yanai A, Taraboulos A. Proteasomes and ubiquitin are involved in the turnover of the wild-type prion protein. EMBO J 2001; 20(19):5383-5391.

(395) Kang SC, Brown DR, Whiteman M, Li R, Pan T, Perry G et al. Prion protein is ubiquitinated after developing protease resistance in the brains of scrapie-infected mice. J Pathol 2004; 203(1):603-608.

(396) Lowe J, McDermott H, Kenward N, Landon M, Mayer RJ, Bruce ME et al. Ubiquitin conjugate immunoreactivity in the brains of scrapie infected mice. J Pathol 1990; 162:61-66.

(397) Yanai A, Huang K, Kang R, Singaraja RR, Arstikaitis P, Gan L et al. Palmitoylation of huntingtin by HIP14is essential for its trafficking and function. Nat Neurosci 2006; 9(6):824-831.

(398) Medori R, Montagna P, Tritschler HJ, LeBlanc A, Cortelli P, Tinuper P et al. Fatal familial insomnia: A second kindred with mutation of prion protein gene at codon 178. Neurology 1992; 42:669-670.

(399) Tzaban S, Friedlander G, Schonberger O, Horonchik L, Yedidia Y, Shaked G et al. Protease-sensitive scrapie prion protein in aggregates of heterogeneous sizes. Biochemistry 2002; 41(42):12868-12875.

(400) Weissmann C. The state of the prion. Nat Rev Microbiol 2004; 2(11):861-871.

(401) Harris DA, Chiesa R, Drisaldi B, Quaglio E, Migheli A, Piccardo P et al. A transgenic model of a familial prion disease. Arch Virol 2000;103-112.

(402) Vorberg I, Raines A, Priola SA. Acute formation of protease-resistant prion protein does not always lead to persistent scrapie infection in vitro. J Biol Chem 2004; 279(28):29218-29225.

(403) Baskakov IV, Aagaard C, Mehlhorn I, Wille H, Groth D, Baldwin MA et al. Self-assembly of recombinant prion protein of 106 residues. Biochemistry 2000; 39(10):2792-2804.

(404) Zhang H, Kaneko K, Nguyen JT, Livshits TL, Baldwin MA, Cohen FE et al. Conformational transitions in peptides containing two putative α-helices of the prion protein. J Mol Biol 1995; 250:514-526.

(405) Lee S, Eisenberg D. Seeded conversion of recombinant prion protein to a disulfide-bonded oligomer by a reduction-oxidation process. Nat Struct Biol 2003; 10(9):725-730.

(406) Hill A, Antoniou M, Collinge J. Protease-resistant prion protein produced in vitro lacks detectable infectivity. J Gen Virol 1999; 80:11-14.

(407) Soto C, Saborio GP, Anderes L. Cyclic amplification of protein misfolding: application to prion-related disorders and beyond. Trends Neurosci 2002; 25(8):390-394.